GENE EXPRESSION IN DWARF MISTLETOE RELATED TO EXPLOSIVE SEED DISPERSAL WITH SPECIAL ATTENTION TO AQUAPORINS

JOANNA URBAN

2018

Gene Expression in Dwarf Mistletoe Related to Explosive Seed Dispersal with Special Attention to Aquaporins

Vom Fachbereich Biologie der Technischen Universität Darmstadt zur

Erlangung des akademischen Grades

eines Doctor rerum naturalium

genehmigte

Dissertation von

Joanna Urban, MSc

Berichterstatter: (1. Referent): Prof. Dr. Ralf Kaldenhoff

Mitberichterstatter (2. Referent): Prof. Dr. Heribert Warzecha

Tag der Einreichung: 10.10.18

Tag der mündlichen Prüfung: 14.12.18

Darmstadt 2018

Joanna Urban: Gene Expression in Dwarf Mistletoe Related to Explosive Seed Dispersal with Special Attention to Aquaporins
Darmstadt, Technische Universität Darmstadt,
Year thesis published in TUprints 2019
URN: urn:nbn:de:tuda-tuprints-000
Date of the viva voce 14.12.18

Acknowledgements

Thank you in particular:

Prof. Dr. Ralf Kaldenhoff for his guidance, his trust, unwavering support and the many stimulating discussions over the years. I am very appreciative of the mentorship that was provided to me during this doctoral journey.

Prof. Dr. Heribert Warzecha for the assessment of the work.

Dr. Cynthia Ross Friedman for originally envisioning this line of research, for the financial support, and the overall expertise on dwarf mistletoe. I am very grateful and appreciative of the passion for this work that was instilled early on.

Beate Otto for discussions on common research interests and working methods, as well as taking good care of me in Germany. I learned many valuable laboratory techniques during my doctoral work that will carry forward with me for a lifetime.

Dr. Norbert Uehlein for his help in the laboratory and making me feel a part of the team.

Dr. Anastassia Butichevskaja for help with bioinformatics analysis of Affymetrix microarray results.

Dr. John Church for helping to finalize the final document and his overall support.

Cameron Boyda for helping with *A. americanum* samples collections in Canada as well as with obtaining qRT-PCR data.

Nadine Priem, Jan Renker, and Magdalena Lachnit for the companionship in the laboratory on the numerous days with extended working hours.

All other former and current members of AG Kaldenhoff for all the good times and cooperation.

List of Figures

Figure 1.1. Lodgepole pine infected with dwarf mistletoe showing witches' brooms and topkill above (adapted from Worrall & Geils, 2006) 2
Figure 1.2. Reproductive shoots from male/staminate (A) and female/pistillate (B) plants of *Arceuthobium americanum* 3
Figure 1.3. Generalized life cycle of *Arceuthobium americanum* (Hawksworth & Wiens, 1972, 1998) 5
Figure 1.4. Diagrammatic longitudinal section through a mature Arceuthobium fruit (left; adapted from Hawksworth & Wiens, 1998) and fruit discharging its seed (right). Photographs by T. Hinds et al. (1993) 7
Figure 1.5. Fruit of *Arceuthobium americanum* as seen in longitudinal sectional view using brightfield microscopy and stained with toluidine blue O (Ross, 2006) 7
Figure 1.6. Hydrated viscin cells (unstained) with helically arranged (f) fibrils and (c) chloroplast (Ross, 2006) 7
Figure 1.7. Generalized phylogeny of Archaeal, Bacterial, and Eukaryal MIPs. Major subfamilies are shown as collapsed sets of nodes with their branches coloured according to a legend. Aquaporins (AQP), aquaglyceroprotein (GLP), plasma membrane intrinsic proteins (PIPs), tonoplast intrinsic proteins (TIPs), uncategorized intrinsic proteins (XIPs), Nodulin 26-like intrinsic proteins (NIPs), small basic intrinsic proteins (SIPs; Abascal et al., 2014) 9
Figure 1.8. (A) Aquaporin model showing the six transmembrane domains (helices; H1 to H6) and two short-pore helices named HB and HE with two NPA motifs in each monomer; (B) Ribbon structure of a single AQP monomer with different colours showing different helices from blue (n-terminal) to red (c-terminal); (C) Crystal stucture of the tetramer consisting of four monomers (adapted from Tani and Fujiyoshi, 2014) 11
Figure 1.9. Evolutionary relationship of all *Populus trichocarpa* MIPs shown along with MIPs from *Arabidopsis thaliana*. Populus MIP subfamilies PtPIPs, PtTIPs, PtNIPs, and PtSIPs are clustered with the corresponding *Arabidopsis* MIP subfamilies. XIPs observed only in *Populus* make a separate group (Gupta & Sankararamakrishnan, 2009, modified) 12
Figure 1.10. Regulation of plasma membrane intrinsic proteins (PIPs) in a cell: endoplasmic reticulum (ER), plasma membrane (PM), PIP2 group (yellow), PIP1 isoforms (green), PIP2s containing a diacidic motif (red circle), coat protein complex II (COPII) of the vesicles, trans-Golgi network (TGN), the syntaxin SYP121 protein. The insert shows the topological structure of an aquaporin

monomer (Murata et al., 2000), which consists of six membrane-spanning α-helices (1–6) connected by five loops (A–E) and N and C termini facing the cytosol. Phosphorylated Ser residues are in green circles (the putative phosphorylated Ser in loop D is not indicated), the protonated Histidine (His) of loop D is in the blue circle, and the Cys residue of loop A involved in disulfide bound formation between monomers is in the purple circle (Adapted from Chaumont and Tyerman, 2014) 14

Figure 2.1. (A) HyperLadder I DNA marker (5 µl, applied to a 1% agarose gel). Image by Bioline. (B) RiboRuler™ High Range RNA Ladder (2 µl, applied to a 1% formaldehyde agarose). Image by Thermo Scientific 23

Figure 2.2. Outline of the Gateway™ Cloning System. (A) Recombination facilitated by the BP enzyme between the attB sites present in the insert (cDNA) and attP sites in the entry vector ([pDonr201] generates the entry clone flanked by the attL sites [pEntry-cDNA]). (B) LR recombinase is used to transfer the insert from the entry vector to the expression vector (pYes-Dest52) to generate expression clone (pYes-Dest52-cDNA). Adapted from Festa et al. 2013……..32

Figure 2.3. Schematic representation of the stopped-flow apparatus. The apparatus consists of the mixing unit (A), the detection unit (B), and the computer with software for analyzing data (not shown). Adopted from UC Davis. 36

Figure 2.4. Graphic illustration of a 96-well plate. The numbers in grey squares indicate the sequence in which the cDNA samples were applied on a slide and then were taken from the respective wells of the plate with the 8 needles of the "array tool." 39

Figure 2.5. Schematic representation of a membrane chip surface (slide): The numbers in grey squares represent the spotting cDNA points. The number 1 indicates the first spot event, 2 is the second, 3 is the third, etc. The letter/number fields (e.g., B1) indicate from which well of the 96 plate the respective DNA sample originates. The 8 array needles are first transferred to the membrane and then transferred to wells A1, A2, A3, A4, B1, B2, B3, and B4, and so forth. After a 96-well plate was completely spotted, columns 1, 9, 17, and 26 were completely filled with cDNA spots (24 spots per column)..... 40

Figure 2.6. Generalized illustration of steps involved in DNA microarray analysis using MicroCaster™, from applying samples to slides to visualization of positive results after hybridization. 41

Figure 2.7. Alkali-labile DIG-11-dUTP (Roche). Digoxigenin DIG) 41

Figure 2.8. Principle of chemiluminescence reaction 44

Figure 2.9. CDP-Star® chemical structure 44
Figure 2.10. Flowchart of a GeneChip System microarray experiment. The labelled ss cDNA was injected into the Affymetrix *Arabidopsis* Gene 1.0 ST arrays and hybridized for 16 hrs at 45°C in a GeneChip® Hybridization Oven 640. Finally, hybridized arrays were washed and stained in an Affymetrix GeneChip® Fluidics Station 450; the fluorescent signals were quantified with an Affymetrix GeneChip® Scanner 3000 7G. Fluidics and scan functions were regulated by the Affymetrix GeneChip® Command Console software (AGCC; version 4.1.3). Figure adopted from Dalma-Weiszhausz et al. (2006)……46
Figure 3.1. Total RNA extracted from a whole mistletoe plant or mistletoe fruit using the RNeasy kit. (A) RNeasy kit with 2% Polyethylene glyco (B) with no addition of 2% polyethylene glycol. Samples from (A) indicate high quality RNA showing two sharp rRNA bands indicating 28S and 18S rRNA with very little smearing. Line 1 represents RNA from a whole plant; line 2 represents RNA from the fruit. All samples from (B) show high RNA degradation – no definite bands of 28S and 18S RNA. Lines 1, 2, and 3 represent a whole plant, lines 4 and 5 fruit tissue..... 54
Figure 3.2. Total RNA extracted from mistletoe fruit using MasterPure™ with 1.5% denaturing agarose gel. Line 1 represents *A. americanum* fruit from a fresh plant. Line 2 represents negative control. Line 3 represents *A. americanum* fruit stored in *RNA*Later solution 54
Figure 3.3. Chips (A-B-C) with positive hybridization results. Black spots ( ) indicate positive chemiluminescence caused by hybridization of the probe to a specific clone of *A. oxycedri*. Numbers 1, 2, 3 on each chip indicate different concentrations of positive control (NtAQP1). 57
Figure 3.4. Aminosilane-coated slide surface (Adapted from Conzone & Pantano 2004) 58
Figure 3.5. Nitrocellulose used to coat a slide surface..... 58
Figure 3.6. Aminosilane Nexterion® slide spotted with PCR products. Black spots indicate the positive hybrids 58
Figure 3.7. Nitrocellulose NEXTERION® NC-C slide spotted with PCR products. Black spots indicate the positive hybrids 58
Figure 3.8. Influence of hybridization intensity thresholds on the number of probes and probe-sets retained in the probe mask following hybridization of *A. americanum* to Affymetrix *Arabidopsis* ATH-1 GeneChip® 60
Figure 3.9. The effect of hybridization intensity thresholds used to generate the probe-mask (computable document format) files on detection of differentially regulated genes following hybridization of labelled *A. americanum* to Affymetrix

Arabidopsis ATH-1 GeneChip®. The 300 threshold intensity cut-off level was used for further investigations 61
Figure 3.10. Phylogenetic comparison of the complete set of 35 different MIPs encoded in the *Arabidopsis* genome. Aquaporins found over-expressed are shown in red squares. The bar indicates the mean distance of 0.05 changes per amino acid residue. (Adopted from Johanson et al., 2001) 67
Figure 3.11. Melting curves from quantitative real time polymerase chain reaction of A) AQP2 gene, B) RuBisCo gene, C) ABC gene generated by an Illumina thermocycler (Bio-Rad, Hercules, CA). The presence of sharp single fluorescence peaks in all examples indicated the presence of single amplicons 69
Figure 3.12. Cq values of three genes obtained during quantitative real-time polymerase chain reaction (qRT-PCR). Data from Table 3.5 were used to generate the graphs 72
Figure 3.13. Blast (NCBI's BLAST) results of in silico translated nucleotide sequence. (A) Alignment of putative PIP2 from *Arceuthobium oxycedri* with similar proteins. (B) Specific sequence example from *Manihot esculenta* (orange box in part A) 74
Figure 3.14. Tree view showing alignment of known different types of aquaporins sequences from At (*Arabidopsis thaliana*) and Os (*Oriza sativa*) with AoAQP sequence (highlighted in yellow) 75
Figure 3.15. Amplification products of polymerase chain reaction on *A. oxycedri* AQP2 complementary DNA clones. M: HyperLadder I DNA marker; 1-5 and 6-7: samples with the gene of interest (insert and primers); 8: negative control; 9: positive control 76
Figure 3.16. Plasmid preparation. M: HyperLadder I DNA marker. Entry clones of AoAQP2 inserted into pDONR201: Lines 1, 2, 3, 4, 5, 6, 10, 11, 12 77
Figure 3.17Polymerase chain reaction on AoPIP2 entry clones. M: HyperLadder I DNA marker; numbers to the left of the marker bands indicate the size of the band in BP. Line 1 and 2: Entry clones of AoAQP2. Clones from line 1 and 2 were used for subsequent LR reaction. Negative control (line 3) was negative. Positive control (line 4) was NtPIP2 77
Figure 3.18. Plasmid isolation of AoPIP2 expression clones for functional analysis (pYES-DEST52). M: HyperLadder I DNA marker. Lines 1 to 8 and 10 and 11: AoPIP2 78
Figure 3.19. Polymerase chain reaction on AoAQP2 expression clones for functional analysis (pYES-DEST52). M: HyperLadder I DNA marker; numbers to the left of

the marker bands indicate the size of the band in BP. Lines 1-7: AoAQP2. 8: positive control (AoAQP2 entry clone). 9: negative control (no template)..... 79
Figure 3.20. Kinetics of stopped-flow water conductance measurements of intact yeast protoplasts expressing AoPIP2;1. Expression of AoPIP2;1 increases water permeability of the yeast membrane. (A) Change of scattered light intensity due to the change in volume of aquaporin-expressing yeast protoplasts and protoplasts whose aquaporin expression was not induced (Kinetics represent averages from 100 individual curves.). (B) Osmotic coefficients of permeability (Pf) in cm s-1 of intact yeast protoplast expressing AoPIP2 (red bar) and not induced (blue bar) as well as standard deviations 80
Figure 3.21. Blast (NCBI's BLAST) results of in silico translated nucleotide sequence. (A) Alignment of putative alkaline/neutral invertase from *Arceuthobium oxycedri* with similar proteins. (B) Specific sequence example from *Sesamum indicum* (orange box in part A)..... 82
Figure 3.22. Plant invertases and synthases. a) Chemical composition of sucrose. b) Invertase as a hydrolase, cleaving sucrose into glucose and fructose. c) Isoforms of sucrose invertase and synthase and their different subcellular compartments (adapted from Sturm and Tang, 1999)..... 83
Figure 3.23. Blast (NCBI's BLAST) results of in silico translated nucleotides sequence. (A) Alignment of putative ABC transporter family protein from *A. oxycedri* with similar proteins. (B) Specific sequence example from *Theobrama cacao* (orange box in part A). 84
Figure 3.24. ABC full transporter. Representative structure of an ABC full transporter containing two transmembrane domains (TMDs), TMD_1 (blue) and TMD_2 (yellow), each containing six transmembrane segments and two nucleotide-binding domains (NBDs), NBD_1 (red) and NBD_2 (green; Deeley et al., 2006). Adapted from Dermauw & Van Leeuwen (2013) 85
Figure 3.25. Blast (NCBI's BLAST) results of in silico translated nucleotide sequence. (A) Alignment of putative Sterol 14-demethylase-like protein from *A. oxycedri* with similar proteins. (B) Specific sequence example from *Sesamum indicum* (orange box in part A). 86
Figure 3.26. Structures of major plant sterols with a similar sterol nucleus (R): sitosterol (24a-ethylcholest-5-en-3b-ol), campesterol (24a-methylcholest-5-en-3b-ol), stigmasterol (24a-ethylcholest-5,22-en3b-ol), and D^5-avenasterol (Z-24-ethylidenecholest-5-en-3b-ol). Adopted from Piironen et al., 2000. 87
Figure 3.27. Cytochrome P450 (CYP) enzyme CYP51 main reactions and sterols biosynthesis. D) 24, 25-dihydrolanosterol; L) lanosterol; M) 24-methylenedihydrolanosterol; N) norlanosterol; O) obtusifoliol; R1) alkyl or

alkylene group; R2) C6 or C7. Red boxes indicate products in plants (Adapted from Lepesheva and Waterman, 2007) 88

Figure 3.28. The detailed sterol biosynthetic pathway in *Arabidopsis thaliana*. A branch in the pathway results from either one or two methylation steps, producing two major end products, stigmasterol and campesterol. Campesterol is the precursor of brassinosteroids. Enzymes catalyzing these steps are shown in purple, and their corresponding mutants are shown in red (Jang et al., 2000; Schrick et al., 2000, 2002, 2004; Men et al., 2008) 89

Figure 3.29. Simplified model of the initial steps of sterol biosynthesis (in red) involved in stomatal development. The EPF–TMM/ER–MAPK cascade, SDD1 and BASL, help bHLH and MYB transcription factors to determine three cell-type differentiations (Casson and Gray, 2008; Lampard et al., 2009; Pillitteri and Torii, 2012). The sterol biosynthetic pathway restricts the cell cycle to affect cell-fate commitment and maintenance of the stomatal lineage after asymmetric division..... 90

Figure 3.30. Blast (NCBI's BLAST) results of in silico translated nucleotide sequence. (A) Alignment of putative RuBisCo enzyme family protein from *A. oxycedri* with similar proteins from different plants. (B) Specific sequence example from *Morus alba var. multicaulis* (orange box in part A)..... 92

Figure 3.31. The quaternary structure of RuBisCo enzymes showing the molecular symmetry. A) The L2S2 unit of form I RuBisCo from spinach viewed along the 2-fold symmetry axis. Large subunits are blue and green, small subunits are yellow, and the substrate mimic (2CABP) is displayed as red spheres. B) The entire L8S8 hexadecamer is shown viewed along the same 2-fold axis (Adopted from Andersson & Backlund, 2008). The gene for the RuBisCO enzyme was used as reference gene for quantitative real time polymerase chain reaction..... 93

Figure 3.32. Images (environmental scanning electron microscopy) of second-year fruit from *Arceuthobium americanum* sampled in (A) late April (B) late August. The fruit body (Fr) is highlighted in green, the sepals are in beige, and the subsidiary cells of each stoma in orange; an epidermal fold (Ef) is evident where the sepals are united and inserted at the top of the ovary (modified from Ziegler and Ross Friedman, 2017b). Scale bar = 400 µm..... 96

Figure 3.33. Generalized plant surface showing the major structural features of the cuticle, epidermal cell layer, and graphic model of cuticular wax secretion. Genes listed are ATP-binding cassette transporter (ABC); ECERIFERUM (CER)5; fatty acid elongase (FAE); lipid transfer protein (LTP); white-brown complex (WBC; Samuels et al., 2008). Only the ABC transporter gene was investigated

in detail in this
thesis. 99
Figure 3.34. Distribution of genes potentially involved in explosive seed dispersal in second-year fruit from *Arceuthobium spp.* (A) Fruit as seen in longitudinal sectional view using brightfield microscopy and stained with toluidine blue O (Ross, 2006). (B) Environmental scanning electron micrograph of fruit (Ziegler & Ross Friedman, 2017b). Fruit (Fr); sepals (Se); aquaporins 2 (AQP2); cytochrome P450 (CYP5), sterol-14 demethylase; ECERIFERUM 1 (CER1); SHN2, SHINE2; stomatal cytokinesis defective2 (SCD2); Movement protein binding protein (MPB2,); alkaline/neutral invertase portion of gene (CINV2). Scale bar = 400 µm..... 105

List of Tables

Table 2.1 *Antibiotic stock and working solutions* 17
Table 2.2 *MasterPure™ kit chemicals* 21
Table 2.3 *Solutions used for formaldehyde gel* 24
Table 2.4 *Buffers (P1, P2, and P3) used during bacterial plasmids extractions* 27
Table 2.5 *Standard PCR program conditions* 30
Table 2.6 *Primers for the fusion of a cDNA with recognition sequences for the Gateway™ System* 33
Table 2.7 *Components of PCR sample for 60 µl volume (A) and PCR cycles (B)* 34
Table 2.8 *Stopped-flow buffers compositions* 37
Table 2.9 *Hybridization buffers compositions* 40
Table 2.10 *PCR batch for labelling cDNA probes (25 uL)* 42
Table 2.11 *Microarray buffers, media, and solutions* 45
Table 2.12 *The thermal profile of qRT-PCR* 50
Table 3.1 *NanoDrop™ results showing total concentration of RNA extracted from the fruits of A. americanum as well as A260/230 and A260/280 ratios for RNA sent for Affymetrix microarray analysis* 55
Table 3.2 *List of genes obtained from hybridization of A. americanum cDNA to Affymetrix Arabidopsis ATH-1 GeneChip® using .cdf value of 300 as the cut-off level* 62
Table 3.3 *Overview of the functional classes of the list of 1,624 genes (GO categories) for biological processes (A) and cellular compartment (B). GOID, gene ontology identifier; Term, GO term name; num_list_annotations, number of genes; list size, total number of genes; % from a gene list, percentage of the genes from a total list size* 63
Table 3.4 *Expression stability of the potential reference genes calculated by BestKeeper software* 71
Table 3.5 *Averages of Cq (Ct) results obtained from quantitative real-time polymerase chain reaction (qRT-PCR) for ABC, RuBisCo, and AQP2 genes from May and September.* 71
Table 3.6 *Fold change values for selected genes (PIP2 and ABC transporter) determined by microarray analysis and quantitative real-time polymerase chain reaction (qRT-PCR).* 73
Table 3.7 *Description of candidate genes potentially involved in explosive seed dispersal in Arceuthobium* spp 95

Table of Contents

1. INTRODUCTION 1

1.1 Dwarf mistletoe (genus Arceuthobium): background 1

1.1.1 Arceuthobium americanum Nutt. ex Engelm. and A. oxycedri (DC.) M. Bieb.: geographical distribution and ecological impact 3

1.1.2 Dwarf mistletoe life cycle 4

1.1.3 Fruit structure and seed dispersal 5

1.2 Aquaporins and other proteins potentially involved in the explosive seed dispersal sequence 8

1.2.1 Aquaporins 8

1.2.2 PIPs expression and regulation within the plant cell 12

1.3. Supporting evidence 14

1.4 Project goals 16

2. MATERIALS AND METHODS 17

2.1 Antibiotics and restriction enzymes 17

2.1.1 Antibiotics 17

2.1.2 Restriction enzymes and modifying enzymes 17

2.2 Sample analysis 17

2.2.1 Plant material 17

2.2.2 Isolating total RNA 18

2.2.3 RNA analysis 21

2.2.4 Microbiological methods 25

2.2.5 Molecular biology methods 30

2.2.6 Physiological study: stopped-flow spectroscopy 35

2.2.7 Heterologous microarray 38

2.2.8 In situ hybridization - Affymetrix microarray 45

2.2.9 Quantitative reverse polymerase chain reaction 49

2.3 Additional Information 50

3. RESULTS AND DISCUSSION 52

3.1 Preface 52
3.2 Material for Analysis 53
3.2.1 Total RNA extraction from fresh A. oxycedri and A. americanum 53
3.3 Analysis of differential gene expression 56
3.3.1 Complementary DNA library construction 56
3.3.2 Heterologous microarray 56
3.4 Characterization of genes identified through MicroCASTer handheld microarray system, their products and putative role in seed dispersal 73
3.4.1 Aquaporin PIP2 and protein (GenBank accession # JN857944) 73
3.4.2 Alkaline/neutral invertase portion of gene (CINV2) coding for neutral/alkaline invertase protein 81
3.4.3 ATP-binding cassette (ABC) transporter family protein, cholesterol/phospholipid flippaseisoform 84
3.4.4 Sterol 14-demethylase-like protein 85
3.4.5 Ribulose-1,5-bisphophate carboxylase/oxygenase 91
3.5 Other genes possibly involved in explosive seed dispersal 94
3.5.1 Stomata development 96
3.5.2 Cuticle and wax production 98
3.5.2.1ECERIFERUM 1 gene 102
3.5.2.2SHINE2 - SHINE clade of AP2 102
3.6 General discussion 102
3.7 Future prospects 106
4. SUMMARY 108
REFERENCES 110
APPENDIX I 136
APPENDIX II 140
APPENDIX III 141
APPENDIX IV 142

1. INTRODUCTION

Mistletoe plants are well known as forest pests throughout the world, and as such, they damage agricultural and natural forests (Shaw et al., 2004). Mistletoe is the common name for the vast number of obligate hemiparasitic plants within the order Santalales. These parasites attach to host trees/shrubs with a structure called a haustorium, through which they extract water and nutrients from the host plant. The parasitic plants are usually endemic, and though they upset the ecosystems in which they exist, they can be beneficial, helping with pollination and decomposition and acting as a food source for animals (Reid & Shamoun, 2008). As pests, they cause major problems for the forestry industry as they can devastate an area, and the damage can be increased by multiple parasitic organisms such as the pine beetle (Jacobi & Swift, 2005).

Within the order *Santalales*, the genus *Arceuthobium*, commonly called dwarf mistletoe, is a genus of 42 species of parasitic plants *(*Nickrent et al., 2004) found within the family *Santalaceae* (formerly in the *Viscaceae*). In western forest ecosystems in North America, many dwarf mistletoe species of this genus are serious forest-borne disease agents. Severe dwarf mistletoe infection can result in a reduction in tree growth, premature tree mortality, reduced cone and seed development, poor wood quality, and an increased susceptibility of host trees to other pathogens and insects. Most commercially important conifers in western North America are parasitized by one or more dwarf mistletoes, and control is challenging. Although much information is available on managing dwarf mistletoe populations with biological, chemical, genetic (Hawksworth & Wiens, 1972; Shamoun et al., 2003) and more radical mechanical control methods, significant research and development is still needed for these control measures to become viable, effective tools. Current control methods need to be improved, and novel approaches are likely needed as well (Shamoun & De Wald, 2002).

1.1 Dwarf mistletoe (genus *Arceuthobium*): background

Dwarf mistletoe infects coniferous trees in the families *Pinaceae* in North and South America as well as *Cupressaceae* in Afro-Eurasia. The parasite consists of aerial shoots (reduced in size) associated with reproductive functions and an extensive endophytic system that obtains water and nutrients from the host. These shoots also produce growth-regulating compounds that negatively affect the host (Heide-Jorgensen, 2008).

Heavy infections caused by *Arceuthobium* spp. kill the host tree by redistributing water and nutrients from healthy areas of the tree to those areas infected with the parasite (Worrall & Geils, 2006). Redirecting water and nutrients results in the formation of characteristic witches' brooms (brooming) and dead, dry, and brittle branches (topkill) above the parasite (Figure 1.1). A witches' broom is a deformity in woody plants, usually a tree, where the plant is radically altered. A dense mass of shoots grows from one single point, and the resulting structure resembles a broom or a bird's nest. It can reduce the wood quality and lifespan of the infected tree by up to 50%, rendering the tree more susceptible to colonization by other parasites or pests, and increasing the fire hazard in the infected areas. As a result, the forestry industry suffers extensive losses worldwide (Worrall & Geils, 2006).

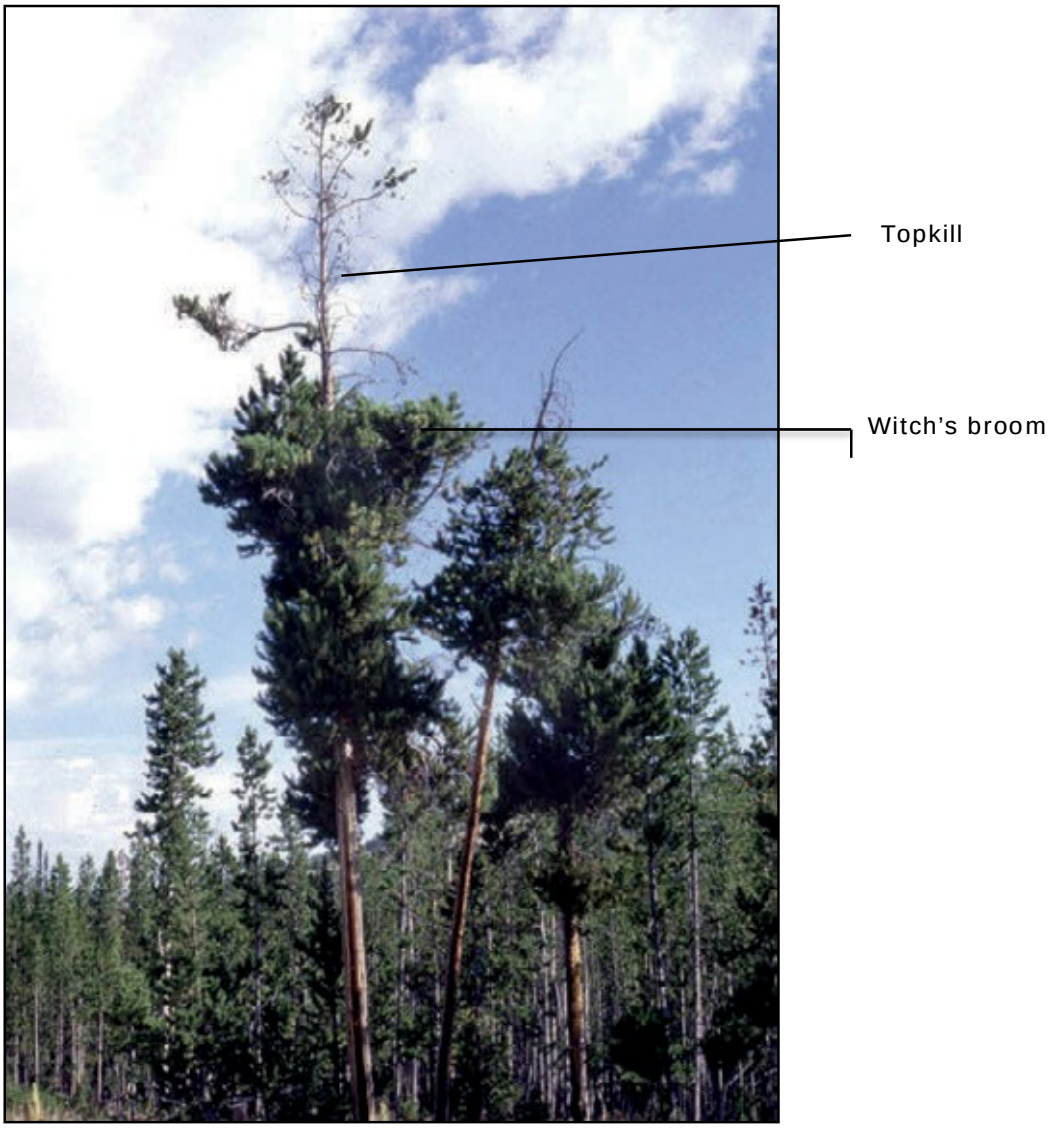

Figure 1.1. Lodgepole pine infected with dwarf mistletoe showing witches' brooms and topkill above (adapted from Worrall & Geils, 2006).

Arceuthobium spp. are dioecious, flowering plants (Figure 1.2) with a very unusual and effective explosive seed dispersal mechanism (Ross, 2006). They also have a few other distinctive features such as a very long life cycle, sometimes as long as 7 years.

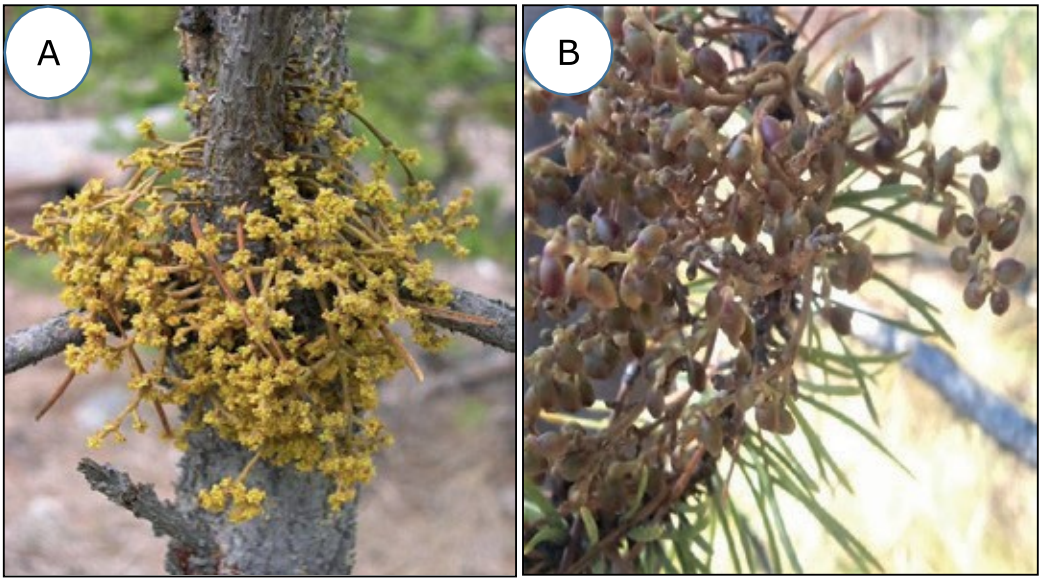

Figure 1.2. Reproductive shoots from male/staminate (A) and female/pistillate (B) plants of *Arceuthobium americanum.*

1.1.1 *Arceuthobium americanum* Nutt. ex Engelm. and *A. oxycedri* (DC.) M. Bieb.: geographical distribution and ecological impact

In North America, *Arceuthobium* spp. host genera in *Pinaceae* include: *Pinus* (pine), *Picea* (spruce), *Abies* (fir), *Pseudotsuga* (Douglas fir), *Tsuga* (hemlock), and *Larix* (larch). As a result, dwarf mistletoe infections are of huge concern, especially in western Canada (British Columbia and Alberta), where the parasite seriously reduces the health of commercially valuable coniferous trees (Hawksworth & Dooling, 1984). In 2003, dwarf mistletoe infections collectively destroyed approximately 3.8 million m^3 in British Columbia alone, and in the western United States, they destroyed approximately 11.3 million m^3 of coniferous forests (Shamoun et al., 2003).

In Canada, *Arceuthobium* comprises six taxa and five species (one species has two subspecies), and each species is found on different principal host species (Hawksworth and Wiens, 1998). *Arceuthobium americanum* Nutt. ex Engelm. is the most widespread of all North American dwarf mistletoes and is found on *Pinus banksiana* (Jack pine) in Saskatchewan and Manitoba and on *P. contorta* Dougl. ex

Loud. (lodgepole pines), predominantly *P. contorta* ssp. *latifolia* (Engelm.) Critchf. in British Columbia and Alberta.

In Eurasia, juniper dwarf mistletoe*, Arceuthobium oxycedri* (DC.) M. Bieb., which has the most extensive geographic distribution of the 42 recognized species of *Arceuthobium* (Ciesla et al., 2002; Nickrent et al., 2004), infects *Cupressaceae* and has been also reported in northern Africa, western Europe, the Balkans, Russia and other former Soviet Republics, the Near East, the Indian subcontinent, and western China. The two species were chosen because they are two widest ranging genera of all dwarf mistletoes, representing both the East and the West.

1.1.2 Dwarf mistletoe life cycle

The generalized dwarf mistletoe life cycle (Figure 1.3) comprises 4 stages, and it takes around 7 years to complete all of them: dispersal, establishment (germination, vegetative growth of endophytic system within the host bark, establishment of the endophyte in the host vascular cambium, linkage to the host xylem), incubation, and reproduction (Hawksworth & Wiens, 1972, 1998).

The fruits of dwarf mistletoe are organized usually in groups of three, and they sit on recurved pedicels. At the end of dispersal season (late August to early September for genus *Arceuthobium*), mature bicoloured and fusiform fruits are 4.2 mm in length and 2 to 2.5 mm in width (deBruyn et al., 2015; Ziegler & Friedman, 2017a). Unlike other mistletoes, which are bird-dispersed, seeds of almost all species of dwarf mistletoes (excepting *Arceuthobium verticilliflorum* Engelm.) are dispersed via explosive dispersal. In this process, a mature fruit will rupture due to immense pressure buildup (1,000 kPA) inside the fruit, and the seed will be ejected from the fruit with a velocity up to 25 m/s (Figure 1.4). The seed can travel as far as 16 m from a parent plant (Hawksworth & Wiens, 1998). After the ejection, the seed, which is covered with a sticky viscous coating (viscin), has a high likelihood of attaching to the needles of other hosts within a proximity of 10 to 16 m, where it then slides down the needle to the bark at the fascicle.

After successful adherence, the seed will enter a dormant period, delaying germination until the spring (Calvin & Wilson, 1996). During germination, the endophyte grows radially from the seed into the host bark (cortex and phloem) as a main haustorial strand or penetration wedge and then expands circumferentially, acropetally, and basipetally as cortical strands in the bark (Calvin & Wilson, 1996). Concurrently, the host cortical cells will usually begin to proliferate in an infection response such that the host branch swells. Occasional parasite sinkers develop

radially towards the host's vascular cambium where the dwarf mistletoe tissues synchronize and establish themselves amongst the host cambial cells. Finally, the sinkers become passively embedded in secondary xylem ray parenchyma as infection rays.

Reproductive shoots emerge from the swollen bark after a 3 to 4 year incubation period, and flowering occurs about 1 to 2 years after the shoots emerge (Hawksworth & Wiens, 1972, 1998). Female plants are predominantly wind pollinated, but some pollinators are believed to be involved as well (Munro et al., 2014). It then takes *A. americanum* another 1.5 years before the fruit matures, ruptures, and releases its single seed, thereby beginning a new cycle.

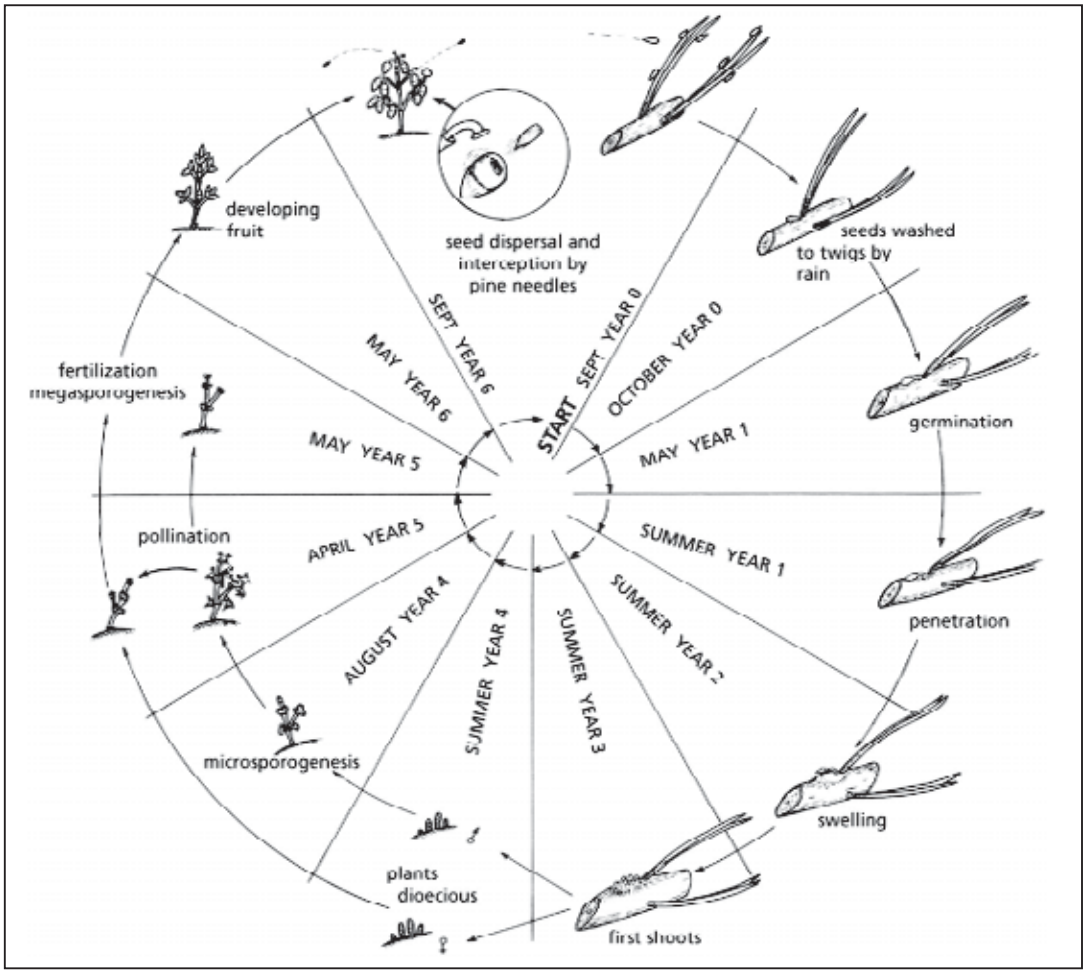

Figure 1.3. Generalized life cycle of *Arceuthobium americanum* (Hawksworth & Wiens, 1972, 1998).

1.1.3 Fruit structure and seed dispersal

The mature fruit of all mistletoes, including dwarf mistletoes, is known as a pseudoberry. These are single-seeded fruits in which the seed is ategmic (lacks

integuments and hence lacks a true seed coat); instead, the embryo and endosperm are surrounded by a tanniferous layer of crushed endocarp cells enveloped by a complex tissue called viscin, which helps the seed adhere to surfaces after seed dispersal (Ross, 2006). Viscin is a unique tissue consisting of two types of cells: viscin and vesicular. Viscin cells are elongated, mucilaginous cells that secrete a pectinaceous mucilage in which uronic acids, xylose, and arabinose are the major sugars (Gedalovich-Shedletzky et al., 1989). Amino acids such as glycine and histidine, as well as the compound ortho-diphenol, are also found in the mucilage. Vesicular cells are isodiametric cells with hydrophobic properties and are found either surrounding or interspersed with the viscin cells, depending on the species.

In the mature *Arceuthobium* fruit, a monolayer of viscin cells surrounds three-quarters of the embryo pole (Figure 1.5), which is in turn enveloped by two to three layers of vesicular cells. The fibrils of the viscin cell walls have a specific helical assembly (Figure 1.6) that is spirally coiled along the long axis of the cell (Ross, 2006). This arrangement is purported to help propel the seed from the fruit during the release of pressure established during the maturation process in which water accumulates. The vesicular cells are also likely involved in the seed dispersal process as parallel with their enlargement, intracellular triacylglycerides (TAGs) mainly composed of 16-carbon and 18-carbon fatty acids, build up. Just before discharge, vesicular cell borders become indistinguishable, generating a lipid mass between the viscin cells and the exocarp (Kelly et al., 2009).

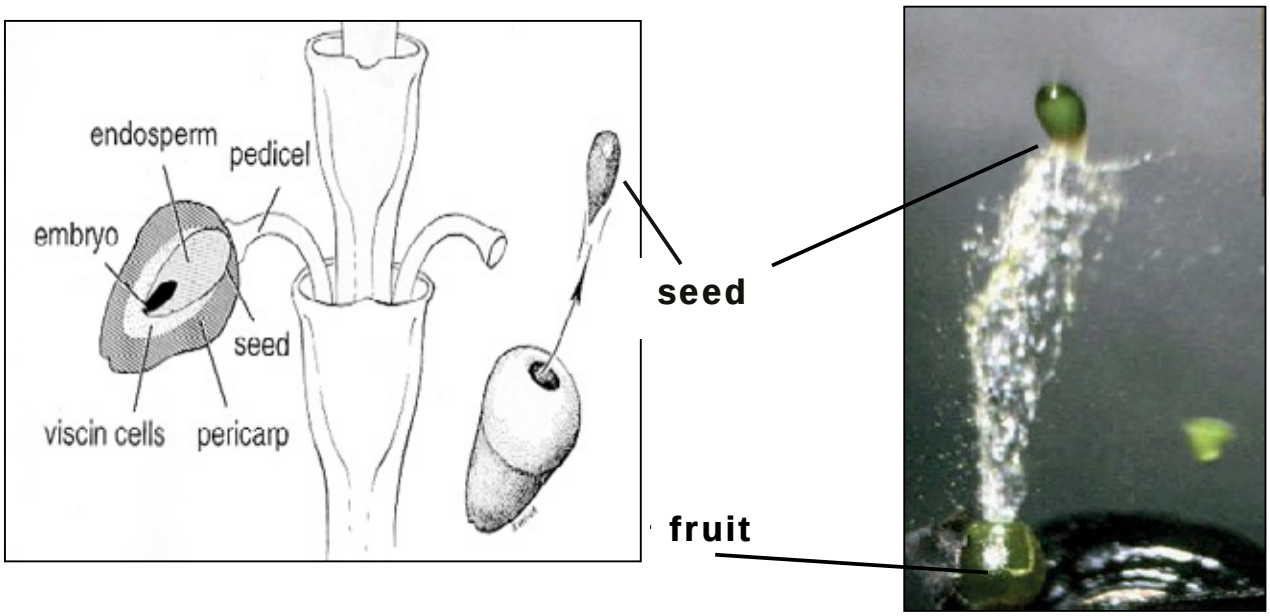

Figure 1.4. Diagrammatic longitudinal section through a mature *Arceuthobium* fruit

(left; adapted from Hawksworth & Wiens, 1998) and fruit discharging its seed (right). Photographs by T. Hinds et al. (1993)

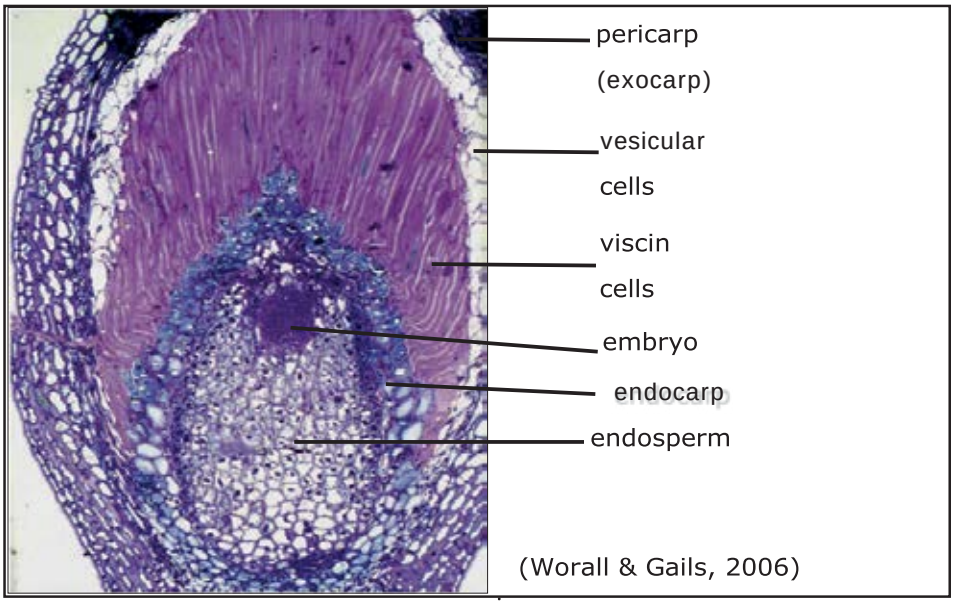

Figure 1.5. Fruit of Arceuthobium americanum as seen in longitudinal sectional view using brightfield microscopy and stained with toluidine blue O (Ross, 2006).

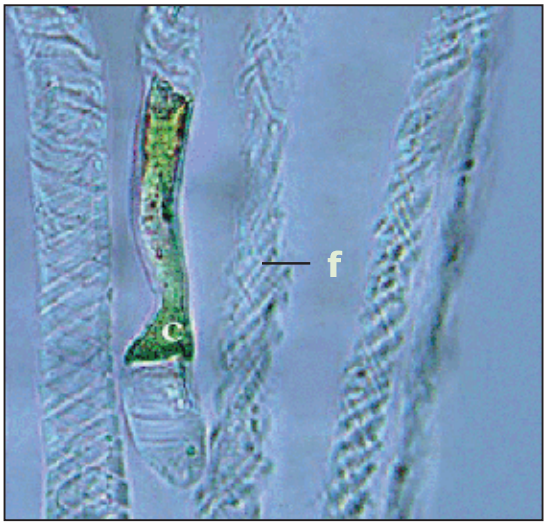

Figure 1.6. Hydrated viscin cells (unstained) with helically arranged (f) fibrils and (c) chloroplast (Ross, 2006).

As water accumulates to form high hydrostatic pressure in the *Arceuthobium* fruit, it is expected that aquaporins (AQP), which are well-known facilitators of membrane water transport in almost all organisms from Archaea to animals, are somehow involved in this unusual means of seed dispersal. Other processes possibly involved in seed dispersal include heat production (thermogenesis; deBruyn et al, 2015), the

lowering of the number of stomata, the thickening of the cuticle on the surface of the fruit (Ziegler & Ross Friedman, 2017b), and the increasing production of lipids and sterols by vesicular cells. The molecular mechanisms of such processes are well worth investigating and will be examined in this thesis as an initial exploration.

1.2 Aquaporins and other proteins potentially involved in the explosive seed dispersal sequence

In view of the fact that a remarkably large amount of water accumulates during fruit and seed maturation, illustrated in part by the great increase in the size of the fruit along with the involvement of hydrostatic pressure, it is intuitive to focus on the transport of water into a fruit and the possible involvement of AQPs. As such, it was decided to focus my investigation into the molecular basis of the explosive seed dispersal process.

1.2.1 Aquaporins

Major-channel proteins called AQPs are homologous to a large superfamily of intrinsic membrane proteins named major intrinsic proteins (MIPs; Kaldenhoff & Fisher, 2006). They are essential for life, highly diversified, and exist in all domains of life: Bacteria, Archea, and Eukarya (Finn & Cerda, 2015). Sequence analysis and functional studies have sorted this superfamily of proteins into two subgroups: AQPs and aquaglyceroporins (GLPs) (Figure 1.7). AQPs are involved mainly in water transport, while GLPs facilitate the transport of glycerol plus water (Uehlein & Kaldenhoff, 2008). Peter Agre et al. (1993) discovered and characterized the first AQPs, finding them in vertebrates. Agre received the 2003 Nobel Prize in Chemistry for this discovery. Then AQPs in plants were identified soon after and found to be more diverse and abundant than their animal counterparts. Such diversity can be attributed not only to plants' sessile lifestyle and their greater need for fine water regulation in response to environmental changes but also to greater compartmentalization of the plant cell in comparison to an animal cell.

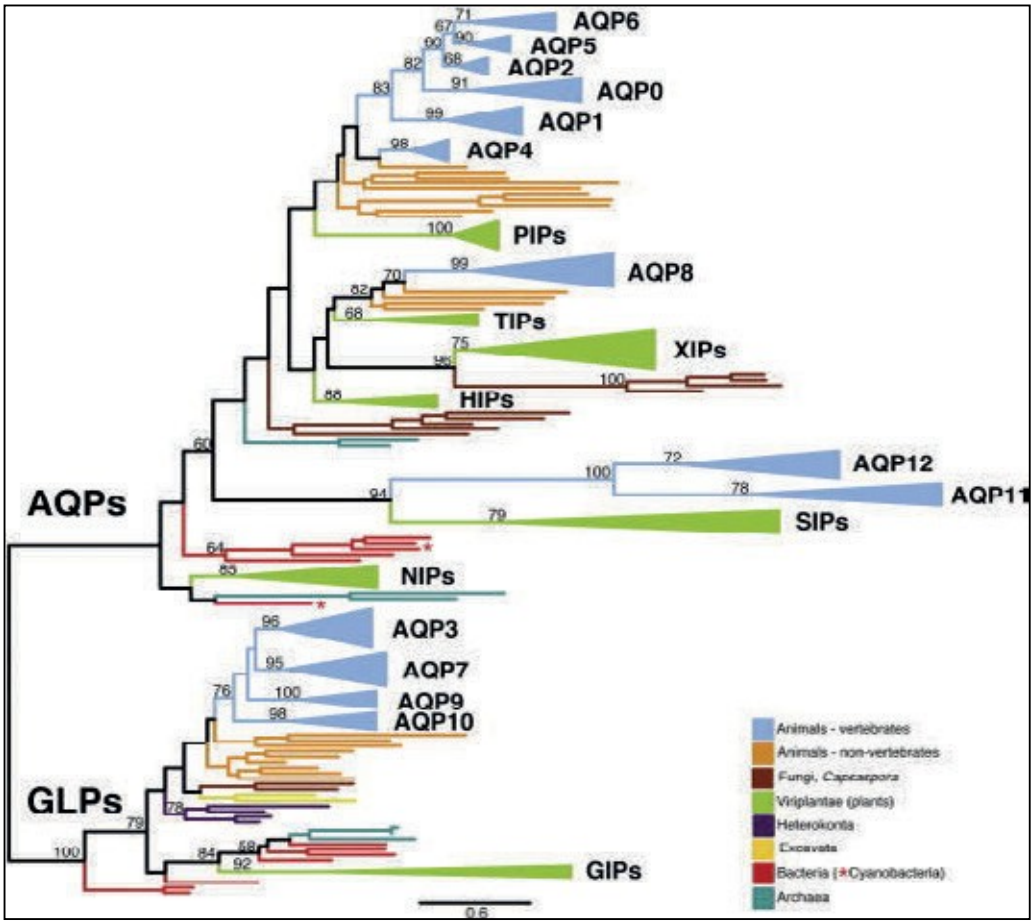

Figure 1.7. Generalized phylogeny of Archaeal, Bacterial, and Eukaryal MIPs. Major subfamilies are shown as collapsed sets of nodes with their branches coloured according to a legend. Aquaporins (AQP), aquaglyceroprotein (GLP), plasma membrane intrinsic proteins (PIPs), tonoplast intrinsic proteins (TIPs), uncategorized intrinsic proteins (XIPs), Nodulin 26-like intrinsic proteins (NIPs), small basic intrinsic proteins (SIPs; Abascal et al., 2014).

When using different gene knock-out techniques, such as antisense, RNAi, virus-induced gene silencing, or T-DNA insertion on AQP genes in plants, and then comparing the resulting plants to control plants, it has been conclusively demonstrated that distinct AQPs contribute to membrane water transport processes in plants (Biela et al., 1999; Siefritz et al., 2002). These AQPs play important roles in root water uptake, cell elongation, plant growth, and plant movement (Kaldenhoff & Eckert, 1999; Kaldenhoff & Fisher, 2006; Kaldenhoff et al., 2007). In addition, AQP-mediated water transport in plants, confirmed in *Xenopus* oocyte- and yeast-functional studies, is important in various physiological processes such as cell elongation, seed germination, and osmoregulation. Some plant AQPs also facilitate the transport of CO_2, and probably many other gaseous substances, across

membranes; although the molecular membrane transport mechanism is not completely understood in these instances. Current data indicate the AQPs involved in gas transport likely function in many other physiological processes, such as photosynthesis, respiration, and growth. It was also found that certain MIPs can be expressed in plant biotrophic interfaces at higher concentrations due to increased water and solute movements between organisms (Opperman et al., 1994; Ikeda et al., 1997; Krajinski et al., 2000; van Dongen et al., 2000). Plant parasitic interfaces involve AQPs either in the process of infection by the parasite or in the function of the interface (Tyerman et al., 2002). When the tomato plant (*Lycopersicon esculentum*) was infected by the higher plant parasite, *Cuscuta reflexa*, an increased expression of *LeAQP2*, a PIP1 family member, was noticed (Werner et al., 2001).

The majority of AQPs have a molecular mass between 26 and 29 kDA, and all consist of 6 transmembrane domains (H1–H6) connected by 5 loops localized on the intra (B, D) and extracytosolic (A, C, E) sides of the cytoplasm (Tani & Fujiyoshi, 2014). Highly conserved NPA (Asn-Pro-Ala) motifs can be found in loops B and E (Figure 1.8 A, B), and the estimated size of AQP molecules is 280 to 300 amino acids long. Three-dimensional structural analyses of AQPs in prokaryotic (Lee et al., 2005; Ringler et al.,1999) and eukaryotic organisms such as mammals and plants (Kukulski et al., 2005) have shown that AQPs form tetramers with a pore (not involved in water transport) in the centre of the tetramer (Figure 1.8C).

The B and E loops of each monomer, carrying an NPA motif, fold as half membrane-spanning hydrophobic α-helices and submerge into the membrane from opposite sides; and together with membrane-spanning helices, form a pore with high specificity that primarily results from two filter regions. The first one is created by the Asp-Pro-Ala motifs of loops B and E that meet at the centre of the channel and represents a first size exclusion zone. The second filter region, aromatic/Arg (ar/R), is made of two amino-acid groups from helices B (HB) and E (HE) and two groups from loop E (LE1, LE2), from the two sides of the NPA motif, and contributes to a size exclusion barrier and the hydrogen bond environment for the substrate transport (Murata et al., 2000). Some studies indicate that the larger, central fifth pore, found between all four monomers, could be involved in the transport of ions such as Na^+, K^+, Cs^+, and tetramethylammonium (Yool & Weinstein, 2002; Kruse et al., 2006).

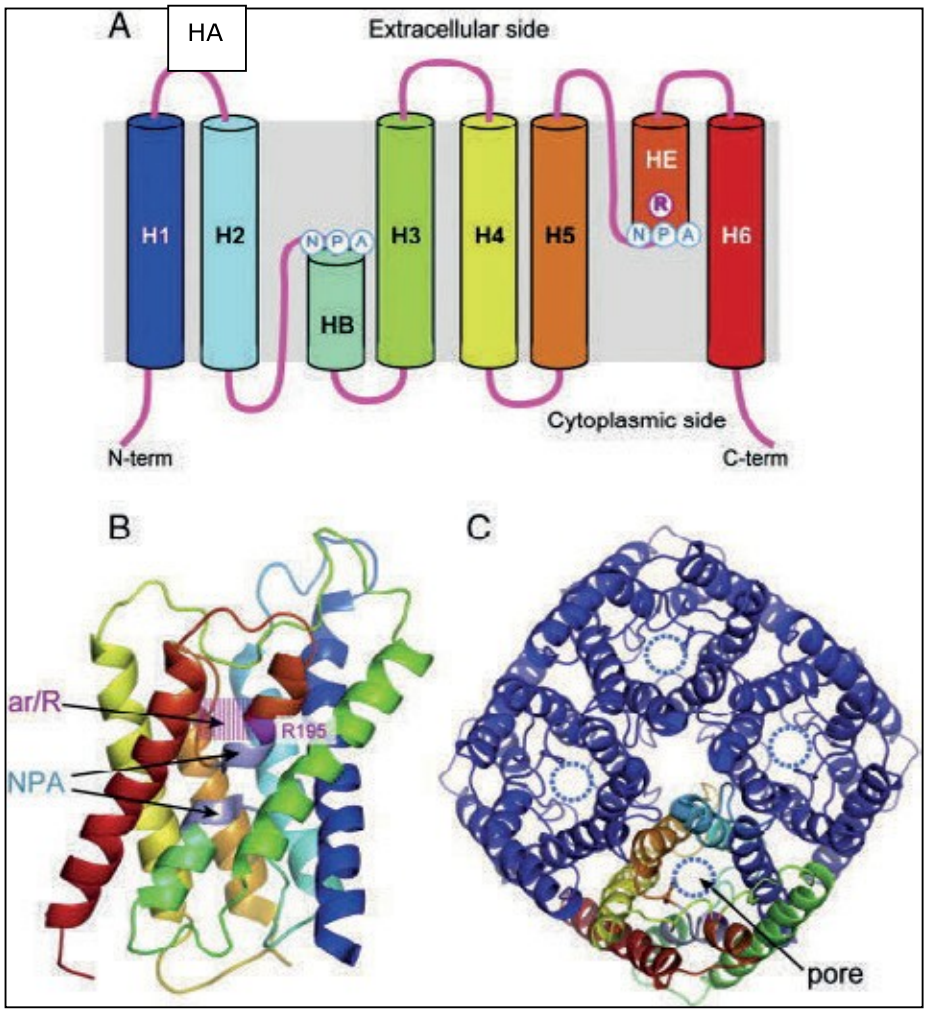

Figure 1.8. (A) Aquaporin model showing the six transmembrane domains (helices; H1 to H6) and two short-pore helices named HB and HE with two NPA motifs in each monomer; (B) Ribbon structure of a single AQP monomer with different colours showing different helices from blue (n-terminal) to red (c-terminal); (C) Crystal stucture of the tetramer consisting of four monomers (adapted from Tani & Fujiyoshi, 2014) .

Compared to other organisms, as mentioned before, plants appear to have a remarkably large number of MIP genes. For example, there are 35 full-length AQP genes in the *Arabidopsis* genome belonging to four different subfamilies: (1) plasma membrane intrinsic proteins (PIPs) having five PIP1 isoforms (PIP1;1 – PIP1;5) and eight PIP2 isoforms (PIP2;1 – PIP2;8), (2) tonoplast intrinsic proteins (TIPs), (3) Nodulin 26-like intrinsic proteins (NIPs), and (4) small and basic intrinsic proteins (SIPs; Figure 1.9; Johanson et al., 2001; Kruse et al., 2006) and uncategorized (X) intrinsic proteins (XIPs) found in *Populus trichocarpa.*

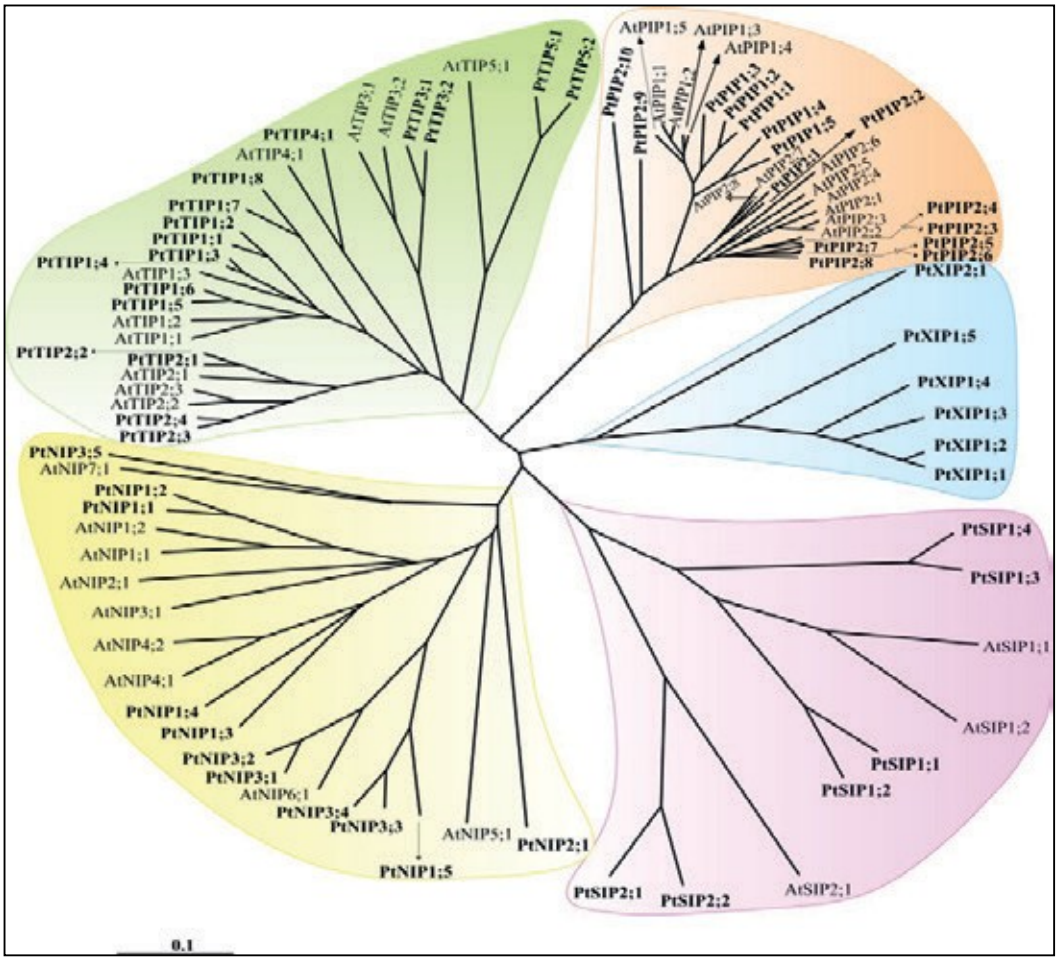

Figure 1.9 Evolutionary relationship of all *Populus trichocarpa* MIPs shown along with MIPs from *Arabidopsis thaliana*. *Populus* MIP subfamilies PtPIPs, PtTIPs, PtNIPs, and PtSIPs are clustered with the corresponding *Arabidopsis* MIP subfamilies. XIPs observed only in *Populus* make a separate group (Gupta & Sankararamakrishnan, 2009, modified).

1.2.2 PIPs expression and regulation within the plant cell

Within the plant cell, MIP gene expression is regulated developmentally in a cell-specific manner via hormones and environmental conditions such as water stress, infection, low temperature, and salinity (Kaldenhoff & Fischer, 2006; Figure 1.10). When PIP genes are transcribed, their mRNA is translated in the rough endoplasmic reticulum (ER), and the proteins are targeted to the plasma membrane. Those PIPs belonging to the PIP2 group form homo- or heterooligomers by associating with PIP1 isoforms. PIP oligomers are transported through the Golgi apparatus and trans-Golgi network (TGN) and are then packed into secretory vesicles and sent to the plasma membrane. Incorporation of PIPs into the plasma membrane is facilitated by the syntaxin SYP121 (vesicle trafficking protein). Then PIPs are recycled with help of the

TGN before being directed back to the plasma membrane or into lytic vacuoles for degradation. Environmental conditions can cause dephosphorylation and internalization of PIPs (salt stress) as well as ubiquitylation of PIPs (drought stress), which are then degraded in the proteasome. The water channel activity or gating of PIPs is regulated by heteromerization, phosphorylation, interaction with SYP121, protonation, pressure gradient, and Ca^{2+} concentration (Kaldenhoff, 2006; Chaumont & Tyerman, 2014).

However, a general expression pattern of MIP genes cannot be distinguished, because the different isoforms being either up- or down-regulated depend on the stimulus and/or the organ studied (Kaldenhoff & Fischer, 2006). The absence of a unique expression pattern represents an important tuning mechanism by which the plant is able to adapt to unfavourable conditions. For instance, in response to water deprivation, most PIPs in *Arabidopsis* leaves are transcriptionally down-regulated; however, the expression of PIP1;4 and PIP2;5 is induced and mRNA levels of PIP2;6 remain constant.

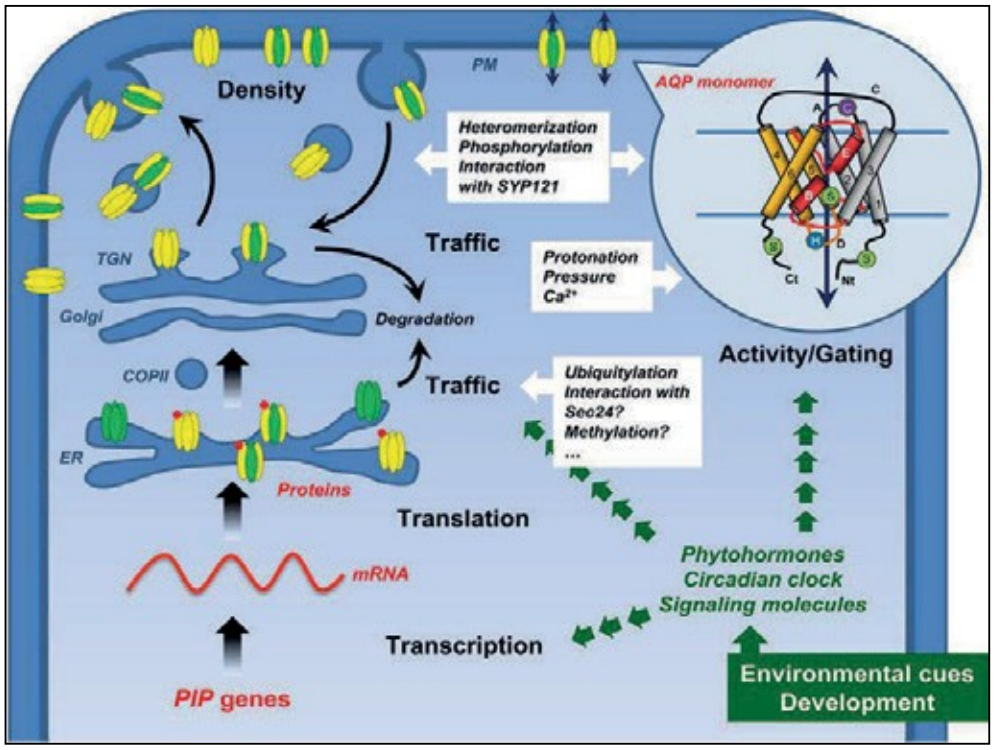

Figure 1.10. Regulation of plasma membrane intrinsic proteins (PIPs) in a cell: endoplasmic reticulum (ER), plasma membrane (PM), PIP2 group (yellow), PIP1 isoforms (green), PIP2s containing a diacidic motif (red circle), coat protein complex II (COPII) of the vesicles, trans-Golgi network (TGN), the syntaxin SYP121 protein. The insert shows the topological structure of an aquaporin monomer (Murata et al., 2000), which consists of six membrane-spanning α-helices (1–6) connected by five loops (A–E) and N and C termini facing the cytosol. Phosphorylated Ser residues are in green circles (the putative phosphorylated Ser in loop D is not indicated), the protonated Histidine (His) of loop D is in the blue circle, and the Cys residue of loop A involved in disulfide bound formation between monomers is in the purple circle (adapted from Chaumont & Tyerman, 2014).

1.3. Supporting evidence

Some studies support the idea that AQPs may be involved in explosive discharge, or at least may be relevant to water relations in dwarf mistletoes. Pollen dispersal in tobacco, *Nicotiana tabacum,* depends on the correct timing of anther dehiscence, and PIP2 AQPs are necessary for this process (Bots et al., 2005). Similarly, research done by Ross Friedman et al. (2010) showed that an antibody raised against the *N. tabacum* PIP2 AQP in combination with a gold-tagged secondary antibody labelled the viscin cell membranes of *A. americanum* fruit at various developmental stages. The validity of the immunolabeling was supported by Western blot analysis, showing a strong signal at about 30 kDa, which is the expected size of a PIP2.

The rapid movement of water correlated with a higher expression of AQPs was demonstrated in studies that examined both the instantaneous and diurnal movements of leaves in *Mimosa pudica* and *Samanea saman*, whose leaves possess a special motor organ called a pulvinus (nyctinastic movement), and also epinastic movement in tobacco (no motor organ). Specifically, seismonastic leaf movement of *Mimosa pudica* plants is associated with high water movement across the cell membranes. Most recently, it was shown that MpPIP1;1 and MpPIP2;2 genes are expressed in seedlings of *Mimosa pudica*; expressing MpPIP2 increases the water permeability as much as 20 times when MpPIP1;1 is coexpressed (Uehlein & Kaldenhoff, 2008). Similarly, a study by Moshelion et al. (2002) showed that SsAQP2, which belongs to the PIP2 family, is linked to the physiological function of diurnal and circadian cell volume changes governing leaf movements in *Samanea saman.* In the case of epinastic movement in tobacco plants, the higher expression of NtAQP1 was regulated diurnally, with the highest concentration of AQP1 observed during the morning hours when increased cellular permeability to water was necessary to change the shape of the leaf (Otto & Kaldenhoff, 2000; Siefritz et al., 2004; Uehlein & Kaldenhoff, 2008).

Additionally, as Hawksworth (1959) and Hinds and Hawksworth (1965) first noticed, the seed discharge from a fruit can be induced by gently heating the fruits in a laboratory setting. This observation led to research done by Ross et al. (2013) to determine if alternative oxidase (AOX) protein, associated with thermogenesis in plants (endogenous heat production; Umekawa et al., 2016)) , could be localized in situ, within *A. americanum* fruit. Thefruit was probed with an anti-AOX antibody/gold- labelled secondary antibody. The immunochemical results were then evaluated by Western blotting. When performed on a whole fruit and mitochondrial proteins, the Western blots revealed a signal at 30–36 kDa, suggestive of AOX, while blots of whole fruit (but not mitochondrial fraction) proteins showed a second band at 40–45 kDa, which was in agreement with the size of another protein: plastid terminal oxidases (PTOXs). The results indicated that the anti-AOX antibody was also labelling PTOX in plastids. Moreover, the plastid labelling only became evident in fruit collected in the final weeks of fruit collection (August), suggesting that PTOX units become more numerous as the fruit matures. These results led to follow-up research completed by deBruyn et al. (2015), which suggested that thermogenesis may indeed play a role in the process of seed dispersal, possibly involving oxidases from plastids and/or mitochondria.

Expanding on that research, in a study of maturing fruit, Ziegler and Ross Friedman (2017b) determined than an increase in the thickness of the waxy cuticle as well as a

reduction in the number of stomata per unit fruit surface is correlated with the process of fruit development and may be involved in the process of seed dispersal via the retention of water within the fruit.

Due to the importance of AQPs in the facilitation of plant water movement and the resemblance of the seed dispersal process in dwarf mistletoe to pollen dispersal in tobacco, AQPs, specifically PIPs (most likely of the PIP2 class), may be involved in establishing the high hydrostatic pressure necessary for dwarf mistletoe seed dispersal. Furthermore, research showing anatomical changes such as enlarging fruit, cuticle thickening, and declining stomata number (density) should be supported by molecular investigations to reveal which genes are involved and how they are expressed.

1.4 Project goals

As previously outlined, the destruction of commercially valuable coniferous trees by North American species of dwarf mistletoes, most notably by *A. americanum*, is a substantial problem in western Canada. Parasitism by these species reduces the lifespan of an infected tree by up to 50% and renders living trees more susceptible to fire and colonization by mountain pine beetles. Therefore, increasing our knowledge of how dwarf mistletoe is dispersed may help foresters develop better methods of controlling the parasite. In this context, finding parasitic genes and the genes involved in explosive seed dispersal would be paramount in developing new strategies to control not only mistletoes, but also other parasitic plants.

The primary aim of this research was to gain insights into the potential involvement of AQPs and other proteins in establishing high hydrostatic pressure within the *Arceuthobium* spp. fruit required for forcible seed discharge and the infection of other hosts. To date, very little molecular data is available for *Arceuthobium* spp. regarding gene sequences and gene expression, so heterologous microarray hybridization was used along with other molecular, biochemical, and physiological approaches to understand PIPs and other genes and their expression in seed dispersal and parasitism.

2. MATERIALS AND METHODS

2.1 Antibiotics and restriction enzymes

2.1.1 Antibiotics

Antibiotics are used extensively in molecular biology. Apart from preventing contamination, several antibiotics can also function as selection agents, used to select and establish transfected/genetically modified cells for research purposes (Table 2.1).

Table 2.1 *Antibiotic stock and working solutions*

Antibiotics	Stock solution (mg/ml) *	Working concentration (µg/ml)
Ampicillin (Roche; Mannheim, Germany)	100 (in water)	100
Gentamicin (Roche; Mannheim, Germany)	50 (in water)	25
Kanamycin (Sigma; Deisenhofen, Germany)	50 (in water)	100

*Stock solutions were stored at -20°C.

2.1.2 Restriction enzymes and modifying enzymes

The restriction enzymes and their buffers were obtained from MBI Fermentas Inc. Life Sciences (ThermoFisher Scientific; St. Leon-Rot, Germany) or New England BioLabs® Ltd. (Frankfurt, Germany). All the modifying enzymes such as T4 DNA ligase, DNase, RNase A and H, T4 DNA polymerase, Superscript II reverse transcriptase, RNase H, Taq DNA polymerase, etc., were purchased from QBiogene (MP Biomedicals, LLC), MBI Fermentas, Stratagene (Agilent Technologies), Roche, Sigma-Aldrich®, Gibco-BRL™ (ThermoFisher Scientific), Amersham Pharmacia Biotech Ltd., and Promega Corporation. Gateway cloning enzymes were purchased from Invitrogen™ (ThermoFisher Scientific; Karlsruhe, Germany).

2.2 Sample analysis

2.2.1 Plant material

2.2.1.1 Samples collection and storage of *Arceuthobium americanum* and *Arceuthobium oxycedri* plants

Arceuthobium americanum female plants were collected near Stake Lake, British Columbia, Canada (coordinates via Google map are 50.506141, -120.486170 at 1,400 m elevation), from infected lodgepole pines during an April-September time frame between 2009 and 2015. Additionally, *A. oxycedri* female plants were collected from infected *Juniperus* spp. in Darmstadt Botanical Garden, Germany.

Twice per week, infected branches from each plant type were clipped and placed in water until they arrived at the laboratory. Dwarf mistletoe samples were then removed from the branches and immediately frozen in liquid nitrogen (LN2), ground (section 2.2.1.2), or placed in autoclaved tinfoil and kept in a -80°C freezer or immersed in RNA*Later* solution for later use.

2.2.1.2 Grinding

The sample was pulverized to enable extraction of RNA. To remove any RNAses that may exist in a sample, the grinding equipment (mortar, pestle, forceps, and tweezers) was autoclaved at 15 psi for 20 min and rinsed with 0.1% diethyl pyrocarbonate (DEPC) treated water before use. Just before the samples were ground, all equipment was chilled with LN2. Fresh samples or samples stored previously in the -80°C freezer were immediately placed in LN2. In the mortar, fruits were separated from the stems easily due to the brittle nature of an LN2-frozen plant. After all stems and fruit were separated, the frozen fruit (10-15 each) and stems were thoroughly ground to a fine powder with a pestle. To keep samples constantly frozen, additional LN2 was periodically added to replace any evaporated LN2 in the mortar. Then the resulting powder was placed in LN2-frozen Eppendorf tubes (around 100 mg) to allow the LN2 to evaporate (20 s). Any remaining frozen samples were kept in an Innova ™ Ultra-low Temperature Freezer (New Brunswick Scientific) at -80°C or used right away for RNA extraction.

To improve the grinding process, modifications were incorporated such as adding sterilized sand during the first stage of grinding.

2.2.2 Isolating totalRNA

To extract all RNA for further testing, the ground material was subjected to many methods commonly used to extract RNA from plants. Dwarf mistletoe fruit contains high levels of polyphenols and polysaccharides that co-precipitate or bind to RNA, so it was extremely difficult to obtain a good quality sample of RNA from the dwarf mistletoe. Many different traditionally and commercially available extraction methods were tested with and without modifications.

2.2.2.1 Lithium chloride method

Approximately 300 mg of tissue was pulverized under LN2, placed in a 2 ml Eppendorf vessel with a 0.8 ml lysis buffe (see below), and quickly thawed under warm, running water. The tissue was then well vortexed, mixed with 0.8 ml of PCI, shaken for at least 30 min (max. 1 h) at room temperature, and then centrifuged for 15 min at 13,000 rpm at room temperature (table centrifuge, approx. 10,000 × g).

Afterwards, the supernatant was removed (approx. 600-800 µl) and mixed with 0.8 ml of PCI, shaken for at least 30 min (max. 1 h) at room temperature, and centrifuged for 15 min at 13,000 rpm at room temperature.

Approximately 300-500 µl of supernatant was transferred to a new Eppendorf tube, and the nucleic acids were precipitated with 0.75 vol. 8 M LiCl for 1 h at 4°C. The sample was then centrifuged for 15 min at 13,000 rpm at 4°C. After removing all the supernatant, the obtained pellet was washed twice with 700 µl of 70% EtOH (-20°C) using centrifugation (table centrifuge, approx. 10,000 × g) for 5 min at 13,000 rpm at 4°C after each wash.

Finally, after all supernatant was removed and the pellet was thoroughly washed, it was air dried and dissolved in 300 µl DEPC-DH_2O. After adding 30 µl NaAc (10%) and 750 µl cold EtOH (100%; 2.5 × vol), the sample was left overnight at -20°C. The next day, the sample was centrifuged for 15 min at 13,000 rpm at 4°C, and the pellet was washed with EtOH, centrifuged, and dried (10 min on ice), repeating as above. To finish, the pellet was dissolved in 50 µl of DEPC-DH_2O (heated to 60°C). All aqueous solutions were treated with DEPC (0.1%) for 1 min, left to rest for 1 hr, and then autoclaved.

Lysis buffer

- 0.6 M NaCl
- 0.1M Tris/HCl, pH 8
- 0.2M Ethylenediaminetetraacetic acid (EDTA)
- 4% Sodium dodecyl sulphate (SDS)
- PCI (no DEPC) phenol: chloroform: isoamyl alcohol = 25:24:1
- 8 M LiCl
- 3 M NaAc or Kac, pH 5
- dH2O
- 70% EtOH, 100 ml: 70 ml 96% EtOH + 30 ml autoclaved DEPC-dH2O
- 96% EtOH (no DEPC)

2.2.2.2 QIAGEN RNeasy Plant Mini Kit (QIAGEN)

To isolate total RNA, the RNeasy Plant Mini Kit was used. Frozen plant powder (section 2.2.1.2) (100 mg) was weighed, and then RNA was extracted according to the manufacturer's protocol.

2.2.2.3 RNeasy Plant Mini Kit (QIAGEN) with modifications

To enhance RNA extraction efficiency, the following modifications were used:

High molecular weight polyethylene glycol HMW-PEG (1-4% w/v) was added to extraction buffers.

Two extraction buffers were used: RLC-extraction buffer (guanidinium hydrochloride buffer) and RLT-extraction buffer (guanidinium isothiocyanate buffer).

Various extraction incubation times were used (5-10 min).

Various washing steps were used.

2.2.2.4 Iandolino Protocol

For each gram of fresh weight tissue, 6.5-8.5 ml of extraction buffer was used. During preparation, the extraction buffer was heated up to 65°C for at least 20-30 min, and 2% 3-mercaptoethanol was added just before the grinding. Samples were ground to a fine powder in LN2 with a pestle and mortar. Then the frozen powdered tissue was added to a 50 ml Falcon™ tube containing the extraction buffer and shaken and vortexed vigorously (Iandolino et al., 2004).

After 30 min of incubation at 65°C, the samples were centrifuged at 5,000 × g for 10 min at 4°C with a swinging-bucket centrifuge. Then the supernatant was poured through a Miracloth filter directly into a 50 ml Teflon® FEP Oak Ridge tube, and the tube was kept on ice and centrifuged at 13,000 × g for 10 min at 4°C to remove any trace of plant material in suspension. In the meantime, equal volumes (12 ml) of the supernatant and chloroform isoamyl alcohol (24:1) solution was combined in a 30 ml Teflon® FEP tube, mixed gently for 1 min by inverting the tube, and centrifuged at 13,000 × g at 4°C for 5 min. The supernatant was then pipetted into a new pair of 30 ml Teflon® FEP tubes, and an equal volume of chloroform isoamyl alcohol (24:1) was added to it, mixed gently, and centrifuged at 13,000 × g for 5 min at 4°C (Iandolino et al., 2004).

The supernatants were combined into one 50 ml Teflon® FEP Oak Ridge tube, and ¼ vol of 10 M LiCl to supernatant was added to it, mixed gently, and precipitated overnight at 4°C. The next day, the sample was centrifuged at 13,000 × g for 30 min at 4°C. Following that, the supernatant was decanted by pipetting without disturbing the pellet. The pellet was washed once with 1 ml of 70% ethanol and centrifuged again at 13,000 × g at 4°C for 5 min. This step was repeated if the pellet did not look white or clear. After the residue was removed, the ethanol pellet was again immediately suspended in an adequate volume of double-distilled DEPC-treated water. The sample was kept on ice and clean-up protocol was initiated immediately as indicated by the manufacturer (e.g., QIAGEN RNeasy Plant Mini Kit protocol). After

final clean up, the RNA was ready for use or storage at -80°C for up to 1 year (Iandolino et al., 2004).

2.2.2.5 MasterPure™ Plant RNA Purification Kit, Epicentre®

This kit uses an optimized plant tissue and cell lysis solution to neutralize and eliminate polyphenols and polysaccharides and to inactivate ribonucleases. As a result, nucleic acids are released from a plant, and precipitation and a rapid desalting process occurs that removes contaminating macromolecules. The MasterPure™-purified RNA can be used in many applications including amplification, hybridization, RNase protection, and RT-PCR.

In the first step, 100 mg of frozen dwarf mistletoe powder was weighed and RNA was extracted according to the manufacturer's protocol. The procedure consisted of three main steps: 1) lysis of tissue sample, 2) precipitation of nucleic acids, and 3) removal of contaminating DNA from RNA preparation. The extraction procedure was performed using the chemicals listed in Table 2.2.

Table 2.2 *MasterPure™ kit chemicals*

Ingredients
2X tissue and cell lysis solution (plant tissue and lysis solution)
MPC protein precipitation reagent
RNase-free water
RNase-free DNase I @ 1 U/µl
proteinase K @ 50 µg/µl
RiboGuard™RNase inhibitor @ 40 U/µl
100 mM Dithiothreito (DTT)
10X DNase Buffer

2.2.3 RNA analysis

2.2.3.1 RNA quantification

2.2.3.1.1 Standard spectrophotometry

From the isolated RNA, a 100 µL sample of a 1:50 dilution was prepared and the concentration of RNA was determined by measuring absorbance at 260 nm (nucleic acids), 280 nm (proteins), and 230 nm (polyphenols and polysaccharides) using a spectrophotometer (Biochrom Biowave WPA S2100). In addition, the ratios of A260/280 and of A260/230 were recorded. The ratios allow estimation of the purity of total DNA or RNA with respect to contaminants (proteins or polyphenols/polysaccharides, respectively).

2.2.3.1.2 NanoDrop™ spectrophotometry

RNA sample concentration and quality for the Affymetrix microarray study was performed using NanoDrop™ 2000 (PEQLAB GmbH, Germany). To zero the

spectrophotometer, 10 mM Tris/HCl pH 7.5 was used. A260/A280 and A260/A230 were calculated. The A260/A80 ratio for isolated DNA (RNA) was about 1.8 (2.0), indicating high quality DNA (RNA).

2.2.3.1.3 Fluorometric method

A Qubit® 2.0 fluorometer (Invitrogen™) was used to determine RNA quantity. The fluorometer uses fluorescent dyes that bind to nucleic acids to calculate the concentration of nucleic acids and proteins in a sample. These dyes have exceptionally low fluorescence until they bind to their targets (DNA, RNA, or protein). Upon binding, they become intensely fluorescent. The measurements were performed according to the manufacturer's protocol.

2.2.3.2 RNA integrity assessment

To assess the integrity and size distribution of extracted RNA, standard spectrophotometry (section 2.2.3.1.1), NanoDrop™ spectrophotometry (section 2.2.3.1.2), and electrophoresis techniques were used.

2.2.3.2.1 Electrophoresis

2.2.3.2.1.1 Native gel to evaluate DNA quality

A solution of 0.8% to 1.0% (w/v) agarose (Invitrogen™) in 1X TAE buffer (Sigma-Aldrich) was prepared by heating the solution in a microwave oven to the boiling point and stirring it until all of the agarose was dissolved. The solution was allowed to cool to about 50°C, and then either ethidium bromide (Sigma-Aldrich, St. Louis, MO) or GelRed® (Biotium) was added to a final concentration of 0.05 µg/µL. Gels were cast by pouring the solution into a casting frame with a comb inserted. The gel was allowed to solidify (30 min), then the casting frame was placed into the electrophoresis chamber filled with 1X TAE running buffer until the top of the gel was covered with a thin film of liquid. DNA samples were applied to the gel in a mixture with 5X DNA loading buffer (Orange G and Ficoll). To evaluate fragment size and the quantity of nucleic acids, a size marker (HyperLadder I, Bioline; Figure 2.1 A) was included in each gel run. Gels were run at a voltage of 10 V/cm. After separation was sufficient, the gels were photographed under UV lighting in a gel documentation chamber (LTF Labortechnik).

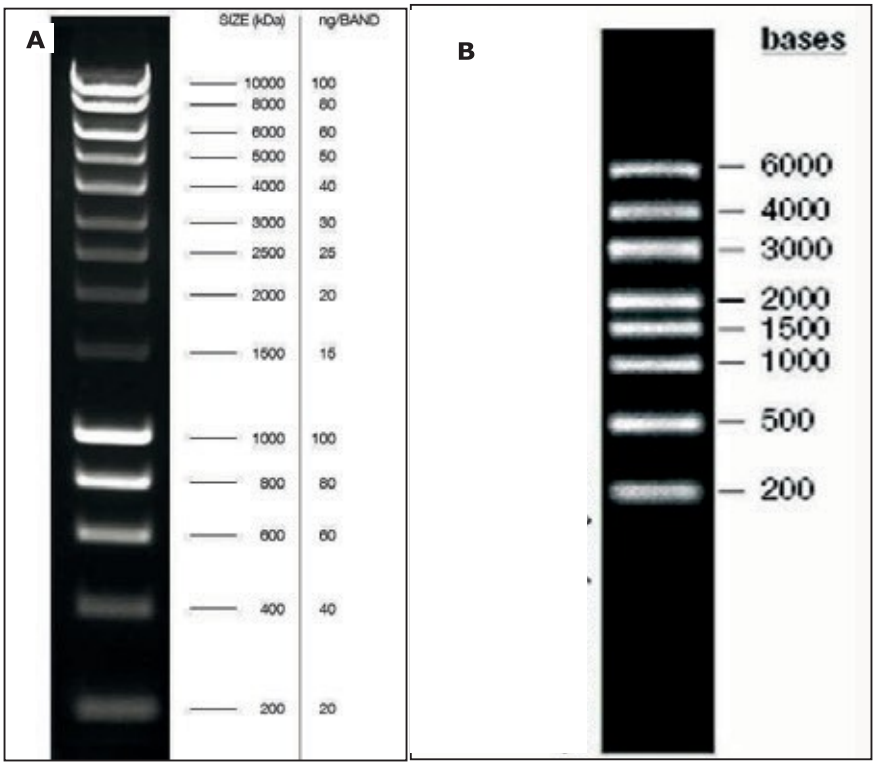

Figure 2.1 (A) HyperLadder I DNA marker (5 µl, applied to a 1% agarose gel). Image by Bioline. (B) RiboRuler™ High Range RNA Ladder (2 µl, applied to a 1% formaldehyde agarose). Image by Thermo Scientific.

2.2.3.2.1.2 Denaturing gel to evaluate RNA quality

2.2.3.2.1.2.1 Formaldehyde gel

Due to the tendency of single stranded RNA to bind to itself or other RNA molecules, a 1% denaturing gel was prepared to ensure the molecules remain single-stranded (Table 2.3). Then, 10 µg of the total RNA was mixed with a volume of the RNA gel loading buffer (Table 2.3) and placed in a 65°C water bath for 10 min. Subsequently, the sample was placed on ice for a period of 2 min. Afterwards, a 1% denaturing 1X MEN agarose formaldehyde gel was loaded with the prepared RNA samples and they were electrophoretically separated at a current voltage of 80 V. Then, the quality of RNA under UV light (ImageMaster VDS, Pharmacia Biotech) or Bio-Rad Gel Doc 2000 (Bio-Rad, Munich, Germany) was assessed. To evaluate fragment size and quantity of RNA, a size marker (RiboRuler™ High Range RNA Ladder; Figure 2.1 B) was used.

Table 2.3 *Solutions used for formaldehyde gel*

Solution	Concentration	Ingredients
10x MEN buffer	200 mM	MOPS*
	10 mM	EDTA**, pH 8.0
	50 mM	sodium acetate
RNA gel loading buffer	0.72 ml	formamide
	0.16 ml	10x MEN
	0.26 ml	37% formaldehyde
	0.18 ml bidest	water
	0.10 ml	80% glycerol
	0.08 ml	2% bromophenol
	3 µl	1% ethidium bromide
MEN agarose gel (35 mL)	0.35g	agarose in the microwave
	3.5 ml	10X MEN and 50°C
	30 ml bidest	water (cooling down)
	2.7 ml	37% formaldehyde

*MOPS - morpholinopropane sulphuric acid
**EDTA - Ethylenediaminetetraacetic acid

2.2.3.2.1.2.2 Bleach gel

As formaldehyde gel is time consuming to prepare and calls for the use of toxic ingredients (formaldehyde), another approach was used to analyze RNA quality. Commercial bleach (Sodium Hypochlorite) was added to a native gel before the gel was loaded with the RNA samples. In the presence of low concentrations of bleach, the secondary structure of RNA was denatured and potentially contaminating RNases were also destroyed (Aranda et al., 2012). Similarly to Aranda et al. (2012), 250 µl of 6% commercial bleach was added to 50 ml of agarose 1% gel.

Bleach gel preparation protocol is listed below:

- 1.0% w/v agarose was added to 1X TAE buffer (e.g., 0.5 g in 50 ml).
- 1.0% v/v (Clorox® bleach) was added to the above and incubated at room temperature for 5 min, swirling occasionally.
- The suspension was heated to melt the agarose.
- The solution was allowed to cool before adding ethidium bromide to a final concentration of approximately 0.5 µg/ml.
- The solution was poured into a gel mold and allowed to solidify into a bleach gel.

Then RNA samples were loaded and run as follows:

- The RNA sample mixed with 10X DNA loading buffer (1.9 mM xylene cyanol, 1.5 mM bromophenol blue, 1.5% Ficoll in sterile dH20; Sigma- Aldrich, St. Louis, MO; Aranda et al., 2013) to a final concentration of 1X was loaded. Then the DNA ladder was also loaded.
- Electrophorese gel in 1X TAE buffer was run at 100 V for approximately 35 min before it was visualized by UV transillumination.

2.2.4 Microbiological methods

2.2.4.1 Escherichia coli

2.2.4.1.1 Cultivation of Escherichia coli

Cultivation of *Escherichia coli* (*E. coli*) was performed using strain DH5alpha (genotype: F- endA1 glnV44 thi-1 recA1 relA1 gyrA96 deoR nupG Φ80dlacZΔM15 Δ(lacZYA-argF)U169, hsdR17(rK- mK+), λ–). Liquid cultures were inoculated with either a colony taken from a Luria-Bertani (LB) (see below) agar plate or with an aliquot of frozen cell suspension from cryostocks using a sterile pipette tip. For overnight cultivation, 3 ml of selective LB medium in standard test tubes was used. Inoculated test tubes were then placed at a slanted angle on a shaker set to 225 rpm. The temperature was set to 37°C by placing the shaker under a temperature-regulating hood.

LB (Luria-Bertani) medium*

- yeast extract
- peptone
- NaCl
- ampicilin**

*pH equilibrated at 7.5 with NaOH sterilized by autoclaving, and stored at room temperature
**antibiotic for selection added just before use

2.2.4.1.2 Preparation of competent cells

To create chemically competent cells for transformation, a protocol developed by Inoue et al. (1990) was used. An overnight *E. coli* starter culture of 3 ml (DH5 without plasmids) was utilized to inoculate 250 ml of a super optimised broth (SOB) medium (See list below) at an OD600 of 0.1. Cultivation was performed under standard conditions, described above, until OD600 of 0.6. At this point, the culture was placed on ice for 10 min, and then cells were harvested by spinning them in a centrifuge for 10 min at 2,500 × g at 4°C. The pellet of cells was then suspended in 80 ml of ice-chilled Tris-Borate (TB; see list below) buffer and incubated for 10 min.

The cells were harvested as before and again suspended in 20 ml of TB buffer. At thispoint, dimethyl sulfoxide (DMSO) was added to a final concentration of 7%. The suspension was incubated on ice for 10 min. and then divided into 200 µL aliquots in microcentrifuge tubes and flash-frozen in LN2. The aliquots were stored at -80°C until use.

SOB Medium*

- yeast extract 0.5% (w/v)
- peptone 2% (w/v)
- NaCl 10 mM
- KCl 2.5 mM
- $MgCl_2$ 10 mM
- $MgSO_4$ 10 mM

*sterilized by autoclaving stored at room temperature

TB Buffer*

- hepes 10 mM
- $CaCl_2$ 15 mM
- KCl 250 mM
- $MnCl_2$ 55 mM

*pH equilibrated at 6.7 with KOH sterilized by filtration stored at 4 °C

2.2.4.1.3 Transformation of competent cells

Aliquots of chemically competent *E. coli* (as described before) were thawed on ice. A total of 50 µL of the competent cells were used per transformation. To each preparation, 1 µL of plasmid DNA was added and gently dispersed among the cells. The mixtures were incubated on ice for 30 min before being subjected to heat shock at 42°C for 45 s. The cells were briefly cooled on ice, and then 250 µL of SOB with catabolite repression (SOC) medium (SOB medium with glucose) was added to each tube. The cells were then incubated for 1 h at 37°C in a shaker, with the tubes fixed horizontally to the shaking surface. After the incubation, cells were harvested by centrifugation (4,000 rpm, room temperature, 5 min). After 220 µL of the supernatant was discarded, the cells were again suspended in the remaining medium (about 80 µL). The concentrated cell suspensions were then spread on selective LB plates. To obtain single colonies, plates were incubated overnight at 37°C. The following day, single colonies were picked and used to inoculate liquid cultures as described in section 2.2.4.1.1.

2.2.4.1.4 Creating Escherichia coli cryostocks

For long-term storage of *E. coli* clones, deep-frozen cryostocks were prepared. First, 370 µL of overnight culture (as described) were mixed with 130 µL of 86% (v/v) glycerol and immediately flash frozen by immersion in LN2. The stocks were then stored at -80°C until further use.

2.2.4.1.5 Plasmid extraction

To isolate plasmid DNA from *E. coli* clones, 1.5 ml of an overnight culture in selective LB medium was harvested by centrifugation (13,000 rpm, 30 s). The supernatant was discarded, and the cells were again suspended in 300 µL of ice-chilled buffer P1 (resuspension buffer). To lyse cells, 300 µL of buffer P2 (lysis buffer) was added, mixing it in carefully by slowly inverting the tube three times. The sample was then incubated for 5 min at room temperature to assure complete lysis, and then 300 µL of ice-chilled buffer P3 (neutralization buffer) was added to neutralize the alkaline pH (Table 2.4). The sample was mixed by slowly inverting it five times. After an incubation period of 15 min on ice, the sample was centrifuged (13,000 rpm, 15 min), and 800 µL of the supernatant was transferred to a new tube.

To precipitate plasmid DNA, 700 µL of isopropanol was added and mixed thoroughly by shaking. Plasmids were pelleted by centrifugation (13,000 rpm, 15 min) and then washed once with pre-cooled ethanol (-20°C, 70% v/v). The supernatant was discarded, and any residual ethanol was evaporated by incubating the tube at 37°C with an open lid. The pellet was again suspended in 30 µL of dH_2O. Plasmids were stored at -20°C until further use.

Table 2.4 *Buffers (P1, P2, and P3) used during bacterial plasmids extractions*

Buffer P1	
Tris/HCl pH 8.0	50 mM
EDTA*	10 mM
RNAse A	100 µg/mL
sterilized by autoclaving RNAse A added after autoclaving stored at 4°C	

*EDTA - Ethylenediaminetetraacetic acid

Buffer P2	
NaOH*	200 mM
SDS**	1 % (w/v)
stored at RT	

*NaOH – Sodium hydroxide
**SDS - Sodium dodecyl sulphate

Buffer P3	
KAc*	3 M
pH equilibrated at 5.5 with CH_3COOH** sterilized by autoclaving stored at 4 °C	

*KAc - Potassium acetate
**CH_3COOH – Acetic acid

2.2.4.2 Cultivation of *Saccharomyces cervesiae*

Functional characterization by stopped-flow spectroscopy was performed in *Saccharomyces cerevisiae* strain SY1 (genotype: Matα, ura3-52, leu2-3,112, his4-619, sec6-4ts, GAL2).

Cultivation of yeast clones lacking specific amino acids for auxotrophic selection (see below) was performed in selective synthetic complete (SC) media (also below). Liquid cultures were inoculated with either a single colony taken from an SC agar plate or with an aliquot of frozen-cell suspension from a deep-frozen stock. The standard size for overnight cultivation consisted of 3 ml of selective SC medium in standard test tubes. The test tubes were placed at a slanted angle on a shaker set to 225 rpm. The temperature was set to 30°C.

2.2.4.2.1 *Induction of protein expression for* Saccharomyces cerevisiae

Yeasts containing putative AQP and cloned into the expression vectors pYES-DEST52 were used for the functional analysis of aquaporins. The expression of the gene of interest was induced by galactose. An overnight starter culture of the yeast clone was prepared in selective SC medium (containing glucose) (see below). The next day, OD600 was measured and the volume of starter culture needed to inoculate an expression culture of the desired size at an OD600 of 0.6 was calculated. The resulting volume of starter culture was harvested by centrifugation (1,000 × g, 5 min) and washed once with sterile dH_2O. The pellet was then suspended again in the appropriate amount of selective SC medium containing galactose instead of glucose. After an induction time of 16 hr (cultivation under standard conditions as described earlier), the expressed culture was used for further study.

2.2.4.2.2 *Preparation of chemically competent yeast cells*

To produce and transform chemically competent yeast cells, yeast cells were cultivated overnight in a 3 ml yeast extract/peptone/dextrose (YPD) medium (strains without the auxotrophy marker; see below) or selective SC medium (strains with the auxotrophy marker) in standard conditions. The culture was used the subsequent day as a starter culture to inoculate 50 ml of YPD at an OD600 of about 0.2. The yeast cells were then grown to an OD600 of 0.6 (30°C, 225 rpm). The cells were harvested by centrifugation
(1,000 × g for 5 min.) and washed once with 10 ml of sterile water. After repeating the centrifugation step, the supernatant was discarded, and the cells were again suspended in 500 µL of 0.1 M lithium acetate (LiAc; pH = 7.5, sterilized by filtration). The suspension was then transferred to an Eppendorf tube and centrifuged another

time. The pellet was again suspended in 200 µL of 0.1 M LiAc and incubated at room temperature for 30 min. The cells were then used for transformation.

SC medium*

- yeast nitrogen base (w/o AA) 0.17 % (w/v)
- $(NH_4)_2SO_4$ 0.5 % (w/v)
- glucose/galactose 2% (w/v)
- amino acid mix for auxotrophy selection 0.115 % (w/v)**

*pH equilibrated at 6.0 with KOH sterilized by autoclaving and stored at room temperature

**Amino acid mix for auxotrophy selection

- alanine, arginine, asparagine, aspartic acid, cysteine, glutamine, glutamic acid – 2 g each
- glycine, isoleucine, lysine, phenylalanine, proline, serine, threonine, tyrosine, valine – 0.2 g each

YPD medium *

- yeast extract 1% (w/v)
- peptone 2% (w/v)
- glucose 2% (w/v)

*sterilized by autoclaving and stored at room temperature

2.2.4.2.3 Transformation of chemically competent yeast cells

Competent yeasts were prepared fresh as described in section 2.2.6.1. A frozen aliquot of salmon sperm DNA (ssDNA, 10 mg/ml) was thawed, boiled at 100°C for 5 min, and then cooled on ice. A total of 10 µL of the prepared ssDNA and 5 µL of plasmid DNA (diluted to 200 ng/µL) were mixed in PCR tubes. A master mix was prepared, which consisted of 70 µL 50% (v/v) polyethylene glycol (PEG), 10.5 µL of 1 M LiAc, 1.5 µL of ssDNA, and 18 µL of competent yeast per transformation. Of this master mix, 100 µL was added to each plasmid-containing PCR tube. The tubes were then incubated for 30 min at 30°C in a thermocycler. Then cells were subjected to heat shock at 43°C for 15 min. After the heat shock, the cells were harvested by centrifugation (1,000 × g, 5 min.), washed once with 100 µL of sterile water, and suspended again in 100 µL of sterile water. Finally, 50 µL of each cell suspension was spread on selective agar plates, and the plates were incubated for 48-72 hr at 30°C to obtain single colonies.

2.2.4.2.4 Plasmid extraction

To isolate plasmids from transformed yeasts, an adapted protocol from Kaiser et al. (1994), was used. First, 1.5 ml of overnight yeast culture was harvested by centrifugation (5,000 × g, 5 min) and the pellet was again suspended in 0.2 ml of DNA release solution (see below). Then, 0.2 ml of a phenol:chloroform:isoamylalcohol (25:24:1) mixture and 0.3 ml of acid-washed glass beads (diameter 0.25 mm) were added, and the cells were disrupted by vortexing at

high speed for 5 min. Phases were separated by centrifugation (14,000 rpm, 5 min, room temperature). A total of 120 µL of the aqueous layer was transferred to a new tube. The DNA was precipitated with 120 µL of isopropanol. After centrifugation, the pellet was washed with 120 µL of 70% (v/v) EtOH, the supernatant was discarded, and residual ethanol was allowed to evaporate. The pellet was then suspended again in 30 µL of DH_2O and stored at -20°C until further use.

DNA release solution*

- Triton X-100 2% (v/v)
- SDS 1 % (W/V)
- NaCl 100 mM
- Tris/HCl pH 8.0
- 10 mM Na-EDTA 1 mM

*stored at room temperature

2.2.4.2.5 Creating yeast cryostocks

For long-term storage of yeast clones, deep-frozen cryostocks were prepared. Firstly, 1.5 ml of overnight culture was harvested by centrifugation (5,000 × g, 5 min) and then suspended in 142 µL of fresh selective SC medium. Then 58 µL of 86% (v/v) glycerol was added and the cells immediately flash frozen by immersion in LN2. The cryostocks were then stored at -80°C until further use.

2.2.5 Molecular biology methods

2.2.5.1 Polymerase chain reaction

A standard PCR program was created using the conditions described in Table 2.5, with adjustments made to primer annealing temperature and elongation time depending on the primers present and the length of the DNA fragment to be amplified. (Appendix) shows all primers used and their respective melting temperature (TM). Annealing temperatures were set to 4°C below TM. Detailed sequence information for each primer is given in the appendix.

Table 2.5 *Standard PCR program conditions*

Step	Temperature	Duration
1. Initial denaturation	95°C	5 min
2. Denaturation	95°C	30 s
3. Primer annealing	Depending on primer	30 s
4. Amplification	72°C	Depending on fragment length
5. Final amplification	72°C	5 min

All PCR reactions were prepared to a final reaction volume of 25 µL. The PCR reactions were prepared by mixing 1 µL of template DNA, 1 µL of forward primer, and 1 µL of reverse primer in a PCR tube. A master mix was prepared, which consisted of 17.5 µL of DH_2O, 2.5 ml of 10X DreamTaq Buffer (Fermentas), 1 µL of

dNTP mix (2.5 µM of each nucleotide), and 1 µL of DreamTaq DNA polymerase (10 units/µL, Fermentas) per reaction. Then, an aliquot of 22 µL of the master mix was added to each PCR reaction. The reactions were placed in a thermocycler (Biometra Gradient) and run under the previously-described conditions. For short-term storage, PCR products were kept at 4°C until further use.

2.2.5.2 Reverse transcription polymerase chain reaction

Synthesized cDNA was used to design a RT-PCR reaction, and a standard PCR (section 2.2.5.1) procedure was used to amplifiy the cDNA in a Multicycler PTC 200 (Biozym, Germany) using 1 to 2 µL cDNA and gene-specific primers. Polymerized fragments were then separated and visualized on agarose gel (section 2.2.3.2.1.1).

2.2.5.3 Purification of PCR product and RNA gel extraction

After the PCR reaction occurred, DNA fragments were purified from primers, nucleotides, polymerases and salts. The purification was performed with QIAquick PCR Purification Kit (QIAGEN, Germany) following the manufacturer's instructions. To purify or extract the target DNA fragment from unspecific fragments in standard or low melting agarose, a QIAquick Gel Extraction Kit (QIAGEN, Germany) was applied according to the manufacturer's protocol. This method was appropriate for extraction and purification of DNA from 70 bp to 10 kb.

2.2.5.4 Digestion by restriction endonucleases

To check the length of insert in a plasmid, the plasmid was cleaved by restriction endonucleases. Restriction endonucleases were chosen depending on the sequence of nucleic acid that flanked the insert. Digests contained about 0.5 µg plasmid DNA (1X reaction buffer). Then 5 units of restriction endonuclease(s) and ddH_2O was added until a volume of 20 µL was reached. The mixture was incubated at 37°C for about 2-3 hrs. The enzyme(s) was (were) deactivated at 65°C for 10 min. The fragments sizes were checked by agarose gel electrophoresis (section 2.2.3.2.1.1).

2.2.5.5 Molecular cloning using the Gateway™ recombination technology

The principle of cloning PCR products using the Gateway™ system is based on the sequence-specific recombination system of the phage λ. Cloning is achieved by using phage-specific recombination enzymes and integration host factor (IHF) from *E. coli*. The DNA sequence containing the necessary recombination recognition sites can then be moved to vectors containing corresponding recognition sites. Adding recombination recognition sites to genes of interest via PCR then allows cloning of these fragments into compatible Gateway™ vectors with an easy recombination reaction. In the process of recombination, the ccdB gene present in Gateway™ vectors is replaced by the gene of interest. The ccdB gene inhibits DNA gyrase in

nonresistant *E. coli* strains (such as DH5α, the strain used for cloning), leading to a lack of growth of clones transformed with non-recombined plasmids, thereby selecting for successful recombination. The recombination reactions are divided into a BP reaction that uses PCR product and a donor vector to produce an entry clone, and an LR reaction using the entry clone and destination vector to produce the expression clone. Figure 2.2 is a schematic overview of BP and LR reactions.

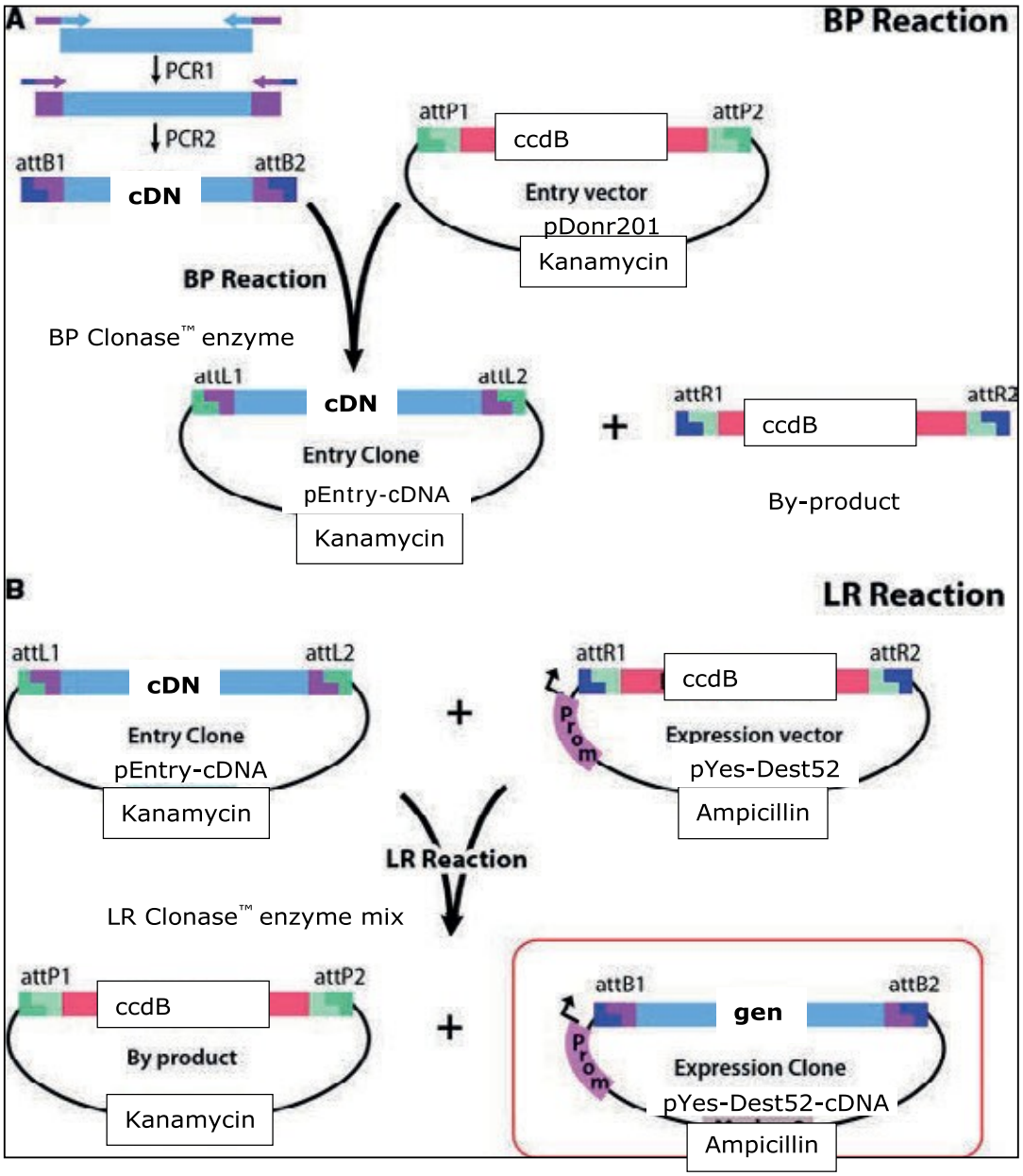

Figure 2.2 Outline of the Gateway™ Cloning System. (A) Recombination facilitated by the BP enzyme between the attB sites present in the insert (cDNA) and attP sites in the entry vector ([pDonr201] generates the entry clone flanked by the attL sites [pEntry-cDNA]). (B) LR recombinase is used to transfer the insert from the entry vector to the expression vector (pYes-Dest52) to generate expression clone (pYes-Dest52-cDNA). Adapted from Festa et al. (2013).

2.2.5.5.1 Generation of cDNA with flanking attB recognition sequences

Via PCR, the cDNA of the aquaporin with the specific recombination recognition sequences attB1 and attB2, for further use with Gateway™ technology, was generated. The required oligonucleotide sequences were created using the Vector NTI software (Invitrogen™) for the PCR reaction. As the PCR product was used for a BP reaction (as described before), attB reaction sites had to be introduced with the primers. These contained the gene-specific sequences and the attB recognition sequences for the integrase (Table 2.6).

Table 2.6 *Primers for the fusion of a cDNA with recognition sequences for the Gateway™ System*

	Sequence
attB1-sense primer	5‘-GGGGACAAGTTTGTAC AAAAAAGCAG GCTTAACCATGGCCAAGGACGTTGAG-3’
attB2 antisense primer	5‘-GGGGAC CACTTTGTAC AAGAAAGCTG GGTATTAATCCATAATTGAGTAAATCAA-3‘

2.2.5.5.2 Cloning the PCR product into an expression vector with the aid of the Gateway™ system

2.2.5.5.2.1 Gateway™ BP reaction

To clone a PCR fragment containing attB1 and attB2 sites into Gateway™ donor vector pDONR201, 50 ng of the PCR product (in a volume of 1 to 5 µL) was mixed with 150 ng of donor vector (in a volume of 1 µL) and 2 µL of 5X BP reaction buffer in a PCR tube. The reaction volume was adjusted with TE buffer (pH 8.0) to 8 µL, then 2 µL of BP Clonase™ mix was added to the reaction. Afterwards, samples were incubated at 25°C for 1 hr. Following the incubation, 1 µL of Proteinase K solution was added to each reaction and again incubated at 37°C for 10 min to inactivate the recombination enzymes. The competent DH5α cells were then transformed with the product of the BP reaction as described before, yielding entry clones.

2.2.5.5.2.2 Gateway™ LR reaction

As soon as transformants containing the genes of interest, cloned into pDONR201 (entry clones,) had been acquired, the resulting plasmids were isolated by standard plasmid preparation (as described before) and used as substrate for the Gateway™ LR reaction. Then 150 ng of the entry clone plasmid DNA (in a volume of 1 to 5 µL) was mixed with 150 ng of destination pYES-DEST52 vector (Invitrogen™) for expression of PIP2 in yeast (in a volume of 1 µL) and 2 µL of 5X LR reaction buffer in a PCR tube. The reaction volume was adjusted with TE buffer (pH 8.0) to 8 µL, and then 2 µL of LR Clonase™ mix was added to the reaction. After incubation (25°C for

1 hr), 1 µL of Proteinase K solution was added to each reaction and incubated at 37°C for 10 min to inactivate the recombination enzymes. Finally, the samples were used for transformation of yeast competent cells, yielding expression clones carrying the gene of interest for functional analysis.

2.2.5.6 Sequencing of DNA

The sequencing of DNA (e.g., PCR products, plasmid DNA) fragments was performed by SEQLAB DNA Sequencing Service (Nucleics; Göttingen, Germany). Following a plasmid DNA preparation from *E. coli*, the purity of the DNA was checked using electrophoretic separation in an agarose gel, and the concentration of the DNA was determined photometrically. Then the instructions from SEQLAB were followed when preparing the sample for sequencing, which included the DNA fragment and the required primer.

2.2.5.7 cDNA library construction

2.2.5.7.1 Producing the first strand of cDNA

To produce the first strand of cDNA from total RNA by RT-PCR, Ready-To-Go PCR beads (Amersham Pharmacia Biotech) were used. The manufacturer's protocol was followed, and 1 µg of total RNA was used for the synthesis, the 3'CDS-primer, and the SMARTIIA-oligo-primer (Takara Bio Europe, France). The 3'CDS-primer consisted of an oligo-dT-sequence of approximately 30 bases at its 3' end and a nucleotide sequence of 25 bases at its 5' end. This primer binds to the beginning of the first strand and to the polyA tail of the mRNAs, such that reverse transcriptase (RT) begins with the elongation of the first strand of cDNA. When the RT arrives at the end of the template strand, i.e., the mRNA, it adds cytosine bases at the 3' end of the newly synthesized ssDNA strand. The SMARTIIA-Oligo-Nucleotide has the same nucleotide sequence of 25 bps at its 5' end as the 3'CDS-primer, and it has some guanosine bases at its 3' end. These complement the C-rich end of the first strand of cDNA, thus serving as an extended template for the RT.

2.2.5.7.2 Duplicating cDNA

The ssDNA (above) was amplified with the aid of the PCR. As the only primer was the nested universal primer (NUP), the cDNA was checked on a gel to ensure that the PCR still ran in a linear range (Table 2.7).

Table 2.7 *Components of PCR sample for 60 µl volume (A) and PCR cycles (B)*

A.

Volume	Ingredient
2.5 µl	ssDNA*
4.0 µl	NUP** (10 pmol/µl)

Volume	Ingredient
1.5 µl	dNTPs (10 mM)
6.0 µl	Advantage® 2 polymerase buffer (10X; Takara)
1.0 µl	Advantage® 2 polymerase mix (Takara)
45 µl	Water (sterile)

*ssDNA – single stranded DNA
**NUP - nested universal primer

The 60 µl were divided equally and added to three PCR reaction tubes and then multiplied in a PCR machine according to the following program:

B.

Step	Temperature	Duration
Denaturation	95°C	5 s
Primer addition	58°C	10 s
Elongation	72°C	3 min

Approximately 10 s before the end of a PCR cycle, the first tube (batch) was obtained from the thermocycler and put on ice. The other two tubes continued analogously for a longer period. Of the three different amplified tubes, 5 µl was used to check the quality of the PCR on a gel.

2.2.5.7.3 Preparing a cDNA library

After controlling the amplified total cDNA on the gel, the samples were reused if no bands were present; just one uniform, distributed band (from 4,000-5000 bps) was seen in the gel.

The plasmids were then transformed into XL1-blue *E. coli* cells, and each 20 µl of the bacteria was placed on LB/AMP/IPTG/X-Gal plates. After incubating them overnight at 37°C, the white colonies were selected and transferred to the single wells of a 96-well plate in which 80 µl LB-amp medium was added. These plates were covered, sealed with Parafilm® (evaporation protection; Bemis® Company, Inc.), and incubated overnight at 37°C. The next day, each culture was overlaid with a drop of 90% glycerin, and the labeled plates were frozen at -80°C. The cDNA library was used for heterologous microarray, Southern blot analysis, and RT-PCR.

2.2.6 Physiological study: stopped-flow spectroscopy

2.2.6.1 Overview

The H_2O conductance of *Arceuthobium* spp. aquaporins was examined in a heterologous yeast expression system using stopped-flow (SF) spectroscopy, a method originally developed to study rapid chemical reactions (Dalziel, 1957) and adapted for various membrane conductance assays (Crandall et al., 1971). This

method relies on the fact that the SF apparatus allows for very fast mixing of different liquid compartments while simultaneously recording optical output signals with very high resolution over time. Figure 2.3 gives a schematic overview of the SF system.

In the case of water conductivity, the shrinking or expanding of yeast protoplasm is observed when it is mixed rapidly with a hypertonic or hypotonic buffer correspondingly. The change in cell size is visualized by measuring the change in intensity of scattered light over time. For example, a yeast protoplast expressing a water-transporting aquaporin suspension can be mixed with a hypotonic solution (mixing buffer), which results in water influx and swelling protoplasts. The incident light scatters when it hits the protoplast surface, and the intensity of light scattering is detected by a photomultiplier (Figure 2.3).

Cell expansion speed is correlated to the water conductance of the plasma membrane; therefore, cell expansion speed is also correlated with the number and function of water-conducting channels. As a result, differences in water conductivity between different aquaporin-expressed clones can be traced back to the water conductivity of the aquaporin being expressed. Negative and positive controls of the same yeast clone are run in a parallel manner and show a difference in water conductivity.

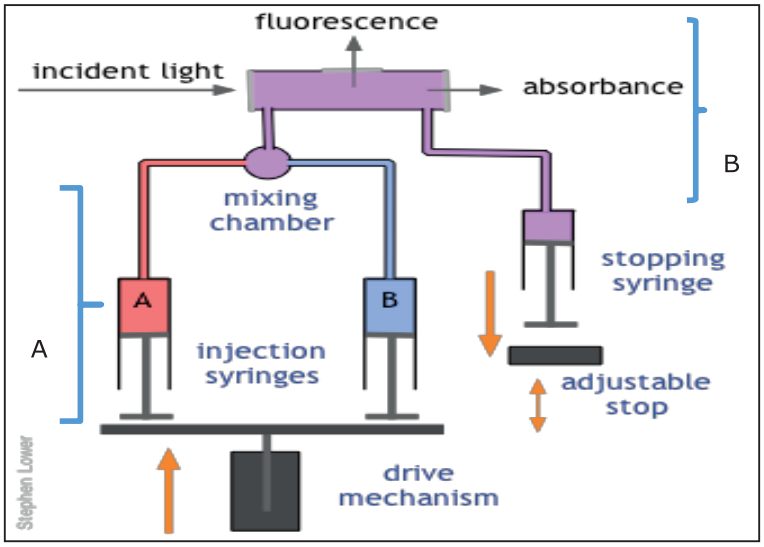

Figure 2.3 Schematic representation of the stopped-flow apparatus. The apparatus consists of the mixing unit (A), the detection unit (B), and the computer with software for analyzing data (not shown). Adopted from UC Davis.
https://chem.libretexts.org/Courses/University_of_California_Davis/UCD_Chem_107B%3A_Physical_Chemistry_for_Life_Scientists/Chapters/2%3A_Chemical_Kinetics/2.10%3A_Fast_Reactions_in_Solution

To measure water conductivity, the change in the size of a yeast protoplast is measured when protoplasts are mixed rapidly with buffers of high or low osmolarity. As result, the change in cell size can be visualized by changes in light diffraction over time.

2.2.6.2 Yeast protoplast preparation

Cultures were grown in liquid SC-Ura or SCGal-Ura on a rotary shaker for 18 h (250 rpm, 30°C). Cells from a 10 ml aliquot were spun down (500 × g, 5 min), suspended again in 3 ml of equilibrium buffer, and equilibrated on a rotary shaker at 30°C for 15 min. Following that, 6 ml of digestion buffer was added, and then the mixture was vortexed and incubated on a rotary shaker for 45 min at 30°C. Protoplasts were harvested by centrifugation (1,000 × g, 5 min), suspended again in an incubation buffer, and kept on ice until use (Bertl at al., 1993).

The yeast protoplast preparation as well as stop flow cytometry was performed using the chemicals listed in Table 2.8.

Table 2.8 *Stopped-flow buffers compositions*

SF Equilibrium Buffer	
potassium phosphate at pH 7.2	50 mM
β-mercaptoethanol	40 mM
Sterilized and autoclaved, stored at room temperature	

SF Digestion Buffer	
Potassium phosphate at pH 7.2	50 mM
β-mercaptoethanol	40 mM
Sorbitol	2.4 M
Bovine serum albumin	50 mg/ml
Zymolyase 20T	0.1-1 mg
Sterilized and autoclaved, stored at room temperature	

SF Incubation Buffer	
Sorbitol	1.8 M
NaCl	50 mM
$CaCl_2$	5 mM
Tris pH 8	10 mM
Sterilized and autoclaved, stored at room temperature	

2.2.6.3 Stopped-flow measurements for water

All H_2O measurements were conducted using a stopped-flow spectrophotometer (BioLogic Science Instruments) that consisted of a light source (arc lamp H-1061-UV), a mixing unit (SF 300), a photomultiplier (PMS 250), and a microprocessor unit (MPS-60) that controlled the mixing unit. The photomultiplier and microprocessor unit were connected to a PC.

Measurements were performed at 10°C with the wavelength of the incident light adjusted to 436 nm. The photomultiplier was put into high voltage mode and adjusted to +600 mV, with the output filter set to 1 ms. The sampling period was set as follows:

- 200 µs, 4,000 data points
- 2 ms, 2,000 data points
- 10 ms, 2,000 data points

This results in a window of measurement of 15 s.

Total injection volume per shot was set to 100 µL (50 µL for each syringe), and the flow rate was set to 10 ml/s. Start of data acquisition was set to 10 ms before stop. A separate raw kinetics file was created for each measurement shot of each sample.

The prepared yeast protoplasts (as described in section 2.2.4.2.2) were again suspended in 2 to 4 ml of SF incubation buffer, taking the relative pellet size into account to create roughly equal cell densities. Syringes 1 and 3 were washed with 10 ml of SF H_2O mixing buffer and SF H_2O buffer III, respectively. Syringe 1 was then filled with 5 ml of SF H_2O mixing buffer. The cell suspension was applied to syringe 3. Trapped air bubbles were removed from both syringes by raising and lowering the plungers several times, then measurement shots were taken. After measuring, both syringes were washed subsequently with 30 ml of dH_2O and 10 ml of their corresponding buffers (as described previously) before applying the next samples.

2.2.7 Heterologous microarray

2.2.7.1 Overview

In a “standard” microarray method, a solution containing an assortment of labeled nucleic acids (the probes), usually (a) known cDNA sequence(s), is used to probe a cDNA array generated from the species of interest. Where similar, these labeled nucleic acids can bind (by hybridization) to the unknown sequences on the array (Bumgarner, 2013). In the traditional array, probes from the same species as the targets (homologous microarray) are used to profile transcriptome dynamics. While heterologous microarrays (probes from closely or unrelated species) are possible, they are not commonly used. There are three basic types of microarrays in regards to how the cDNA array is attached to the substrate: spotted arrays on glass substrates, in situ synthetized arrays, and self-assembled arrays. During my research, two technologies were used: a modified spotted array (DeRisi et al., 1996) and an in situ synthetized array developed by Affymetrix.

2.2.7.2 Spotted heterologous microarray - MicroCASTer handheld microarray system

In principle, the modified spotted array method consists of the following:

1. spotting a substrate with cDNA from the species of interest
2. preparing digoxigenin (DIG)-labelled probes with known sequences
3. hybridizing
4. detecting

NEXTERION® nitrocellulose (NC-C; Schott Nexterion) slides and aminosilane-coated slides (NEXTERION®) were spotted with Mistletoe cDNA clones (Southern blot) from the mistletoe cDNA library (800-1,000 cDNA clones on each slide) according to Schleicher and Schull BioScience GmbH (now Whatman, GE Healthcare Group) instructions and using a hand-held MicroCaster™ array tool (Figure 2.4 and 2. 6). Initially, all clones were transferred, using a pin applicator, to new 96-well plates (Figure 2.4) filled with a nutrient broth (section 2.2.4.1.1). Plates were incubated overnight, and colony screening by PCR was done using M13 primers for pDrive vector. Then the PCR products were diluted in either a 3X saline-sodium citrate (SSC) buffe (Table 2.9) or DMSO for further application (Figure 2.5: a schematic representation of a membrane chip surface [slide] using a DNA concentration of 70-100 ng). Directly after spotting, DNA was denaturated by soaking the slide for 5 min in a denaturation buffer (Table 2.9) and then neutralized for 5 min in a neutralization buffer (Table 2.9). Subsequently, the DNA was immobilized to a nitrocellulose membrane via cross-linking using UV light (150 mjoules/cm^2). Finally, the slide was rinsed for 5 min in H_20 to remove salts from the chip and allowed to air dry before it was stored in a dry, cool place (+4°C).

	1	2	3	4	5	6	7	8	9	10	11	12
A	1	1	1	1	5	5	5	5	9	9	9	9
B	1	1	1	1	5	5	5	5	9	9	9	9
C	2	2	2	2	6	6	6	6	10	10	10	10
D	2	2	2	2	6	6	6	6	10	10	10	10
E	3	3	3	3	7	7	7	7	11	11	11	11
F	3	3	3	3	7	7	7	7	11	11	11	11
G	4	4	4	4	8	8	8	8	12	12	12	12
H	4	4	4	4	8	8	8	8	12	12	12	12

Figure 2.4 Graphic illustration of a 96-well plate. The numbers in grey squares indicate the sequence in which the mistletoe cDNA samples were applied on a slide and then were taken from the respective wells of the plate with the 8 needles of the "array tool."

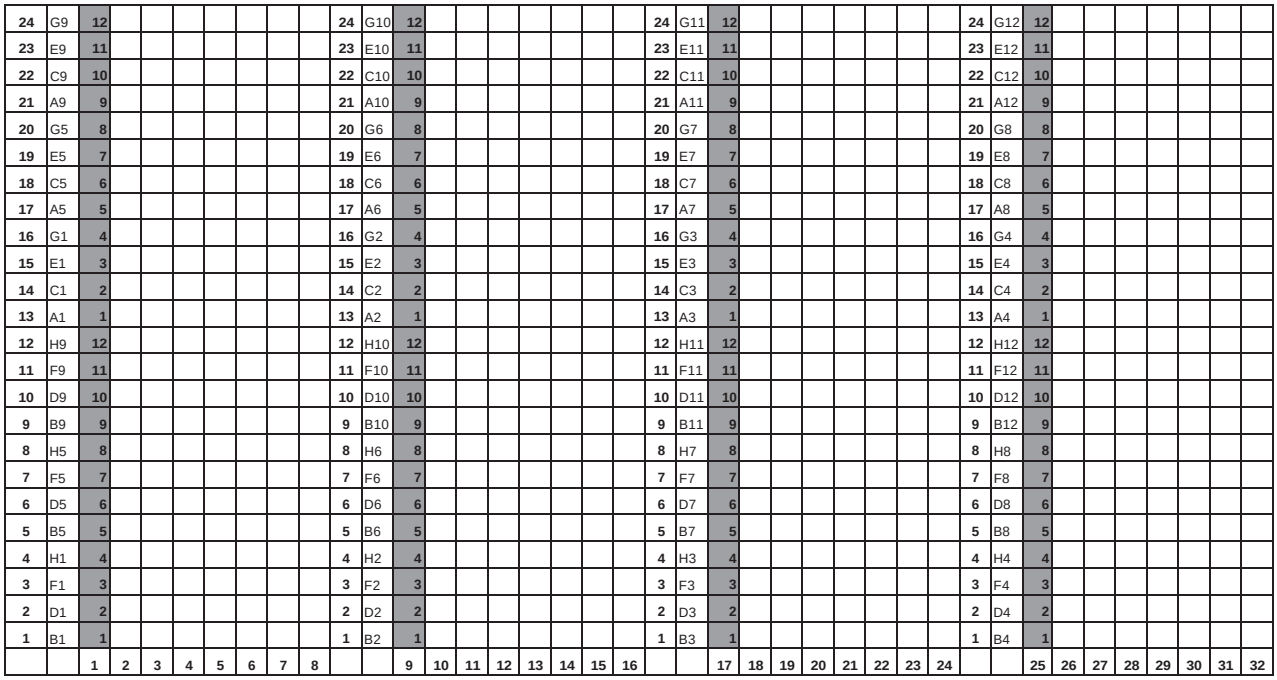

Figure 2.5 Schematic representation of a membrane chip surface (slide): The numbers in grey squares represent the cDNA spotting events. The number 1 indicates the first spot event, 2 is the second, 3 is the third, etc. The letter/number fields (e.g., B1) indicate from which well of the 96 plate the respective DNA sample originates. The 8 array needles are first transferred to the membrane and then transferred to wells A1, A2, A3, A4, B1, B2, B3, and B4, and so forth. After a 96-well plate was completely spotted, columns 1, 9, 17, and 26 were completely filled with cDNA spots (24 spots per column).

Table 2.9 *Hybridization buffers compositions*

Buffer	Ingredients
3X SSC* Buffer	1.5 M NaCl
	0.15 M Na3-Citrate, pH 7.0
Denaturation buffer	0.4 M NaOH
	3 × SSC*
	10 mM EDTA**
Neutralization buffer	0.5 M TRIS-HCL pH 7

*SSC - saline-sodium citrate

**EDTA - ethylenediaminetetraacetic acid

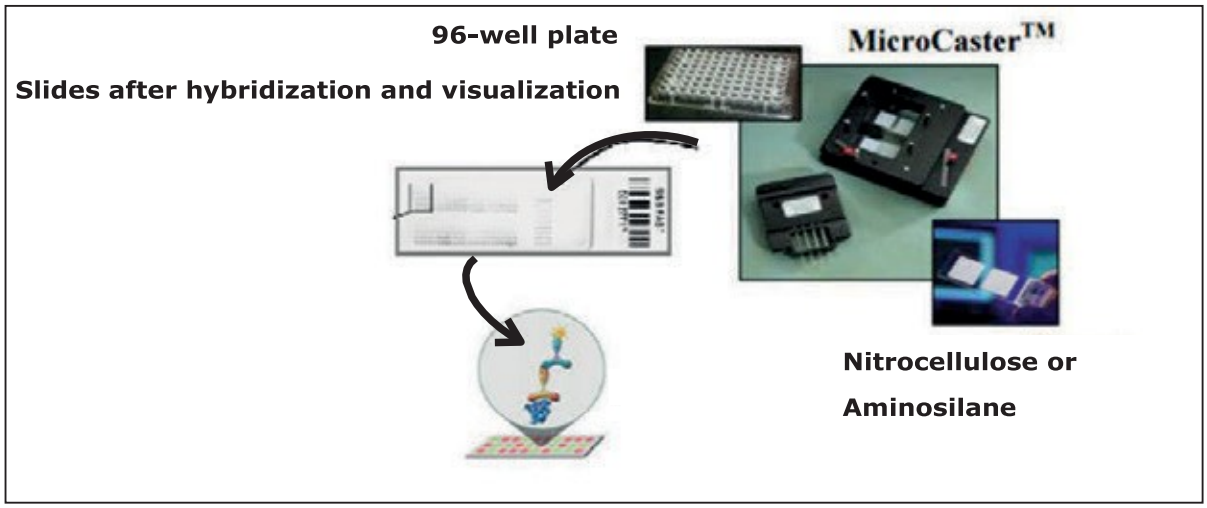

Figure 2.6 Generalized illustration of steps involved in DNA microarray analysis using MicroCaster™, from applying samples to slides to visualization of positive results after hybridization.

2.2.7.3 Preparing probes

A DIG nonradioactive system to label nucleic acids was used. The system employs alkali-labile DIG-11-dUTP (Roche; Figure 2.7), where an alkaline phosphatase conjugate is bound to the desired gene and an anti-DIG antibody binds to the hybridized probe. The antibody-probe hybrids were visualized with chemiluminescent alkaline phosphatase substrates.

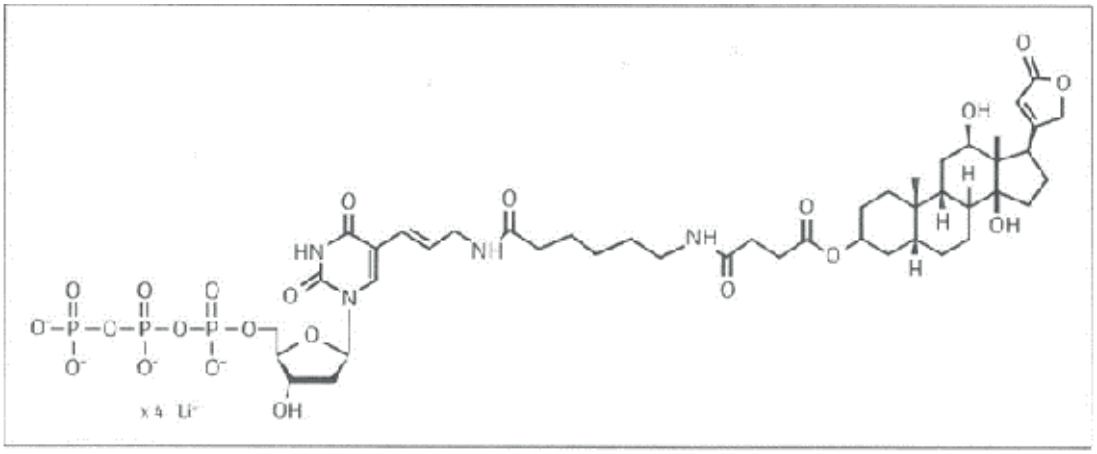

Figure 2.7 Alkali-labile DIG-11-dUTP (Roche). Digoxigenin (DIG).

Probes were prepared for various AQPs from different plants such as *Arabidopsis thaliana* (At), *Nicotiana tabacum* (Nt), *Oryza sativa* (Os), *Samanea saman* (Ss), and *Cleome spinosa* (Cleome):

1. Nt AQP1
2. NtTIP PGEM

3. Cleome PIP2
4. Cleome PIP1
5. OsPIP1.2
6. OsPIP2.1
7. OsPIP2.2
8. NtPIP2.1
9. SsIpQE
10. SsIIpQE
11. AtPIP1.2
12. AtPIP2.3
13. At PIP2.1
14. AtNIP1.2

The PCR-labelling method was chosen from many different methods of probe preparation, as this method required a small amount of template and gave a high yield of labeled probes. Probes were prepared according to the instruction manual using the Biometra TGradient thermal cycler.

Table 2.10 *PCR batch for labelling cDNA probes (25uL)*

Chemical	Volume	Concentration
dNTPs	2 ul	(2.5 mM each)
DIG*-11- UTP	2.7 ul	(10 mM)
primer 1	0.5 ul	10 pmol/ul)
primer 2	0.5 ul	(10 pmol/ul)
buffer x 10 with 1.5 mM MgCL	2.5 ul	
Taq-S polymerase	1 ul	(2.5 to 5 U)
template	0.5 ul	(endoconcentration 1 ng/ul)
H_2O to total volume of 25 ul	15.3 ul	

* DIG-11- digoxigenin

PCR conditions 25 cycles of 30 s at 94°C:

Step	Temperature	Duration
1. Initial denaturation	95°C	3 min
2. Denaturation	95°C	30 s
3. Primer annealing	Depending on primer	60 s
4. Amplification	72°C	60 s
5. Final amplification	72°C	10 min

After each probe was synthesized, evaluation of probe-labelling efficiency was performed using gel electrophoresis. Next, the PCR products were cleaned using a NucleoSpin® Kit (Takara) and then added to 5 ml of hybridization buffer (DIG Easy Hyb hybridization buffer, Roche).

2.2.7.4 Hybridization with probes

The prehybridization/conditioning of slides was performed using either DIG Easy Hyb solution (Roche). A total of 3 ml of the solution was applied on the slide and incubated for 60 min at 42^{o}C using a glass chamber. The chamber was agitated gently during this step. After prehybridization, the slide was removed from the solution and immersed in a hybridization buffer that contained DIG Easy Hyb buffer with a DIG-11-dUTP probe at a concentration of 50 ng/ ml of DIG Easy Hyb buffer.

To prepare the labeled probe for hybridization, the probe was mixed with DIG Easy Hyb (1:1) and denaturated before use by placing the mixture in a 95°C water bath for 10 min and then chilling it on ice for 2 min. Immediately after this step, the probe was placed in a 68°C water bath for 7 min. Then it was prewarmed in the DIG Easy Hyb buffer and mixed well by inversion. The hybridization solution was then added to the blot (slide), and it was left overnight at 42°C in an incubator with agitation so hybridization would occur. The next morning, the slide was removed from the chamber and placed in a plastic container to undergo a washing procedure to remove unattached probes from the surface of a blot. A low stringency buffer was added to the container and it was placed on a shaking platform or in a shaking water bath. The incubation times, temperatures, and ingredients of the washing buffers are listed in order of procedure below:

1. 1 × 10' in 2×SSC @ room temperature
2. 1 × 30' in 2×SSC 1% SDS @ 60^{0}C
3. 1 × 15' in 2×SSC 1% SDS @ room temperature

After the washing procedure, the slides were air dried and either kept at 4°C for further use or used to perform the detection procedure immediately.

2.2.7.5 Detection of hybridization probes on blot

After stringency washes to detect probe-target hybrids, alkaline phosphatase-conjugated anti-DIG-AP antibodies (Roche) and CDP-Star (Roche), a chemiluminescent (light-generating) substrate for alkaline phosphatase, were used. Alkaline phosphatase causes dephosphorylation of the substrate, producing unstable anions that immediately disintegrate and emit light (Figure 2.8). The resulting chemiluminescence was then detected using the ChemiDoc™ MP Imaging System (Bio-Rad Laboratories, Inc.). This method is the one of the most sensitive methods for detecting hybrids using the Southern blot technique.

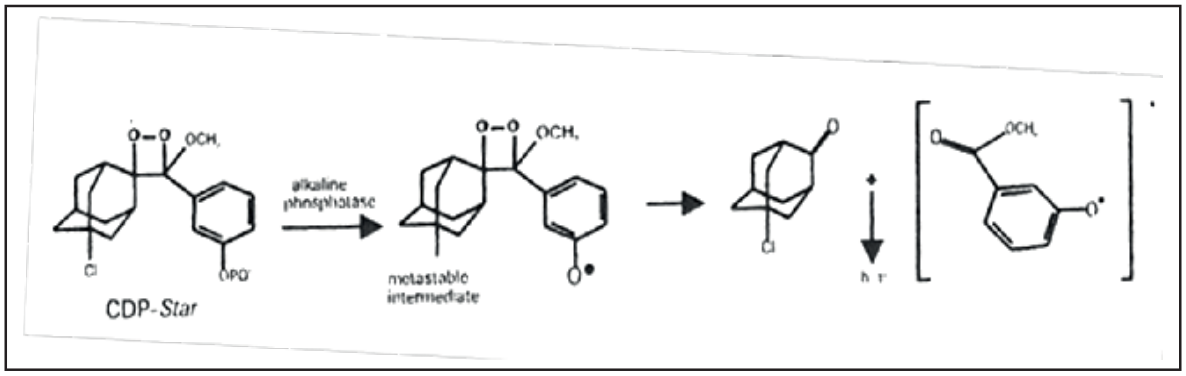

Figure 2.8 Principle of chemiluminescence reaction

After washing was complete, the washing buffer was discarded, and, to prevent unspecific binding of an antibody to the membrane, a blocking solution (Table 2.11) was added to the slide, after which it was incubated for 30 min with agitation. Following that, the membrane was incubated with alkaline phosphatase-conjugated anti-DIG-AP antibodies (Fab fragments; Roche). The antibody was prepared according to Roche protocol, and it was diluted 1:10,000 in 1 volume of blocking solution with gentle shaking at room temperature. After 1 hr, the antibody solution was discarded and the slide was gently washed 3 times for 15 min per wash in a washing buffer with shaking. Afterwards, the buffer was poured off and the membrane was equilibrated two times/1 min with a detection buffer (Assay B; Table 2.11). Then a Nitro-Block II™ (ThermoFisher Scientific) solution, diluted 1:20 in Assay B for 5 min, was applied. Nitro-Block II™was applied to enhance bioluminescence. The slide was then washed for 5 min in a washing buffer. Finally, a CDP-Star®-diluted substrate (Sigma- Aldrich (1:50 in Assay B; 1 ml solution per 100 cm^2 membrane; Figure 2.9) was applied to the slide. The slide was then covered with Saran™ wrap, spreading the solution evenly to remove any air bubbles that formed. The excess liquid also was squeezed out and the slide was sealed.

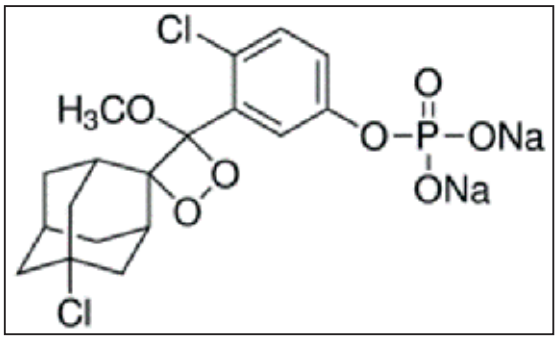

Figure 2.9 CDP-Star® chemical structure

2.2.7.6 Detection with ChemiDoc™

Chemiluminescence was detected with the ChemiDoc™ XRS$^+$ System (Bio-Rad Laboratories, Inc.), a chemiluminescent detection device.

2.2.7.7 Microarray buffers and other media used

Table 2.11 *Microarray buffers, media, and solutions*

10 × PBS buffer (1 L)	**Concentration**	**Chemical**
	82.3 g	Na_2HPO_4
	23.5 g	NaH_2PO_4-H_2O
	40 g	NaCl
Detection buffer (Assay B)	**Concentration**	**Chemical**
	200 mM	Tris/HCL pH 9.8
	10 mM	$MgCL_2$
DIG-blocking solution	**Concentration**	**Chemical**
	5%	milk powder
	1×	PBS
	0.5%	TWEEN® 20 (Sigma-Aldrich)
Wash Buffer	**Concentration**	**Chemical**
	1×	PBS
	0.5%	TWEEN® 20

2.2.8 In situ hybridization - Affymetrix microarray

GeneChip microarrays have been the most frequently used technology for genome-wide expression profiling; from the various available microarray platforms, the Affymetrix GeneChip® Instrument System has been the most frequently utilized (Auer et al., 2009). In my experiment, the *Arabidopsis thaliana* GeneChip®AraGene-1.0 ST containing 37,409 probe sets was used. The probes (oligonucleotides) of a specific length (25 bases long) were directly synthetized on a quartz wafer in a known location. Each *A.thaliana* gene was represented on the array by a series of different oligonucleotide probes.

2.2.8.1 Genome-wide microarray analyses using Affymetrix ATH1 GeneChip® cRNA (antisense copy RNA) preparation, microarray hybridization, and processing

Sample preparation for the microarray hybridization was performed as described in the Affymetrix GeneChip® WT PLUS Reagent Kit User Manual (Affymetrix Inc., Santa Clara, CA). Sample processing was done by an Affymetrix Service Provider and Core Facility, KFB - Center of Excellence for Fluorescent Bioanalytics (Regensburg, Germany). Double-stranded cDNA was built using 200 ng of total RNA extracted from *A. americanum* fruits. Next, 15 µg of synthesized cRNA was purified and reverse transcribed into sense-strand (ss) cDNA. Purified ss cDNA was then fragmented using

a mixture of uracil DNA glycosylase (UDG) and apurinic/apyrimidinic endonuclease 1 (APE 1), and labelled using biotin. The flow of the experiment after the sample labelling is described in the Figure 2.10.

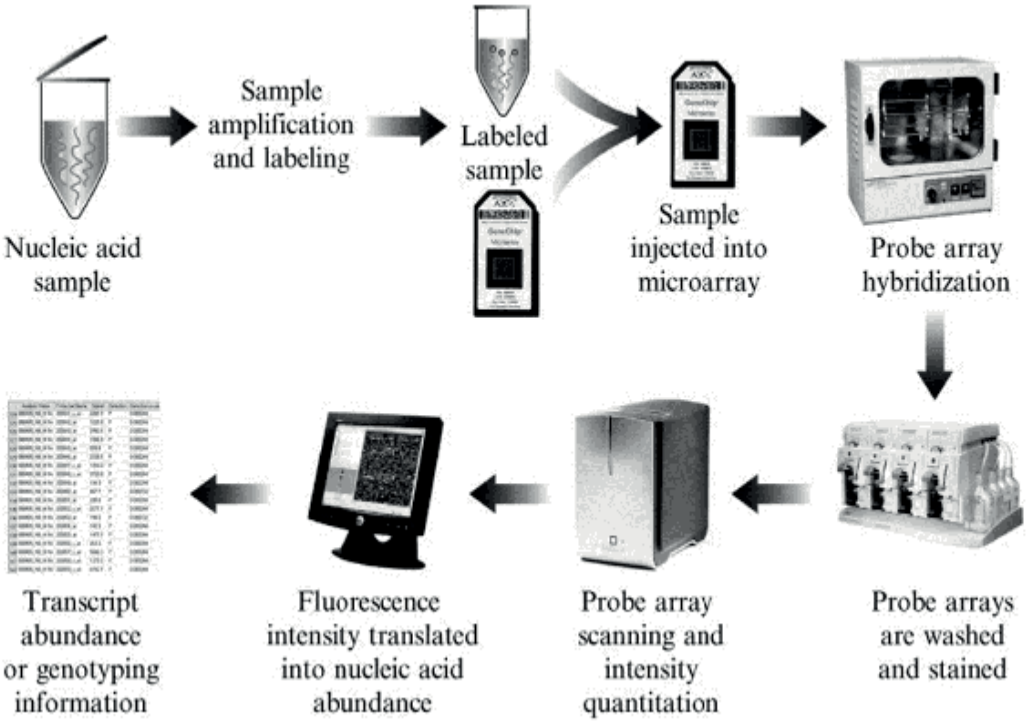

Figure 2.10 Flowchart of a GeneChip System microarray experiment. The labelled ss cDNA was injected into the Affymetrix Arabidopsis Gene 1.0 ST arrays and hybridized for 16 hrs at 45°C in a GeneChip® Hybridization Oven 640. Finally, hybridized arrays were washed and stained in an Affymetrix GeneChip® Fluidics Station 450; the fluorescent signals were quantified with an Affymetrix GeneChip® Scanner 3000 7G. Fluidics and scan functions were regulated by the Affymetrix GeneChip® Command Console software (AGCC; version 4.1.3). Figure adopted from Dalma-Weiszhausz et al. (2006)

2.2.8.2 In silico methods

After the scanning process, the fluorescence values were converted into the corresponding numerical values that represent the fluorescence intensities, which are stored as pixel values comprisingcomprising the image data files (.dat file). Then, files containing probe cell intensity data (.cel files) were generatedgenerated from the .dat files by Affimetrix AGCC; the files contain information about the hybridization intensities between *A. americanum* cDNA fragments and all *Arabidopsis thaliana* probes. For further analysis, special programs designed for the correction of differences in probe labeling efficiency, RNA concentration or hybridization efficiency were used (Harr & Schlotterer, 2006).

2.2.8.2.1 Construction of probe mask file

To visualize the quality of raw data on each array, a program called RMAExpress (version 1.1.0; Irizarry et al., 2003) was used. Probe pairs from the .cel file were carefully chosen for follow-up transcriptome analysis using a .cel file parser script created in the Perl programming language as used in Davey et al. (2009). This program generates a probe mask (computable document format; .cdf file) that permits the extraction and further consideration of only those probe pairs with a perfect-match (PM) probe. To be considered “perfect”, the PM probe must have an intensity value higher than a stipulated hybridization intensity threshold empirically deduced from the .cel files. The threshold value is one that maximizes the number of probe sets and minimizes the number of lower-intensity probe-pairs. Only those probe sets represented by at least one PM probe pair per probe set were retained for analysis (Davey et al., 2009).

Initially, a probe-mask .cdf file based on the .cel file from May (May .cdf) was created to obtain information about differentially expressed genes (DEGs) in May, and then—based on the Perl masking script—the .cdf files with hybridization intensity thresholds (from 0 to 1,000) were constructed. The optimal .cdf file was established empirically. Also, a probe-mask .cdf file based on the .cel file from September (September .cdf) was produced to investigate genes expressed in September (Appendix III:1).

2.2.8.2.2 Statistical analysis

To produce robust multichip average (RMA) expression values, a May .cdf file with a hybridization intensity threshold ranging from 200 to 700 was applied to 6 .cel files. All probe-set signals were analyzed (recapped, normalized, and $\log_2$ transformed) using the RMA summarization algorithm in the program RMAExpress (version 1.1.0; Irizarry et al., 2003). The uniformity of technical replicates was controlled by the Pearson correlation coefficient. The correlations between replicates within the May or September groups were all > 0.9, demonstrating the accuracy of expression measures. Then, average signal values and significance P-values (*t*-test) between two groups of arrays were calculated. All probe sets with P-values < 0.05 were additionally reduced by adjusting for the false discovery rate (FDR; Benjamini & Hochberg, 1995). Also, each September .cdf file with a hybridization intensity threshold range from 200 to 700 was applied to the same 6 .cel files. RMA-normalized expression data were created, and t-test statistics were determined.

2.2.8.2.3 Gene ontology and functional characterization

A number of high-throughput enrichment tools were used to analyze the large gene list; and help to organize and display the genes in the context of already existing biological knowledge. Functional classification was based on The *Arabidopsis* Information Resource (TAIR) TAIR10 genome annotation. As such, the GO::TermFinder (Ashburner et al., 2000; Boyle et al., 2004) was used to evaluate whether specific biological pathways were over-represented among the differentially

expressed genes and within specific gene clusters. To accentuate a molecular interaction network among the genes representing a certain GO category, the software program GeneMANIA (Montojo et al., 2010) was used. GeneMANIA finds other genes related to a set of input genes using a very large set of functional association data like protein and genetic interactions, pathways, co-expression, co-localization, and protein domain similarity (Montojo et al., 2010). Also, the MapMan (Thimm et al., 2004) was used to visualize functional categories of genes with altered expression levels between the May and September transcriptomes.

2.2.9 Quantitative reverse polymerase chain reaction

2.2.9.1 Quantitative real-time polymerase chain reaction primer design

2.2.9.1.1 Primers designed on the basis of sequences of the genes obtained using handheld Microaray system

The quantitative real-time PCR (qRT-PCR) primer design and verification of amplification primers of each gene were performed by the platform OligoPerfect Designer (Invitrogen™), with an optimal melting temperature of 60°C, optimal guanine-cytosine (GC) content of 50%, and optimal primer size of 20 bp. Product size was between 100 and 300 bp. Each primer showed good specificity and efficiency.

2.2.9.1.2 Primers designed on the basis of Affymetrix probes

Orginal Affymetrix probe sequences with signal intensity 300 or higher were used as inputs for primer-designing sofware (Primer-BLAST, Oligo Calc: Oligonucleotide Properties Calculator) and for other online analysis tools (internet resources for molecular biologists) (Section 2.3). Parameters routinely used for designing optimal primers for qRT-PCR reactions were applied, and standard procedures for degenerative primer design were used.

2.2.9.2 Quantitative polymerase chain reaction

All qRT-PCR experiments were conducted in the The Eco™ Real-Time PCR System (Illumina, Inc.), which combines the gene amplification, detection, and data analysis steps together using thermal profile shown in Table 2.12. A 20 µL reaction system volume was used for amplification. Each reaction contained 10 µl SYBR™ Green qPCR Kit Master Mix (ThermoFisher Scientific), 0.5 µL each of forward and reverse primer, 0.2 µL buffer, and 2 µL cDNA synthesized from total RNA.

Table 2.12 *The thermal profile of qRT-PCR*

Cycle	Time	Temperature
Initial Denaturation	5 min	95^0C
Denaturation	15 s	95^0C
Annealing	30 s	60^0C
Extension	30 s	72^0C for 40 cycles

Three technical replicates were used in the qRT-PCR experiments, and the average Cq, also known as Ct values, were used for quantification (Appendix II:3). "No template" controls were used as a negative control for each pair of primers. The PCR products were checked by 1.5% agarose gel electrophoresis to verify the specificity and expected sizes of amplicons.

2.2.9.2.1 Housekeeping genes

Before any gene is chosen as a standard, a comprehensive search and testing is needed to ensure that no significant regulation occurs. This can, however, be a circular problem, as the expression data of the tested standard has to be standardized. A possible solution might be to use more than just one housekeeping gene (HKG) in the form of a weighted expression index. To circumvent this issue, an Excel-based spreadsheet software application, BestKeeper, can be used. The software uses descriptive statistics of the derived crossing points (CP) to compute for each HKG: the geometric mean (GM), arithmetic mean (AM), minimal (Min) and maximal (Max) value, standard deviation (SD), and coefficient of variance (CV). All CP data were compared over the entire study, including control and all treatment groups. Three genes were ultimately investigated as possible housekeeping genes. The x-fold over- or under-expression of individual samples towards the geometric mean CP were calculated, and the multiple factors of their minimal and maximal values, expressed as the x-fold ratio and its standard deviation, are presented.

2.2.9.2.2 The relative expression levels calculations

Relationships between the quality and the Cq values were measured by correlating Cq values and intensity ratio values. The Cq values were gathered from qPCR data, and relative expression levels of the genes were calculated using the $2^{-\Delta\Delta Ct}$ method (Pfaffl, 2001; Schmittgen and Livak, 2008), which represents the Cq (cycle threshold) difference between the reference ribulose-1,5-bisphophate carboxylase/oxygenase (RuBisCo) gene and the target gene product.

2.3 Additional Information

BestKeeper: http://www.gene-quantification.de/bestkeeper.html

GeneMania: https://genemania.org/

GO annotation: http://go.princeton.edu/cgi-bin/GOTermFinder

MIPS Arabidopsis Thaliana DataBase:
https://www.hsls.pitt.edu/obrc/index.php?page=URL1096992371

MapMan: http://mapman.gabipd.org/

NCBI (BLAST analyses): http://www.ncbi.nlm.nih.gov/

NCBI (Primer BLAST): http://www.ncbi.nlm.nih.gov/tools/primer-blast/

OligoPerfect Designer (Invitrogen™):
https://www.thermofisher.com/ca/en/home/life-science/oligonucleotides-primers-probes-genes/custom-dna-oligos/oligo-design-tools/oligoperfect.html

Online Analysis Tools (Internet Resources for Molecular Biologists):
http://molbiol-tools.ca

Primer3: http://www-genome.wi.mit.edu/cgi-bin/primer/primer3_

The Arabidopsis Information Resource (TAIR) http://www.arabidopsis.org/

3. RESULTS AND DISCUSSION

3.1 Preface

The primary aim of this research was to gain insights into the potential involvement of PIPs (AQPs) and other proteins in establishing high hydrostatic pressure within the *Arceuthobium* spp. fruit, ultimately resulting in explosive discharge. Other processes possibly involved in seed dispersal include heat production (thermogenesis; deBruyn et al., 2015), the lowering of the number of stomata (density), the thickening of the cuticle on the surface of the fruit (Ziegler & Ross Friedman, 2017a,b), and the increasing production of lipids and sterols by vesicular cells (Kelly et al., 2009) Heterologous microarray hybridization was used along with other molecular, biochemical, and physiological approaches to understand PIPs and other genes and their expression in seed dispersal.

Due to the large number of identified genes, diversity of techniques, and obtained results, the findings are discussed separately after each section. Finally, encompassing conclusions are given at the end of this chapter.

During the initial research in Germany, entire aerial shoots of *Arceuthobium oxycedri* from the Botanical Garden in Darmstadt, Hesse, were used (these will be referred to as “plants”, keeping in mind the endophytic system could not be readily acquired). Initially, this species was used because the samples imported from Canada did not reveal RNA, as it degraded during transport, even though they had been preserved in RNA*Later* solution (QIAGEN). As *Arceuthobium oxycedri and Arceuthobium americanum* are closely related species (same genus), and as both are the most ranging species in their respective continents, it was decided to first use *A. oxycedri* for RNA extraction. Later in the study, RNA from *A. americanum*—the whole plant or just the fruit—was used. The first step in the research was to extract and establish a sufficient RNA-extraction technique for this genus. At the time, little molecular research had been done with that genus, so the process began with established methods for model plants such as *Arabidopsis thaliana*, for recalcitrant plants tissue such as tree leaves (pine, Norway spruce, ginkgo), and for plants known for high concentrations of phenols and carbohydrates such as *Vitis vinifera* fruits (Gehrig, 2000).

3.2 Material for Analysis

3.2.1 Total RNA extraction from fresh *A. oxycedri* and *A. americanum*

There are several standard and modified methods for isolating RNA from eukaryotic organisms (Vomelová et al. 2009). However, RNA extraction from plants is frequently more difficult in comparison to its extraction from other kingdoms. The fruits of many plants are even more problematic in this regard, as they possess vast amounts of secondary metabolites such as polysaccharides, polyphenols, terpenoids, and nitrogen- and sulphur- containing compounds (Hu et al., 2002). Therefore, the procedure has to be tailored to the plant species, and additional modifications of standard methods are needed in terms of types of extraction buffers, addition of polyethylene glycol (PEG), polyvinylpyrrolidinone K30 (PVP) and other chemicals, and length and temperature of extraction.

Both spectroscopic (NanoDrop™ and standard analysis in UV-vis light) and fluorometric methods (Qubit) were used to analyze RNA or DNA quantity and quality. As nucleic acids display optimum absorbance at 260 nm (Winfrey et al., 1997), spectroscopic analysis, in addition to the quantity of the nucleic acid, was used to determine the A260/230 and A260/280 ratios (quality). Such spectroscopic analysis provided insight into possible contaminants in the sample that may affect cDNA library preparation, microarray study, or qRT-PCR analysis. An A260/280 ratio was used for protein contamination, and an A260/230 ratio was used to evaluate contamination by polyphenols and polysaccharides (Loulakakis et al., 1996). While ratios A260/280 and A260/230 are usually good indicators of contamination, they are not necessarily good indicators if RNA is intact (Imbeaud et al. 2005; Die and Roman, 2012). Table 3.1 shows the yield and quality of RNA extracted from *A. americanum* fruits obtained using the NanoDrop™ technique.

Additionally, the samples were run on a denaturing gel. The method relies on the assumption that rRNA quality reflects the mRNA (constituents of total RNA) (Sambrook et al. 1989). The rRNA quality is evaluated visually using the intensities of ribosomal bands with high quality RNA showing at least two sharp rRNA bands indicating 28S (5kb) and 18S (2K) bands with some smearing between the bands (Figure 3.1), and, if run long enough, also showed 16S and 23S bands. Generally, mRNA is not easily visualized on the gel as mRNA has many different sizes, but smearing between strong rRNA bands indicates mRNA.

After many trials, the QIAGEN-made RNeasy kit with 2% (w/v) polyethylene glycol (PEG) added to a lysis buffer was chosen for a whole plant extraction, and

MasterPure™ (Epicentre) was chosen for fruit extraction. These were the two techniques of many that gave the best results in terms of the quality of RNA obtained to ensure that RNA was suitable for qRT-PCR and microarray hybridization. Figures 3.1 and 3.2 show the results obtained, respectively, using each technique.

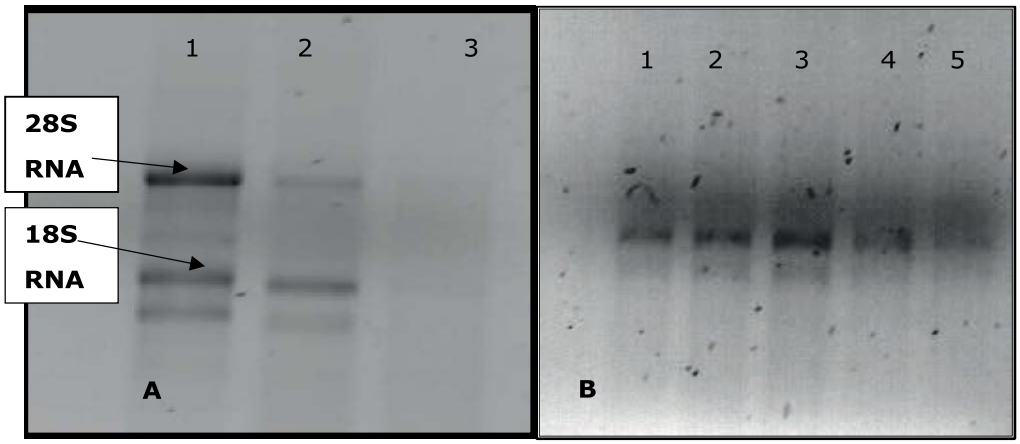

Figure 3.1 Total RNA extracted from a whole mistletoe plant or mistletoe fruit using the RNeasy kit. (A) RNeasy kit with 2% Polyethylene glyco (B) with no addition of 2% polyethylene glycol. Samples from (A) indicate high quality RNA showing two sharp rRNA bands indicating 28S and 18S rRNA with very little smearing. Line 1 represents RNA from a whole plant; line 2 represents RNA from the fruit. All samples from (B) show high RNA degradation – no definite bands of 28S and 18S RNA. Lines 1, 2, and 3 represent a whole plant, lines 4 and 5 fruit tissue.

However, as fruits are richer in the chemicals listed earlier, the MasterPure™ (Epicentre) kit was used for extracting RNA from the fruits of *A. americanum* as it shows better results in terms of the quality of RNA obtained.

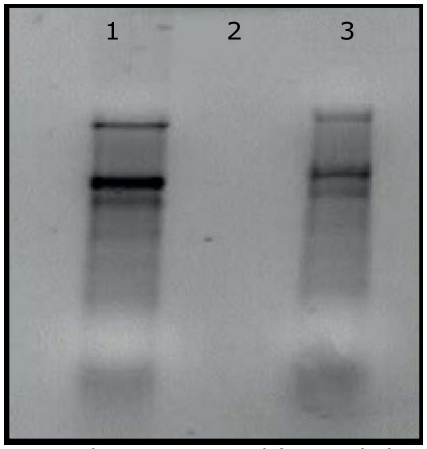

Figure 3.2 Total RNA extracted from mistletoe fruit using MasterPure™ with 1.5% denaturing agarose gel. Line 1 represents *A. americanum* fruit from a fresh plant. Line 2 represents negative control. Line 3 represents *A. americanum* fruit stored in RNA*Later* solution.

Table 3.1 *NanoDrop™ results showing total concentration of RNA extracted from the fruits of A. americanum as well as A260/230 and A260/280 ratios for RNA sent for Affymetrix microarray analysis.*

Sample	Concentration	A260/280	A260/230
A (May 26)	209.9 ng/µl	1.72	1.98
B (July 25)	186.5 ng/µl	1.17	1.89
C (August 25)	86.2 ng/µl	0.79	1.80
D (September 2)	207.9 ng/µl	1.22	1.85

3.2.1.1 Discussion

Numerous standard protocols and commercially available kits for RNA extraction were used, and they gave unsatisfactory results for various dwarf mistletoe tissue (for both plants without fruit, and in particular, with fruit). The LiCl precipitation method has been employed for years to extract RNA from diverse plants, because it offers many advantages over other methods, such as avoiding DNA, carbohydrate, or protein precipitation (Barlow et al., 1963), in contrast to RNA that is precipitated efficiently. Moreover, modifications such as the addition of chloroform/phenol extractions as well as further additions such as CTAB, PVP and Spermidine (Birtić & Kranner, 2006.) could be used. Therefore, methods designed by Chang et al. (1993) using CTAB, PVP, and Spermidine, and by Iandolino et al. (2004) using 2% beta mercaptoethanol in an extraction buffer, and chloroform-isoamyl alcohol for DNA precipitation were applied. Commercial chemical combinations (without any modifications) such as RNeasy (column method; QIAGEN), which combines the selective binding properties of a silica-based membrane with the speed of microspin technology, and MasterPure™ (Epicentre®) were used as well. The latter relied on a gentle salt precipitation of nucleic acid without the use of a column (contrary to the Qiagen method), which frequently reduced the RNA yield. However, as dwarf mistletoe fruit contains, in addition to many polyphenolics and polysaccharides, fatty acid methyl esters (Kelly et al., 2009), extraction was more challenging than first thought, so additional modifications were needed. It was discovered that addition of HMW-PEG (Gehrig et al. 2000), helped to remove some polyphenolics and polysaccharides. Therefore, HMW-PEG modification was used with the RNeasy kit by adding HMW-PEG to a lysis buffer. Ultimately, after many trials, the QIAGEN RNeasy kit with 2% (w/v) PEG added to a lysis buffer was chosen for a whole plant extraction; and MasterPure™ (Epicentre) was selected for fruit extraction. These were the two techniques of many that gave the best results in terms of the quality and quantity of RNA obtained that was suitable for PCR, cDNA library construction, two microarray analyses, and the qRT-PCR experiments described in the following sections.

3.3 Analysis of differential gene expression

3.3.1 Complementary DNA library construction

cDNA library construction is a technique aiming at placing pieces of DNA into plasmid vectors (cloning), which are then inserted into a bacterial host such as *E. coli* using a process called transformation. By doing this, cloned DNA can be stored and replicated as needed and used for identifying genes of interest as well as for detecting their differential expression. After positive cloning using SMARTer™ RACE (Clontech Laboratories Inc./Takara) technology and pDrive vector, all positive colonies (4,000) from LB/AMP/IPTG/X-Gal plates were transferred into 96 well trays with LB AMP broth for growth and consecutive storage.

3.3.2 Heterologous microarray

DNA arrays are a group of technologies in which DNA sequences are either deposited or synthesized in a two- or three-dimensional array on a surface. An original, very simple version of a DNA array was created in the 70s by Grunstein and Hogness (1975). The technology progressed more rapidly in the 90s and 2000s with the development of more advanced methods involving better substrates for DNA attachment; or different modes of detection of hybridization such as fluorescent or chemiluminescent detection. As a result, many variations of the array method eventually entered the scientific market that are differing from the original method. If a target and probe are from the same species, a homologous microarray is deployed. However, when closely related – or unrelated – organisms are involved, then the microarray is referred as heterologous. While homologous microarrays are more common, it has been demonstrated that microarrays from closely related, heterologous species can be used to probe the transcriptomes of non-model plants (Davey et al., 2009).

For this research, two types of heterologous microarrays were used: a spotted array (MicroCASTer handheld microarray system), and an in situ synthesized array developed by Affymetrix.

3.3.2.1 Spotted array- MicroCASTer handheld microarray system

As explained in Materials and Methods, PCR with M13 primers for a clone from each well (96) was performed initially, and then NC-C slides (microarray chips – see section 3.3.2.1.1 below) were spotted with the PCR products (cDNA) using a MicroCASTer handheld microarray system and MicroHybridization kit protocol. The PCR products were also stored (-20°C) for further study. Afterwards, using a mixture of DIG-11-dUTP-labelled probes from variety of plants (Materials and Methods), a

blot hybridization was performed on the chips to screen the library for AQPs and other genes potentially related to the dwarf mistletoe explosive seed dispersal. Bright, positive chemiluminescent spots (Figure 3.3) were detected on the chips, indicating hybridization of the probe to a specific clone. The position of positive spots was then used to find cDNA clones from an *A. oxycedri* library using a scheme (Materials and Methods) designed once the slides were spotted for microarray analysis. Their sizes were confirmed by PCR and after sequencing, sequence similarity to the genes: PIP2; Alkaline/neutral invertase portion of gene (CINV2), ATP-binding cassette transporter family, Sterol 14-demethylase, and Ribulose-1,5-bisphophate carboxylase/oxygenase were found (described in Section 3.4).

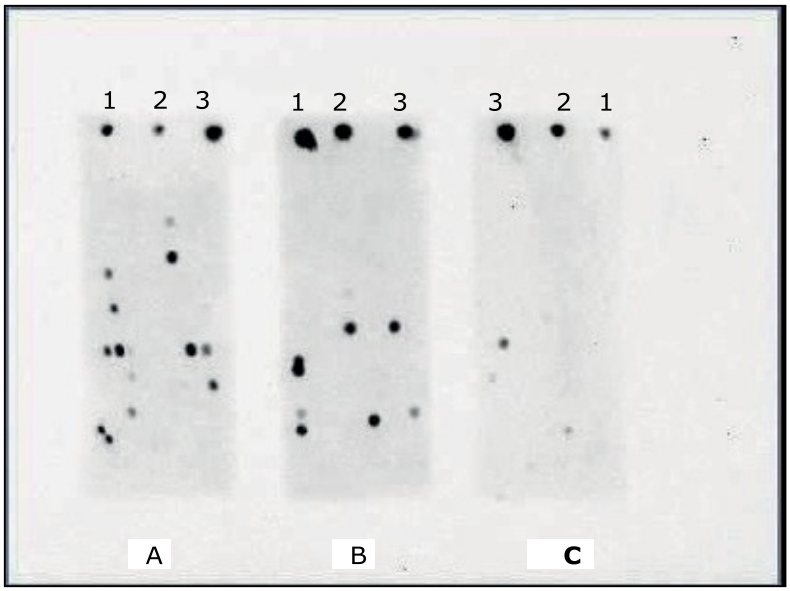

Figure 3.3 Chips (A-B-C) with positive hybridization results. Black spots ( ) indicate positive chemiluminescence caused by hybridization of the probe to a specific clone of *A. oxycedri.* Numbers 1, 2, 3 on each chip indicate different concentrations of positive control (NtAQP1).

3.3.2.1.1 Choosing the best solid medium for heterologous microarray analysis

The microarray technique needs a supportive, solid medium and coating to absorb a sample. Usually, as a solid support, a borosilicate glass slide is used, and then the slide is covered with a unique coating that provides a uniform surface for a biomolecule attachment**.** There are a few types of coatings used, with aminosilane-coated slides (Schott's NEXTERION® Slide A+) being the most popular for application of long oligonucleotides (Conzone & Pantano, 2004) and PCR products. Aminosilane, being positively charged, is perfectly suited, adsorbing negatively charged DNA molecules (Figure 3.4). However, as the research was done in a laboratory supplied with new nitrocellulose-coated slides (Figure 3.5) characterized with a very small pore size (Schott's NEXTERION® Slide NC-C), these slides were also tested for their

usefulness in DNA microarray analysis. NEXTERION® Slide NC-C is coated with a new nitrocellulose formulation that contains a higher cellulose nitrate content than older versions. This improved nitrocellulose membrane also possesses a higher density polymer and a smaller pore size (SCHOTT Technical Glass Solutions GmbH, 2010).

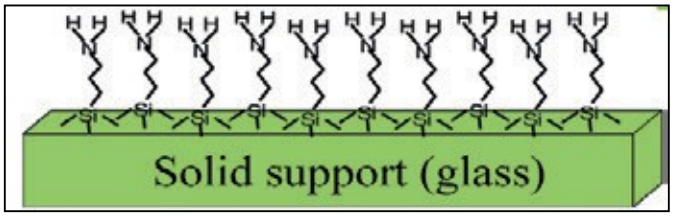

Figure 3.4 Aminosilane-coated slide surface (Adapted from Conzone & Pantano, 2004).

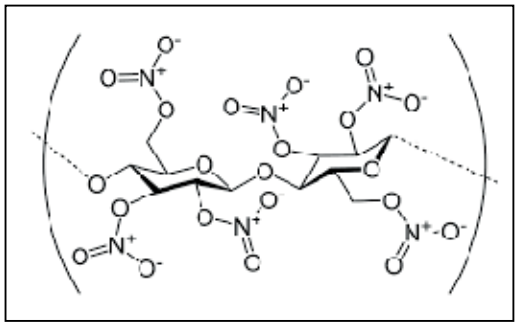

Figure 3.5 Nitrocellulose used to coat a slide surface.

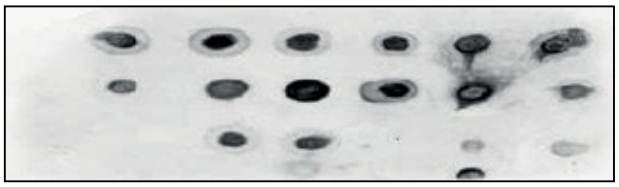

Figure 3.6 Aminosilane Nexterion® slide spotted with PCR products. Black spots indicate the positive hybrids.

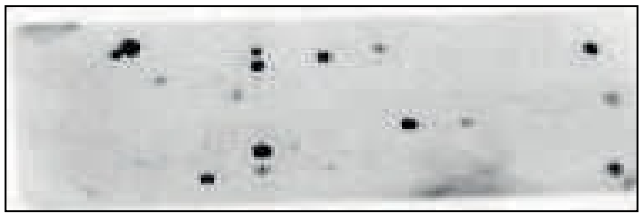

Figure 3.7 Nitrocellulose NEXTERION® NC-C slide spotted with PCR products. Black spots indicate the positive hybrids.

3.3.2.1.2 Discussion regarding the MicroCASTer handheld microarray system

Nitrocellulose is produced by treating cellulose with nitric acid to get each glucose unit in the cellulose polymer esterified with nitrate groups, which are responsible for the negative charge of nitrocellulose at neutral pH (Figure 3.4). Even though

nitrocellulose membranes were originally used only to filter out bigger particles, they are now used primarily to adsorb macromolecules throughout the filter matrix (pore size); and mostly hydrophilic and electrostatic interactions are responsible for binding macromolecules to the filter. The nitrocellulose slide performance is strongly dependent on the internal, three-dimensional membrane structure and surface quality. However, how macromolecules bind to nitrocellulose is still not well known; but electrostatic and hydrophobic interactions are proposed as probable binding mechanisms (Nakamura et al., 1989). To attach molecules such as DNA, molecules first have to be dissolved in an SSC buffer and then they can be applied on a slide. Pilot tests were run with both types of slides, Aminosilane NEXTERION® and NEXTERION® NC-C slides, and the results (spots) using NC-C-coated slides (Figure 3.7) were clearer and better defined in comparison to aminosilane slides using the same concentrations of samples (Figure 3.6).

The heterologous approach allowed us to obtain sequences of five genes from the non-model organism, *Arceuthobium oxycedri*. The genes sequences were used for further investigations.

3.3.2.2 Affymetrix microarray

3.3.2.2.1 Affymetrix heterologous microarray and identification of differentially expressed genes

Encouraged by the positive results obtained using the heterologous approach with the MicroCASTer handheld microarray system, the Affymetrix microarray with heterologous probes was used to obtain the broader profile of gene expression in *Arceuthobium* spp. This approach was used because it is less expensive than the homologous approach in the case of non-model organisms, as there is no need to produce species-specific chips, and instead it utilizies commercially available *Arabidopsis thaliana* chips (Davey et al., 2009, Boudichevskaia et al., 2015). Difficulties related to sequence divergence between the test and reference organism exist, but they can be overcome by using appropriate data analyzing tools. Each individual gene transcript on the *Arabidopsis* ATH-1 GeneChip® microarray is represented by a set of eleven 25 bp probe pairs that make a probe set. Using the standard approach, like in case of homologous approach, signals are first calculated as the mean value; and then used to determine the expression level for a gene. In contrast, for the case of the heterologous approach, the strategies used by Hammond et al. (2005) and Davey et al. (2009) were employed where the similarity between the target and the individual probe sequences were monitored before signal averaging. This procedure enabled removal of very weak or non-hybridizing individual probes and kept only strong signal probes.

To investigate the transcriptome profile of dwarf mistletoes based on an *Arabidopsis* Gene 1.0 ST array, the expression level of individual probes was first analyzed within a probe-set related to each transcript. A script written in the Perl programming language (Davey et al., 2009) was used to analyze an Affymetrix Aragene-1_0-st .cdf file of the chip from the May sample. This process recognizes and eliminates those individual probes within each probe-set with perfect match probe intensities below a distinct cut-off value. Similar to Hammond et al. (2005) and Davey et al. (2009), the hybridization intensity threshold used for probe exclusion was set arbitrarily and ranged from 0 (no probe selection) to 1,000 (Figure 3.8). The requirement for a probe-set to be determined as present necessitates that the hybridization has at least one visible probe pair within that probe-set. The resulting modified .cdf files (May .cdf files) with hybridization intensity thresholds from 0 to 1,000 were generated. As in Figure 3.8, the quantity of individual retained probes within a probe set decreased significantly with expanding hybridization intensity threshold. Concurrently, the quantity of test sets retained diminished moderately. Consequently, the number of probe-sets available for the transcriptome analysis remained high enough to obtain a rough, comprehensive view of expression trends for those genes in *A. americanum*.

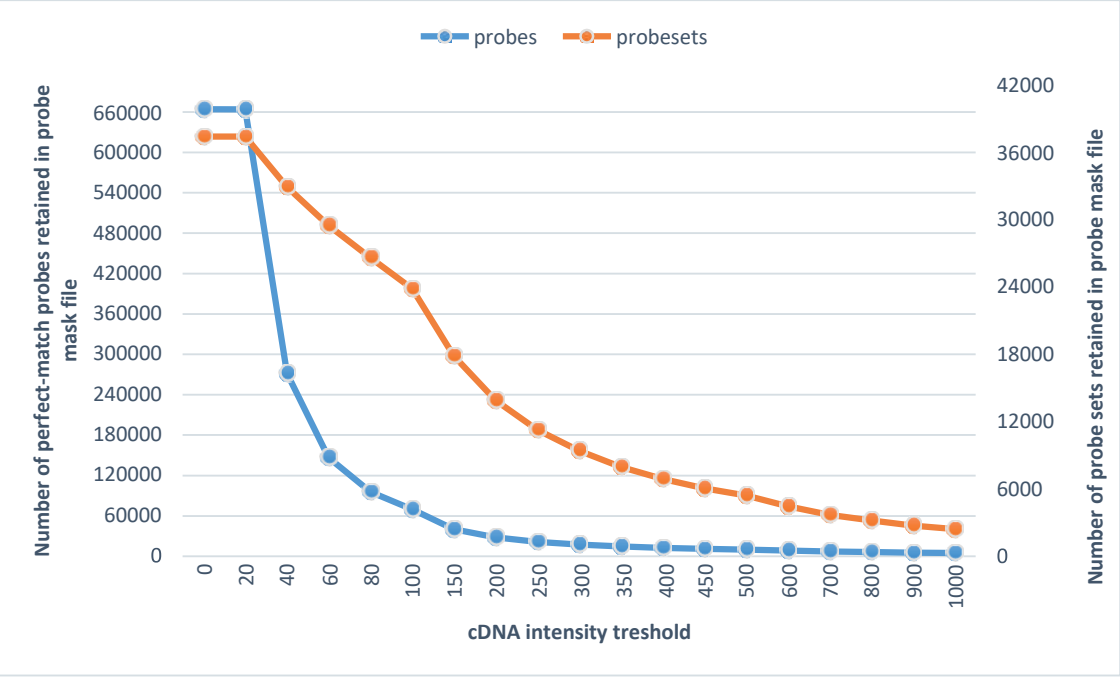

Figure 3.8 Influence of hybridization intensity thresholds on the number of probes and probe-sets retained in the probe mask following hybridization of *A. americanum* to Affymetrix Arabidopsis ATH-1 GeneChip®.

Additionally, to measure transcript abundance, the new probe-masking files with thresholds range 0-700 were used for RNA hybridization-based transcriptome analysis. Each May .cdf file that had a corresponding intensity with 6 .cel file arrays

(May 1-3 and September 1-3) were processed by a robust multi-array average (RMA) algorithm and log2 transformed by the RMAExpress program to get data of differentially expressed genes in May (Appendix III:1). Log2 values were giving the fold change of the expression and a +/- sign showing the up or down regulation in comparison to the May or September expression. Later, the transcripts showing a log2 fold change ≥1 or ≤−1 with a p-value below 0.05 were accepted as significant. In a view of t-test and false discovery rate (FDR) adjustments of p-values, a list of differentially expressed genes for each May .cdf file was acquired. As shown on Figure 3.9, the highest number of differentially expressed genes was discovered utilizing a May.cdf value of 300.

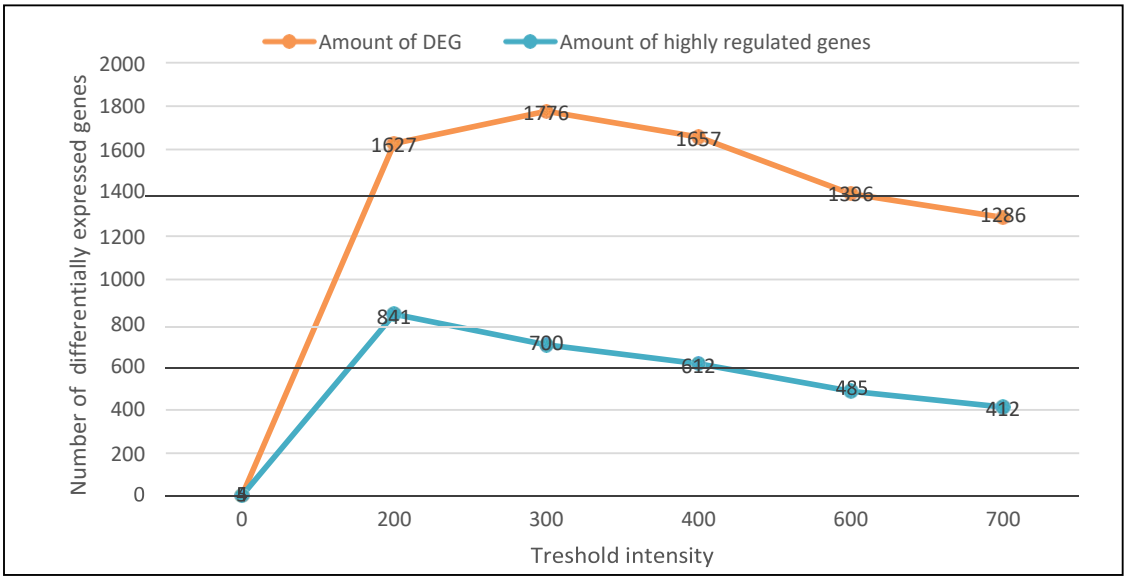

Figure 3.9 The effect of hybridization intensity thresholds used to generate the probe-mask (computable document format) files on detection of differentially regulated genes following hybridization of labelled *A.americanum* to Affymetrix Arabidopsis ATH-1 GeneChip®. The 300 threshold intensity cut-off level was used for further investigations.

Using a 300 intensity threshold as the cut-off level, 9,036 probe-sets out of 37,409 probe-sets representing 24.2% of *Arabidopsis* Gene 1.0 ST array were hybridized to *A. americanum* RNA. From 9,036 probe-sets, 1,776 probe-sets corresponding to 1,624 genes were differentially expressed in May with 700 probe-sets (661 genes) were highly differentially expressed. To further analyze the expression profile in the developing fruit of dwarf mistletoe based on data obtained with the May .cdf value of 300 was used.

To examine other differentially expressed genes activated in September that might be filtered out in May .cdf files, the Aragene-1_0-st .cdf file of one chip from the

September sample was analyzed. The same procedure described for the May sample was applied to data created with the September .cdf file. At a cut-off level of 300, 1,690 differentially expressed genes in September were identified. Among them, 767 genes were highly differentially expressed (Table 3.2). The differentially expressed genes obtained with the September .cdf value of 300 were used in comparative analysis to elucidate the biological processes specific to the mature fruit before seed dispersal.

Table 3.2 *List of genes obtained from hybridization of A. americanum cDNA to Affymetrix Arabidopsis ATH-1 GeneChip® using .cdf value of 300 as the cut-off level.*

	September	**September with high expression All log2 fold change with a p-value below 0.05**	**May**	**May with high expression All log2 fold change w p-value below 0.05**
Number of highly differentially expressed genes (DEG)	1,690	767	1,624	661

3.3.2.2.2 Gene Ontologies

The amount of differentially expressed genes based on the heterologous approach depends on the similarity between the probes' sequences and the RNA as well as the hybridization intensity threshold cut-off values (.cdf values) used to create the probe-mask file (Davey et al., 2009). As a result, many genes can be filtered out; thus, a list of candidate genes may not be entirely representative. Consequently, the results of the functional classification of genes based on a gene ontology tool such as the GO::TermFinder (Boyle et al., 2004) have to be interpreted with discretion. The gene list from May and September with intensity threshold 300 was examined for significant GO terms accompanying the same biological process. Detailed information about identified GO categories (FDR-adjusted *p*-value <0.05) for 63 biological processes and 30 cellular compartment groups from May is shown in Table 3.3. Additionally, Appendix III:3 and III:4) contains additional dataanalysis.

Table 3.3 *Overview of the functional classes of the list of 1,624 genes (GO categories) for biological processes (A) and cellular compartment (B). GOID, gene ontology identifier; Term, GO term name; num_list_annotations, number of genes; list size, total number of genes; % from a gene list, percentage of the genes from a total list size.*

A

GOID	TERM	NUM_LIST_ANNOTATIONS	LIST_SIZE	% from the gene list
GO:0009987	cellular process	966	1624	59.48275862
GO:0008152	metabolic process	876	1624	53.9408867
GO:0044699	single-organism process	816	1624	50.24630542
GO:0071704	organic substance metabolic process	802	1624	49.38423645
GO:0044237	cellular metabolic process	762	1624	46.92118227
GO:0044238	primary metabolic process	755	1624	46.49014778
GO:0044763	single-organism cellular process	653	1624	40.20935961
GO:0043170	macromolecule metabolic process	630	1624	38.79310345
GO:0044260	cellular macromolecule metabolic process	584	1624	35.96059113
GO:0009058	biosynthetic process	539	1624	33.18965517
GO:1901576	organic substance biosynthetic process	520	1624	32.01970443
GO:0044249	cellular biosynthetic process	509	1624	31.34236453
GO:0006807	nitrogen compound metabolic process	499	1624	30.72660099
GO:0034641	cellular nitrogen compound metabolic process	468	1624	28.81773399
GO:0044710	single-organism metabolic process	456	1624	28.07881773
GO:1901360	organic cyclic compound metabolic process	444	1624	27.33990148
GO:0006725	cellular aromatic compound metabolic process	429	1624	26.41625616
GO:0046483	heterocycle metabolic process	409	1624	25.18472906
GO:0006139	nucleobase-containing compound metabolic process	376	1624	23.15270936
GO:0009059	macromolecule biosynthetic process	368	1624	22.66009852
GO:0034645	cellular macromolecule biosynthetic process	359	1624	22.10591133
GO:0010467	gene expression	357	1624	21.98275862
GO:0090304	nucleic acid metabolic process	337	1624	20.75123153
GO:0044271	cellular nitrogen compound biosynthetic process	336	1624	20.68965517
GO:0071840	cellular component organization or biogenesis	323	1624	19.88916256
GO:0032502	developmental process	315	1624	19.39655172
GO:0044767	single-organism developmental process	311	1624	19.15024631
GO:1901362	organic cyclic compound biosynthetic process	310	1624	19.08866995
GO:0016070	RNA metabolic process	299	1624	18.41133005
GO:0016043	cellular component organization	295	1624	18.16502463
GO:0032501	multicellular organismal process	295	1624	18.16502463
GO:0051179	localization	289	1624	17.7955665
GO:0019438	aromatic compound biosynthetic process	289	1624	17.7955665
GO:0019222	regulation of metabolic process	276	1624	16.99507389
GO:0018130	heterocycle biosynthetic process	274	1624	16.87192118
GO:0051234	establishment of localization	269	1624	16.56403941
GO:0006810	transport	262	1624	16.13300493
GO:0034654	nucleobase-containing compound biosynthetic process	243	1624	14.96305419
GO:0060255	regulation of macromolecule metabolic process	242	1624	14.90147783
GO:0031323	regulation of cellular metabolic process	239	1624	14.71674877
GO:1902578	single-organism localization	238	1624	14.65517241
GO:0044765	single-organism transport	236	1624	14.5320197
GO:0032774	RNA biosynthetic process	220	1624	13.54679803
GO:0044281	small molecule metabolic process	219	1624	13.48522167
GO:0006351	transcription, DNA-templated	219	1624	13.48522167
GO:0097659	nucleic acid-templated transcription	219	1624	13.48522167
GO:0043933	macromolecular complex subunit organization	125	1624	7.697044335
GO:0006811	ion transport	119	1624	7.327586207
GO:0048518	positive regulation of biological process	105	1624	6.465517241
GO:0009416	response to light stimulus	102	1624	6.280788177
GO:0022607	cellular component assembly	92	1624	5.665024631
GO:0006812	cation transport	88	1624	5.418719212
GO:0071822	protein complex subunit organization	80	1624	4.926108374
GO:0065003	macromolecular complex assembly	76	1624	4.679802956
GO:0070271	protein complex biogenesis	72	1624	4.433497537
GO:0034622	cellular macromolecular complex assembly	71	1624	4.371921182
GO:0006461	protein complex assembly	70	1624	4.310344828
GO:0006091	generation of precursor metabolites and energy	68	1624	4.187192118
GO:0000003	reproduction	67	1624	4.125615764
GO:0043623	cellular protein complex assembly	62	1624	3.81773399
GO:0015979	photosynthesis	52	1624	3.201970443
GO:0019684	photosynthesis, light reaction	40	1624	2.463054187
GO:0015672	monovalent inorganic cation transport	38	1624	2.339901478

B

GOID	TERM	NUM_LIST_ANNOTATIONS	LIST_SIZE	% from gene list
GO:00056	cell	1358	1624	83.62068966
GO:00444	cell part	1354	1624	83.37438424
GO:00056	intracellular	1239	1624	76.29310345
GO:00444	intracellular part	1236	1624	76.10837438
GO:00432	intracellular organelle	1117	1624	68.78078818
GO:00432	organelle	1117	1624	68.78078818
GO:00432	intracellular membrane-bounded organe	1090	1624	67.1182266
GO:00432	membrane-bounded organelle	1090	1624	67.1182266
GO:00057	cytoplasm	808	1624	49.75369458
GO:00444	cytoplasmic part	665	1624	40.94827586
GO:00160	membrane	445	1624	27.40147783
GO:00444	intracellular organelle part	326	1624	20.07389163
GO:00444	organelle part	326	1624	20.07389163
GO:00095	plastid	280	1624	17.24137931
GO:00095	chloroplast	275	1624	16.93349754
GO:00444	membrane part	236	1624	14.5320197
GO:00329	macromolecular complex	178	1624	10.96059113
GO:00432	protein complex	135	1624	8.312807882
GO:00444	plastid part	114	1624	7.019704433
GO:00444	chloroplast part	110	1624	6.773399015
GO:00319	organelle subcompartment	67	1624	4.125615764
GO:00095	chloroplast thylakoid	48	1624	2.955665025
GO:00319	plastid thylakoid	48	1624	2.955665025
GO:00444	thylakoid part	44	1624	2.709359606
GO:00426	thylakoid membrane	41	1624	2.524630542
GO:00343	photosynthetic membrane	41	1624	2.524630542
GO:00095	chloroplast thylakoid membrane	40	1624	2.463054187
GO:00550	plastid thylakoid membrane	40	1624	2.463054187
GO:00095	photosystem I	11	1624	0.677339901
GO:00095	chloroplast ATP synthase complex	4	1624	0.246305419

3.3.2.2.3 Discussion regarding the Affymetrix heterologous approach

An improved and increased variety of gene expression analysis tools, such as gene arrays and Next Generation Sequencing (NGS), may be used in research related to development, seed dispersal, and transport, as well as host resistance mechanisms and patterns of parasite gene expression. Molecular data has proven to be a valuable supplement to both microscopic and physiological data, providing deeper and more comprehensive insight. Recently, a number of publications have demonstrated the utility of NGS techniques in transcriptome analysis of non-model parasitic plants (Westwood et al., 2012; Honaas et al., 2013; Ranjan et al., 2014; Yang et al., 2015). However, despite the obvious advantages of the NGS approach, challenges such as standardization of procedures, productivity, speed, cost, data analysis and storage still exist; therefore, microarray analysis still appears to be a very valuable tool for a large-scale gene expression profiling as well as it provides highly consistent data and using well-established analytical pipelines. Finally, results obtained using microarray techniques are much easier to interpret in comparison to NGS (Zhao et al., 2014).

As such, following the successful results obtained using the handheld heterologous microarray methodology, a heterologous microarray approach based on highly annotated *Arabidopsis* Gene 1.0 ST Arrays (Affymetrix) was employed. The high

probe coverage across the entire transcript of *A. thaliana* specific to this array made the identification of genes expressed in the non-model plant, dwarf mistletoe, very promising. Knowing that potential mismatches between probe and target sequences require special considerations (heterologous approach), a script to parse an Affymetrix .cdf file of the selected chip to identify and remove those perfect match probe intensities below a defined cut-off value was used (Hammond et al., 2005; Davey et al., 2009). The cut-off value of 300 was chosen arbitrarily based on previously obtained results. As a result, despite sequence significant divergence between the two species, 24.2% of *Arabidopsis* Gene 1.0 ST array was hybridized to *A. americanum* RNA at this cut-off level. This allowed the opportunity to identify approximately 1,000 genes that are highly differentially expressed in dwarf mistletoes during fruit development.

It was shown that application of the heterologous GeneChip approach could provide a global overview of physiological processes. Results from this study can be used as a good starting point for planning further research related to specific issues of dwarf mistletoe parasitism, physiology, and seed dispersal or control strategies.

3.3.2.2.4 Dwarf mistletoe and gene ontology

Filtering out perfect match probe intensities below a defined cut-off value efficiently reduces the number of gene transcripts that can be measured in heterologous microarray experiments (Kassahn, 2008) and artificially decreases the number of differentially expressed genes that potentially belong to the same functional category. It is expected that, in case of heterologous microarrays, experiments are more effective in measuring gene responses at conserved gene loci, while genes that have diverged significantly are expected to show poor cross-hybridization (Kassahn, 2008). Regardless, despite the problems mentioned above, the use the heterologous approach allowed to obtain a comprehensive view of expression tendencies for genes differentially expressed in fruit of dwarf mistletoe.

3.3.2.2.4.1 General information about water, nutrients, and transport

Even though dwarf mistletoes are hemiparasites, they appear to have limited photosynthesis (Těšitel et al., 2010). As such, to survive, they must also obtain water and nutrients from the host plant. GO term “Transport” (GO:0006810; Table 3.3 A), includes 262 genes that were over-represented in the gene list (FDR-adjusted *p*- value <0.01). This category connects genes related to transport of amino acids, calcium, potassium, sugars, metals, sulfates, and others (Appendix III:2). Among highly expressed genes in developing dwarf mistletoes fruits are three aquaporin genes (PIP1;4; PIP2;4; PIP2B) encoding water channel proteins. All of them are up

regulated in May and down regulated in September with the PIP2B (AT2G37170) showing the highest expression (log_2 value of 2.21). Figure 3.10 shows the phylogenetic tree of the three aquaporin genes in relation to other AQPs, possibly found in plants. Additionally, 10 significantly differentially expressed genes encoding amino acid transporters were found. Six were highly up-regulated in May (fold difference ≥2). Amino Acid Permease, AAP3 (AT1G77380), with a log_2 value of 4.56, had the highest expression. This transporter is responsible for a transport of variety of amino acids like proline, which is known as a major osmolite, so it helps in the accumulation of osmotically active compounds in a male flower and roots (Okumoto et al., 2004). AAP3 expression in female flowers and fruits hasn't been yet observed, but Affymetrix results indicate that AAP3 transporter is remarkably active in the *Arceuthobium* fruit, and so might be involved in creation of osmotic pressure, which would be particularly noteworthy with respect to explosive seed dispersal. Additionally, the AAP3 is acknowledged for its crucial role in the parasitism of the root-knot nematode of *Arabidopsis*. It was shown that disruption of amino acid transport had negative influence on nematode parasitism (Marella et al., 2013; Elashry et al., 2013).

Dwarf mistletoe was found to use a variety of sugars in its metabolism, including those acquired from the host. A total of 12 differentially expressed genes involved in sugar transport (Appendix III:2) were found. Eight of them were up-regulated in developing fruit, and four of those were highly induced (log_2 min ≥1). At the same time, genes representing inositol transporter ATINT2 and UDP-GALACTOSE TRANSPORTER 6 were highly down-regulated in May. Other genes highly up-regulated in May were those with gene products involved in transport, including metal transporters, ATP-binding cassette (ABC) transporters, zinc transporter, potassium transporter, and boron transporter. Calcium transporter CAX4 and its activator CXIP2 are also highly induced in dwarf mistletoe fruit. Similarly, Up-regulated genes encoding transporters such as the ABC transporter, sugar transporter, and amino acid transporter were identified to be enriched in haustorial tissue of the another plant parasite, *Cuscuta* (Ranjan et al., 2014) and at least two species of parasitic *Orobanchaceae* (Yang et al., 2015).

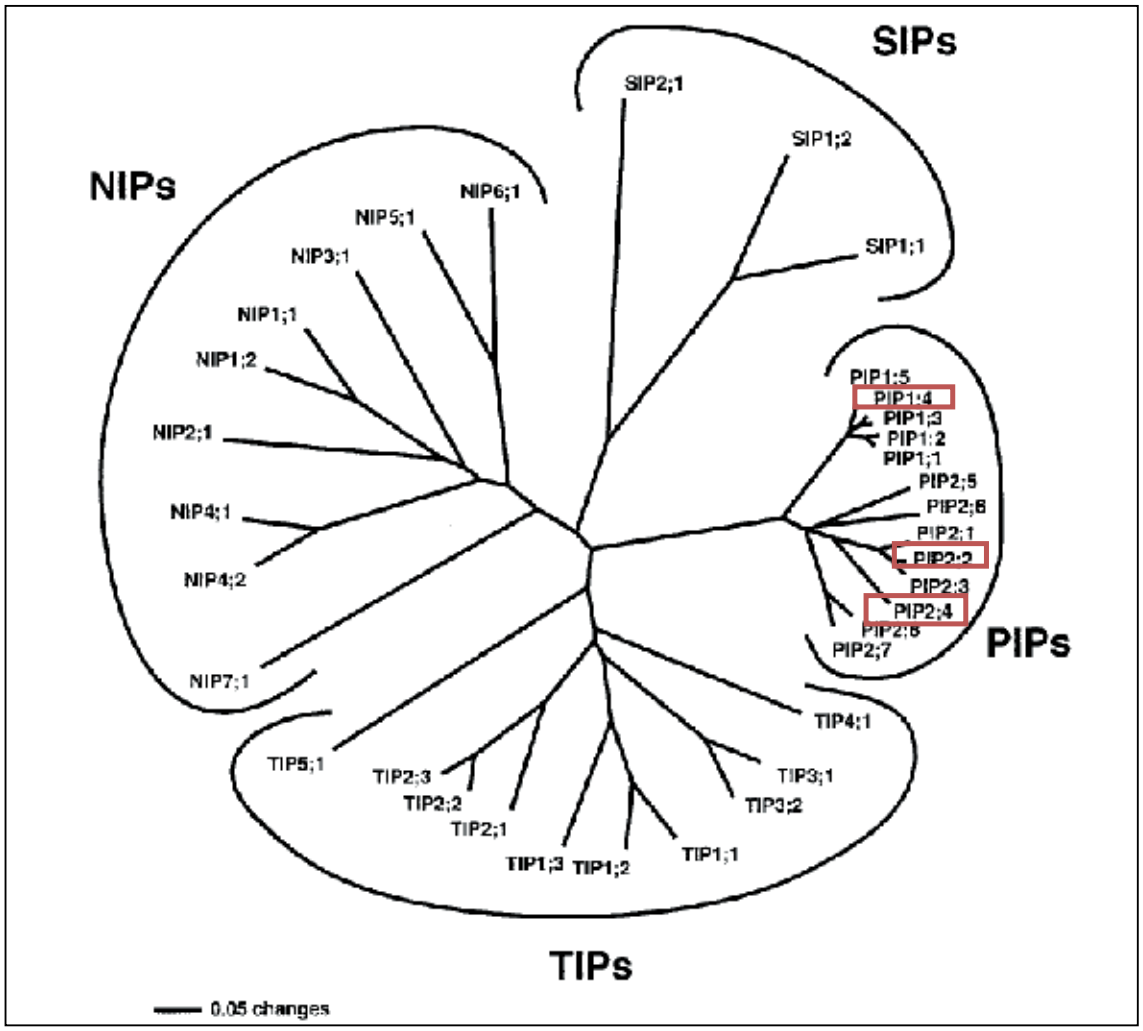

Figure 3.10 Phylogenetic comparison of the complete set of 35 different MIPs encoded in the *Arabidopsis* genome. Aquaporins found over-expressed in dwarf mistletoe are shown in red squares. The bar indicates the mean distance of 0.05 changes per amino acid residue. (Adopted from Johanson et al., 2001)

3.3.2.2.5 Verification of Affymetrix results by quantitative real time polymerase chain reaction

3.3.2.2.5.1 Quantitative polymerase chain reaction

Microarray, and, more recently, NGS techniques are regularly used to study gene expression. In both techniques, RTPCR or qRT-PCR is used to confirm the results. Generally, qRT-PCR is known to be a very sensitive and reliable method. However, to properly interpret qRT-PCR results, they must be normalized using a standardizing gene or genes, against which the level of gene expression for genes of interest is determined. All qRT-PCR methods use fluorescent dyes (for example, SYBR-Green I or fluorophore-containing probes) that bind to double-stranded DNA) to measure the amount of amplified product in real time (Heid et al., 1996). To run qRT-PCR, gene-

specific primers (Appendix II:2) were designed. Neither primers painstakingly designed using the Affymerix probes as a template nor a large number of degenerative primers gave expected results; therefore, primers obtained according to the sequences of the three genes (AQP, RuBisCo, and ABC), as attained from a hand held heterologous microarray (section 3.3.2.1), were employed. Primer efficiencies for each gene were as follows: AQP 96.87% R^2 0.997, RuBisCo 100.29% R^2 0.992, and ABC 103.06 R^2 0.99. Gel electrophoresis revealed a single band, indicating amplification of a single product in each case.

Additionally, the dissociation curves created automatically by the instrument were evaluated. This post-amplification dissociation-curve analysis is a simple way to check RTPCR reactions for primer-dimer artifacts and to ensure reaction specificity. Figure 3.11 shows post-amplification dissociation curves of the three genes under investigation (AQP2, RuBisCo, and ABC). The theory behind is that when double-stranded DNA intercalated with SYBR® Green I dye (highest fluorescence) is heated, a rapid decrease in fluorescence is detected at the moment when the melting point is reached due to dissociation of the DNA into single strands and consequent dye release. When the fluorescence is plotted against temperature (Figure 3.11) and then the -ΔF/ΔT (change in fluorescence/change in temperature) is plotted against temperature, a clear view of the melting dynamics is obtained. (Figure 3.11).

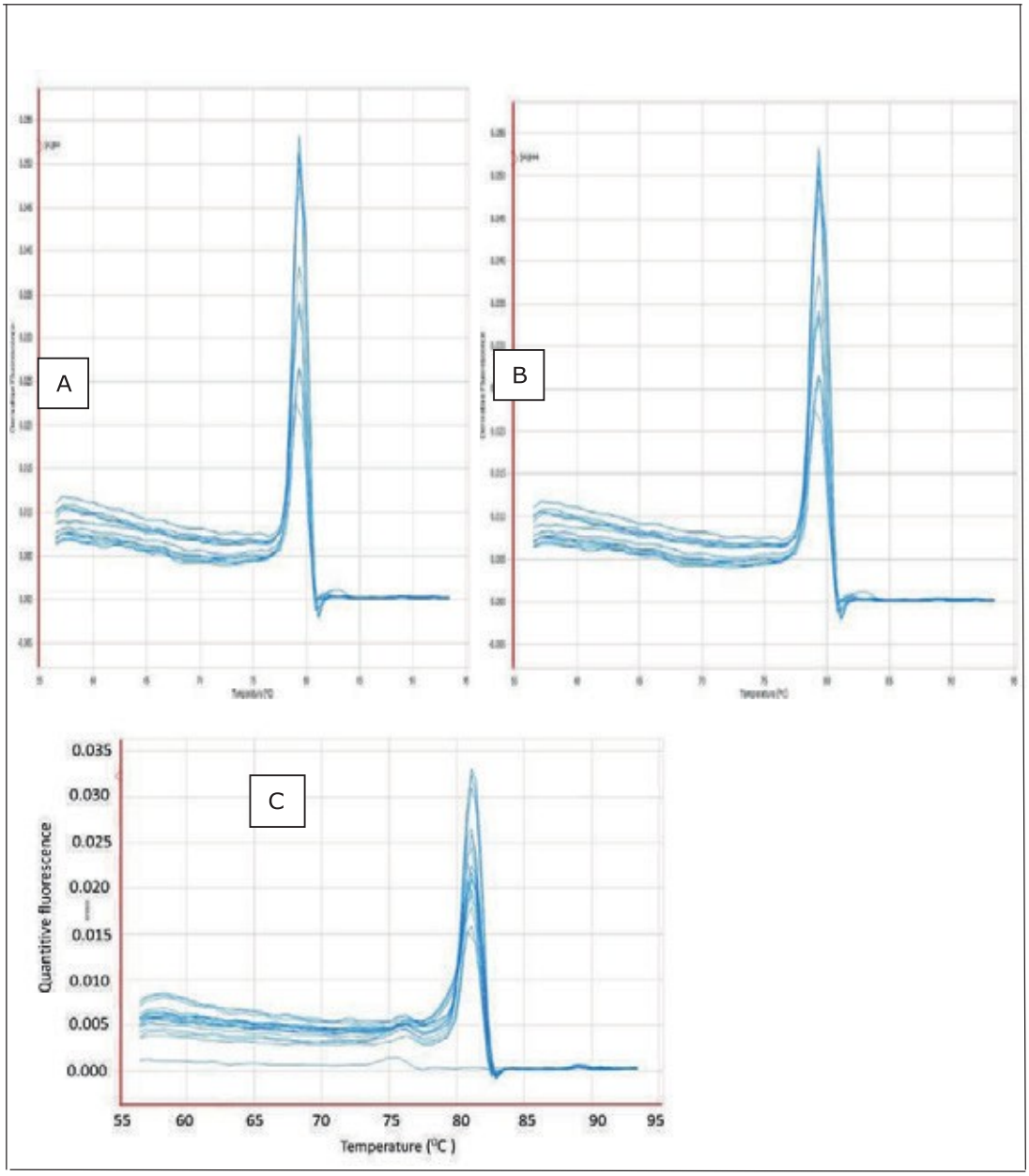

Figure 3.11 Dissociation curves from quantitative real time polymerase chain reaction of A) AQP2 gene, B) RuBisCo gene, C) ABC gene generated by an Illumina thermocycler (Bio-Rad, Hercules, CA). The presence of sharp single fluorescence peaks in all examples indicated the presence of single amplicons.

A key step in designing an appropriate qRT-PCR is to find relevant reference genes. During the search, many different potential reference genes from various plants, including those closely related to dwarf mistletoe as well as distantly-related ones, such as *A. thaliana*, were used. Before relative quantification can be measured in a sample, the suspected reference genes must be checked to validate their consistent expression throughout the experimental conditions (Suzuki et al., 2001 et al., Thellin et al., 1999; Thellin et al., 2009). Usually, genes involved in crucial and essential processes necessary for cell survival (housekeeping genes) are used, as they seem to fulfill the aforementioned criteria for many plants.

It was difficult to decide what gene or genes should be used as reference genes because no *A. oxycedri* and *A. americanum* reference gene sequences existed. Moreover, attempts to use gene sequences that are traditional reference genes used in model organisms, such as ubiquitin, actin, alpha-tubulin, 60S ribosomal protein L2, TIP41-like protein, elongation factor 1-alpha, cyclophilin, histone H2A and DNAJ-like protein, and eukaryotic initiation factor 4A-2 (EIF4A2) were not successful, regardless if the sequence was from a closely or more distantly related plant. Also, as attempts to use primers designed on the basis of Affymetrix probes or degenerative primers were not successful, five genes sequences obtained using the handheld heterologous microarray were ultimatley used. Three of them were tested and two of them were suspected to be able to work as reference genes: ABC and RuBisCO. The expression of these two genes was checked for potential use as reference genes even though neither of them are classic reference genes; however, they have previously been successfully used as reference genes in experiments run by Gadkar and Filion (2015) as well as Gao et al. (2017).

The relative expression levels of Cq (formerly called Ct) values from different years (2013, 2014, 2015) and different months (May, June, July, August, early September) were determined and used for determining housekeeping genes. Generally, it is advised to use a set of two to three reference genes for normalization, but this opportunity was not possible as the BestKeeper Microsoft Excel-based software that utilizes descriptive statistics of the derived crossing points for each potential housekeeping gene indicated only that the RuBisCo gene could be used as a reference gene (Table 3.4).

Table 3.4 *Expression stability of the potential reference genes calculated by BestKeeper software.*

	ABC	**RuBisCo**
N	23	23
GM [CP]	27.49	27.21
AM [CP]	27.50	27.22
Min [CP]	26.10	25.53
Max [CP]	28.95	29.00
SD[±CP]	0.77	0.64
CV [%CP]	2.80	2.34

Note: Reference genes were identified as the most stable genes; i.e., those with the lowest coefficient of variance (CV) with standard deviation (SD).
Abbreviations: N: number of samples; GM [CP]: the geometric mean of CP; AM [CP]: the arithmetic mean of CP; Min [CP] and Max [CP]: the extreme values of CP; SD [± CP]: the standard deviation of the CP; CV[%CP]: the coefficient of variance expressed as a percentage on the CP level; Min [x-fold] and Max [x-fold]: the extreme values of expression levels expressed as an absolute x-fold over- or under-regulation coefficient; SD [± x-fold]: standard deviation of the absolute regulation coefficients

Data from late May and early September was used to calculate averages (Table 3.5) and generate Figure 3.12, which illustrates the down regulation of ABC and PIP2 genes as well as the consistency of the housekeeping gene, RuBisCo (Figure 3.12).

Table 3.5 *Averages of Cq (Ct) results obtained from quantitative real-time polymerase chain reaction (qRT-PCR) for ABC, RuBisCo, and AQP2 genes from May and September.*

Time	ABC Cq	RuB Cq	AQP2 Cq
Late May	26.87	28.85	26.37
Early September	29.06	28.95	28.4

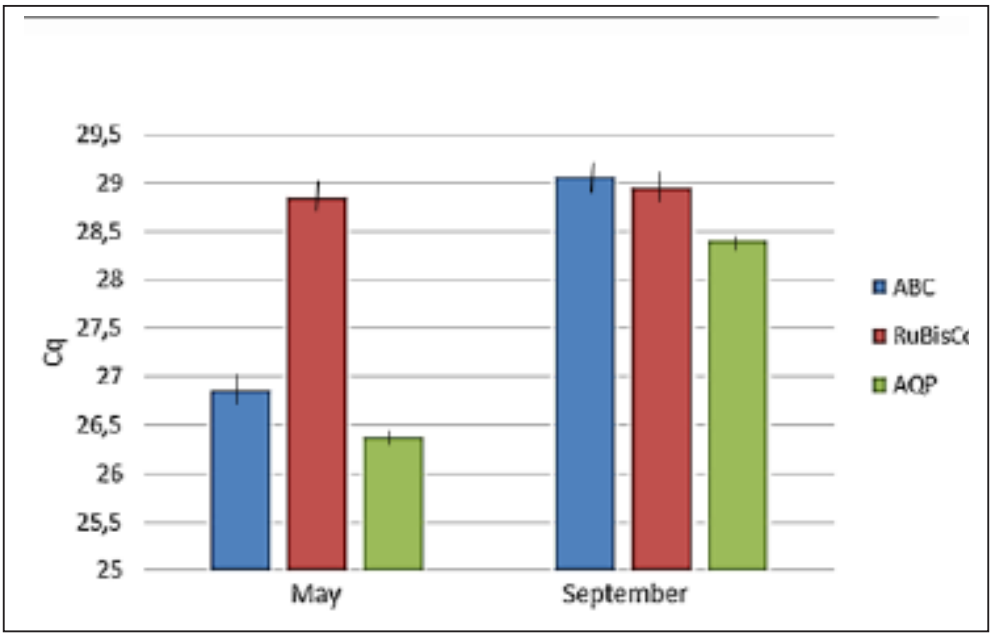

Figure 3.12 Cq values of three genes obtained during quantitative real-time polymerase chain reaction (qRT-PCR). Data from Table 3.5 were used to generate the graphs.

Aquaporins PIP2 and ABC were then used as genes of interest to confirm reliability of Affymetrix microarray data. In this case, cDNA from late May and early September (Table 3.5) and the same RNA and cDNA used in the Affymetrix microarray were employed in the calculation of fold-change values. The relative expression levels of the genes were calculated using the $2^{-\Delta\Delta Ct}$ method (Pfaffl, 2001; Schmittgen and Livak, 2008), which represents the Cq difference between the reference RuBisCo gene and the target gene product. All the genes had similar expression patterns for microarray and qRT-PCR values of fold-change (Table 3.6). The changes in expression levels observed using qRT-PCR were greater than the levels obtained by microarray analysis (Table 3.6). The levels of gene expression change determined by Affymetrix microarray analysis underestimated those determined by qRT-PCR. This type of result has been observed previously in comparison of microarray and PCR-based estimates of gene expression changes (Iyer et al., 1999; Dowd et al., 2004; López al., 2005; Coram & Pang, 2006). Therefore, the RT-PCR data serves to verify the Affymetrix microarray results.

Table 3.6 *Fold change values for selected genes (PIP2 and ABC transporter) determined by microarray analysis and quantitative real-time polymerase chain reaction (qRT-PCR).*

Gene	Affymetrix Array	qRT-PCR
PIP2	-2.21	-3.73
ABC transporter	-1.54	-4.25

3.3.2.2.5.2 Discussion

qRT-PCR was performed using gene sequences obtained from the handheld microarray and Southern blot analysis. The genes were then used to design primers, using the Primer 3 designer program for qRT-PCR, as any attempts at obtaining working primers from the Affymetrix microarray probes failed. The situation was further complicated by the fact that housekeeping genes, suggested by other plant researchers as being important for normalizing qRT-PCR, were not available or did not work (i.e., the expression was not steady for the time under the investigation). The results obtained by qRT-PCR, using *RuBisCo* as the reference gene, validated the Affymetrix microarray results by showing the same general trends in gene expression of *PIP2* and *ABC*.

3.4 Characterization of genes identified through MicroCASTer handheld microarray system, their products and putative role in seed dispersal

After finding corresponding, positive clones using heterologous microarray, their sizes were confirmed by PCR and they were sent for sequencing to Microsynth Seqlab (Göttingen, Germany). Subsequently, using NCBI BLAST, sequence similarity to the genes listed in section 3.3.2.1 was determined.

3.4.1 Aquaporin PIP2 and protein (GenBank accession # JN857944)

Using the NCBI BLAST, sequence similarity to an AQP PIP2:1 and PIP2:2 gene was found in one of the positive samples sent for sequencing. Figure 3.13 shows alignment of putative *Arceuthobium oxycedri* PIP2 (AoPIP2) to highly similar PIP2 AQPs.

Additionally, multiple sequence alignment of predicted amino acid sequence of *Arceuthobium oxycedri* PIP2 (AoPIP2) with other PIP2 (300 aa) aquaporins from different plant groups using ClustalW was performed (Appendix I).

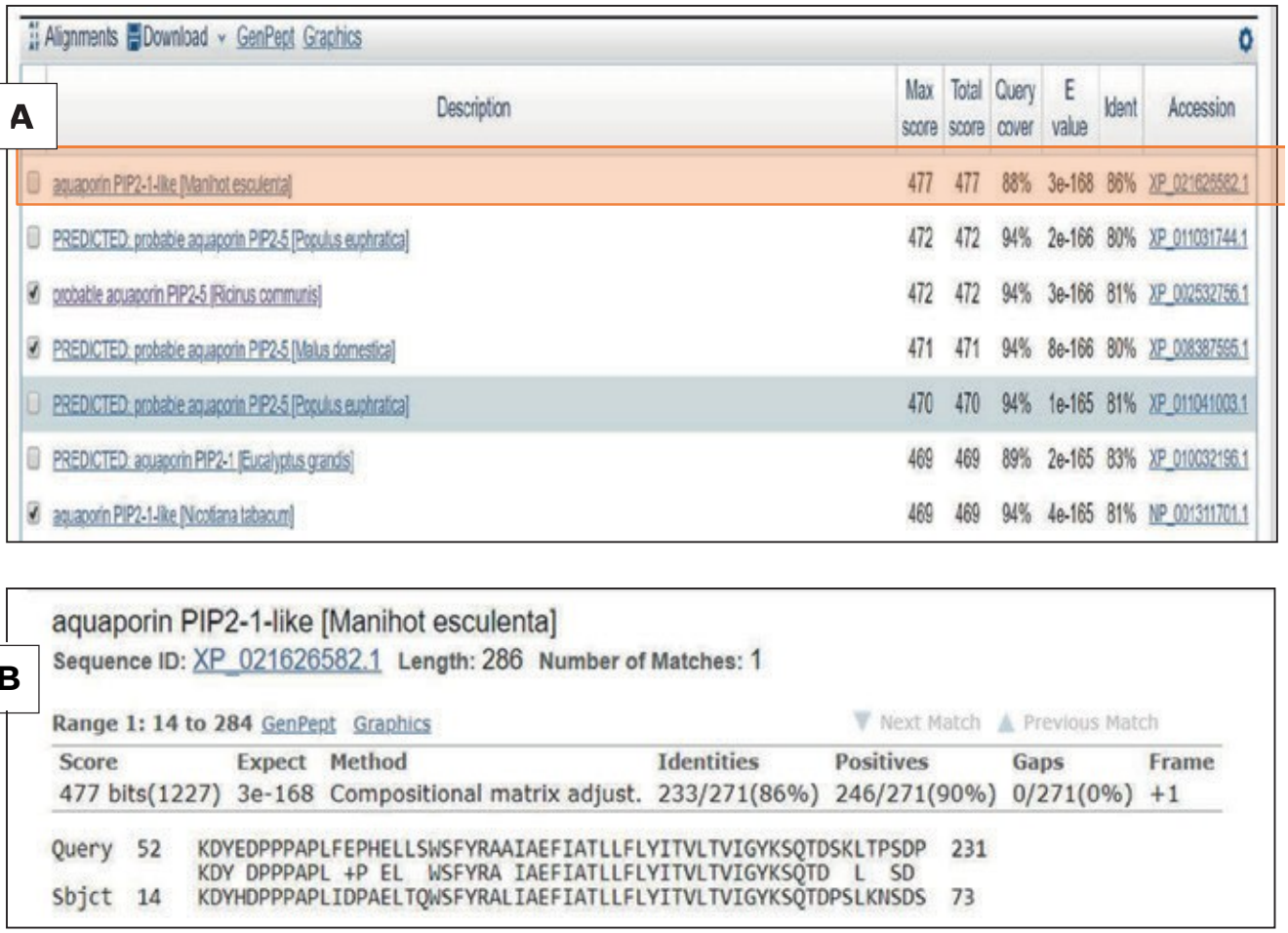

Figure 3.13 Blast (NCBI's BLAST) results of in silico translated nucleotide sequence. (A) Alignment of putative PIP2 from *Arceuthobium oxycedri* with similar proteins. (B) Specific sequence example from *Manihot esculenta* (orange box in part A).

Using the AQP sequence from *A. oxcycedri* (AoPIP2) and a variety of AQPs sequences from plants used for alignments in Figure 3.13 and other sequences availble, a tree view (Figure 3.14) was built to show relationships among known aquaporin sequences from At *(Arabidopsis thaliana) and* Os (*Oriza sativa*) with the discovered AoPIP2.

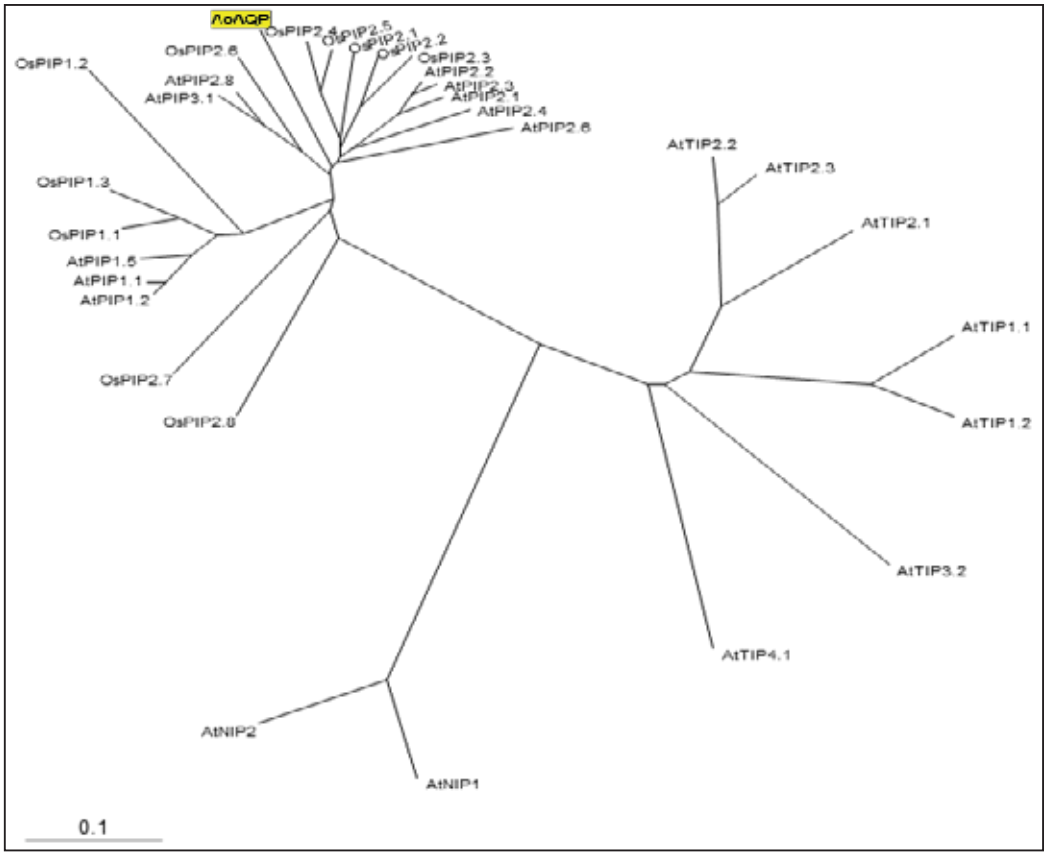

Figure 3.14 Tree view showing alignment of known different types of aquaporins sequences from At (*Arabidopsis thaliana*) and Os (*Oriza sativa*) with AoAQP sequence (yellow colour).

3.4.1.1 Functional analysis: stopped-flow spectrophotometry

The PIP2 gene was a key gene to examine in order to establish support for its involvement in dwarf mistletoe seed dispersal. The product of this gene, PIP2 protein, was further subjected to stopped-flow spectrophotometry analysis. Other sequenced genes were used mainly to find reference genes for qRT-PCR to confirm the Affymetrix microarray analysis results.

3.4.1.1.1 Water conductivity measurements of the PIP2 gene product

The system for stopped-flow water measurements relies on the AQPs under examination being present in the yeast plasma membrane (*Saccharomyces cerevisiae* or *Pichia pastoris)*; if there is a noticeable difference in water conductivity between yeast cells expressing AoPIP2 constructs and a negative control (known yeast cells that do not express the protein), this can be an indication that the AQP is indeed present in the yeast plasma membrane. To perform the assay of the cDNAs encoding potential, *Arceuthobium oxycedri* PIP2 was inserted into the pYES-DEST52

yeast expression vector using Gateway™ technology, which consisted of the following steps:

1. Amplify cDNA genes for use in Gateway™ cloning:
   First, to create fragments suitable for Gateway™ cloning, attB1 and attB2 recombination recognition sites were added to the gene of interest (PIP2) via PCR. The plasmids containing the PIP2 were extracted from *E.coli*. Then PCR with primers designed for this gene was run to confirm the gene's presence. Figure 3.15 shows the resulting PCR amplification product.

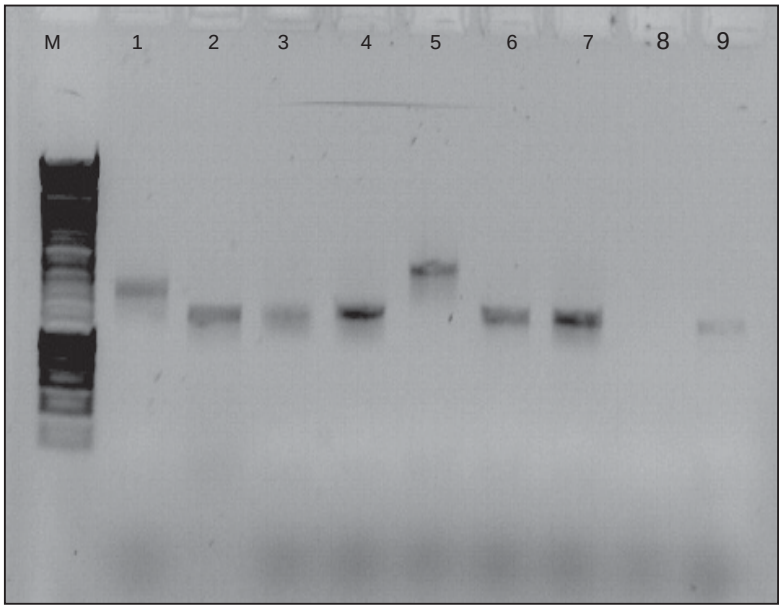

Figure 3.15 Amplification products of polymerase chain reaction on *A. oxycedri* AQP2 complementary DNA clones. M: HyperLadder I DNA marker; 2-4 and 6-7: samples with the gene of interest (insert and primers); 8: negative control; 9: positive control.

2. Synthesize expression clones for Gateway™ amplification:
   Amplified fragments (Figure 3.15) were excised from the gel and purified with a gel purification kit (NucleoSpin® Extract II; Macherey-Nagel) according to the manufacturer's instructions. To clone the purified amplification fragments into pDONR201 (yielding entry clones), the Gateway™ BP reaction was performed as described in Materials and Methods. Then, DH5α *E.coli* was transformed with the constructs. The PIP2 gene plasmid was isolated (entry clones; Figure 3.16), and then, to validate the presence of the correct insert, PCR was performed on all of the plasmids using the same primer pairs originally used for insert preparation (Figure 3.17).

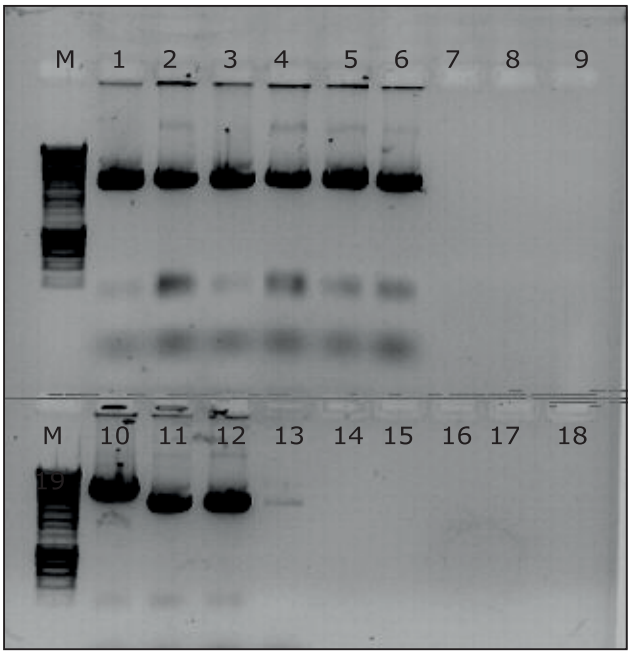

Figure 3.16 Plasmid preparation. M: HyperLadder I DNA marker. Entry clones of AoAQP2 inserted into pDONR201: Lines 1, 2, 3, 4, 5, 6, 10, 11, 12.

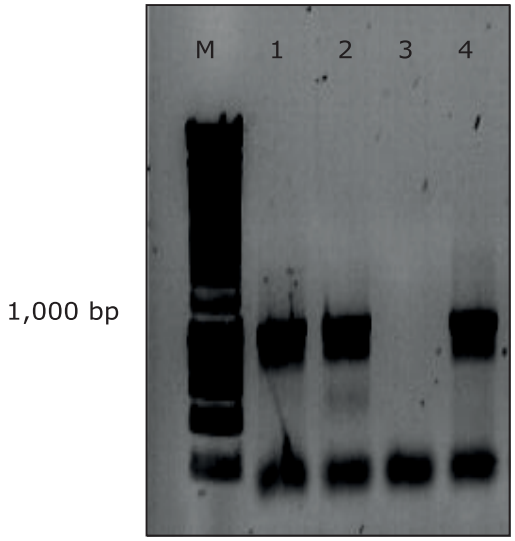

Figure 3.17 Polymerase chain reaction on AoPIP2 entry clones. M: HyperLadder I DNA marker; numbers to the left of the marker bands indicate the size of the band in BP. Line 1 and 2: Entry clones of AoAQP2. Clones from line 1 and 2 were used for subsequent LR reaction. Negative control (line 3) was negative. Positive control (line 4) wasNtPIP2.

The entry clones were used for a series of Gateway™ LR reactions as described in Materials and Methods. Inserts were cloned into the pYESDEST52 yeast expression vector. Plasmids were isolated (Figure 3.18), and all constructs were verified by PCR (Figure 3.19).

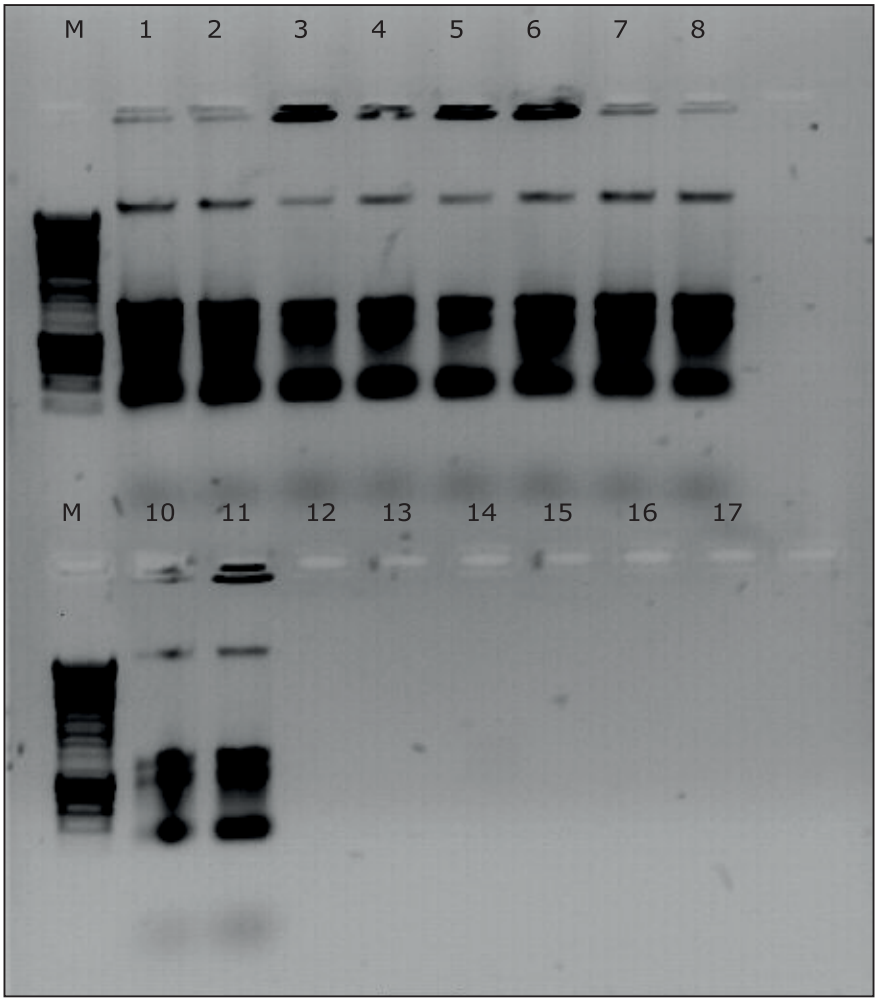

Figure 3.18 Plasmid isolation of AoPIP2 expression clones for functional analysis (pYES-DEST52). M: HyperLadder I DNA marker. Lines 1 to 8 and 10 and 11: AoPIP2.

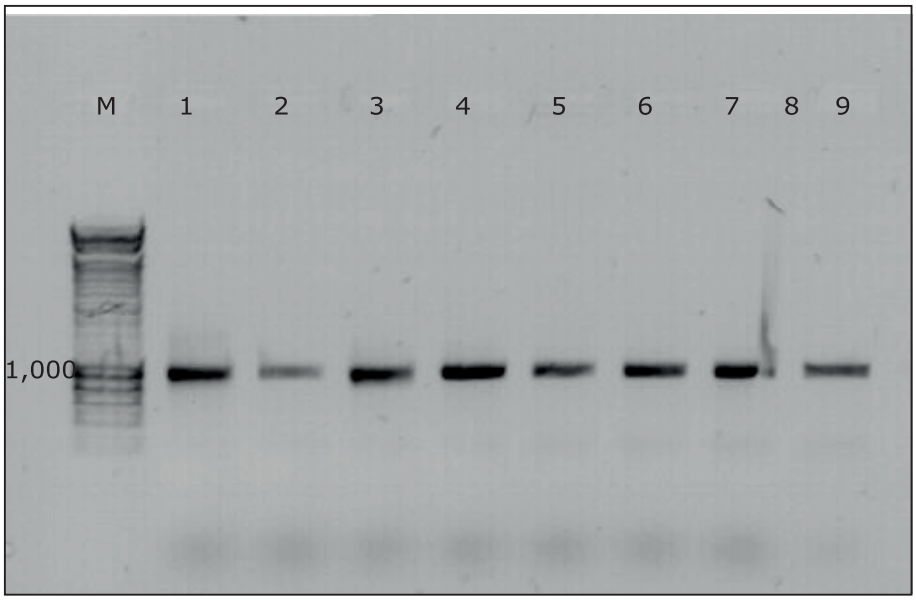

Figure 3.19 Polymerase chain reaction on AoAQP2 expression clones for functional analysis (pYES-DEST52). M: HyperLadder I DNA marker; numbers to the left of the marker bands indicate the size of the band in BP. Lines 1-7: AoAQP2. 8: positive control (AoAQP2 entry clone). 9: negative control (no template).

The expression of AQP constructs for water permeability of intact yeast protoplasts was tested using stopped-flow spectrophotometry. Yeast cells were transformed with pYES-DEST52 containing AoAQP2, and negative controls (pYES-DEST52 alone) were used. Swelling kinetics for the AoAQP2 constructs indicate a large increase in swelling and water influx into the yeast protoplasts possessing additional AQPs compared to the negative control (Figure 3.20; Appendix IV).

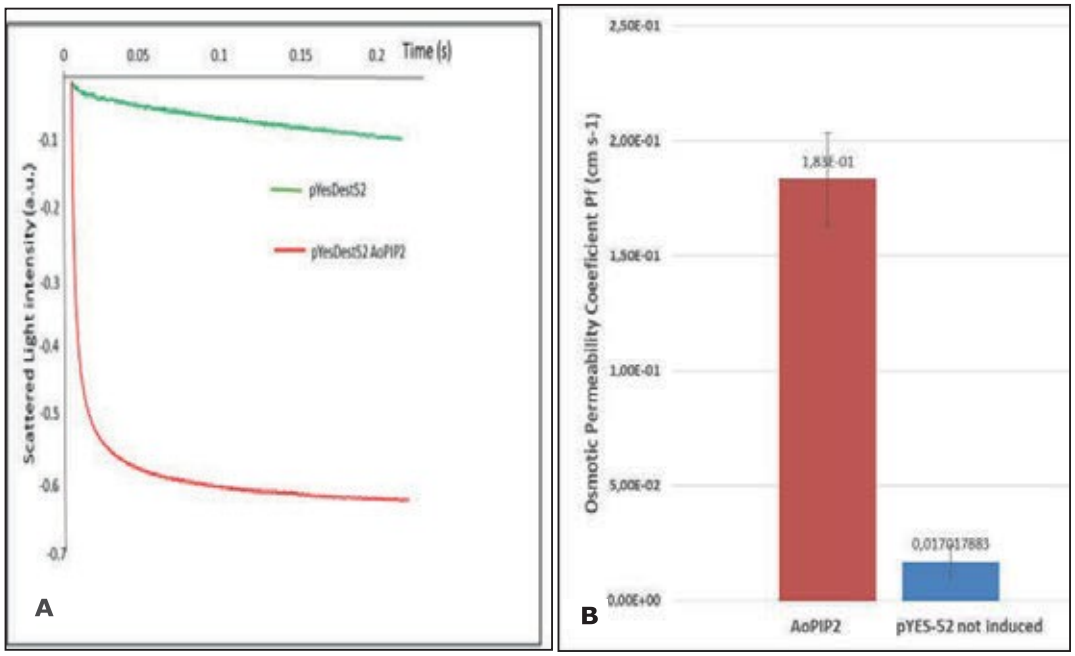

Figure 3.20 Kinetics of stopped-flow water conductance measurements of intact yeast protoplasts expressing AoPIP2;1. Expression of AoPIP2;1 increases water permeability of the yeast membrane. (A) Change of scattered light intensity due to the change in volume of aquaporin-expressing yeast protoplasts and protoplasts whose aquaporin expression was not induced (Kinetics represent averages from 100 individual curves.). (B) Osmotic coefficients of permeability (Pf) in cm s-1 of intact yeast protoplast expressing AoPIP2 (red bar) and not induced (blue bar) as well as standard deviations.

3.4.1.1.2 Discussion

The results of the stopped-flow cytometry validated that the AoPIP2 gene was responsible for inducing the production of the AQP type 2 involved in water movement.

As the yeast cells in this experiment had their cell walls removed (i.e., were protoplasts; Materials and Methods), their plasma membrane can expand without any difficulties. When the cell suspension was filled in with a syringe of the mixing unit of the stop-flow spectrophotometer with the hypo-osmolar buffer, an osmotic gradient across the plasma membrane of the protoplasts of 300 m Osmol was formed. This induced a water influx into the protoplasts, which led to an increase in volume inside the protoplasts and an increase in the size of the cells. The enlargement of the protoplasts surface decreased the intensity of scattered light at an angle of 90° to the incident light. This decrease in scattered light intensity was detected by the photomultiplier. The kinetics of the scattered light intensity was determined by the water conductivity of the plasma membrane.

Quantification of water conductivity was attained by computationally fitting a single exponential function on the initial 100 ms on the swelling kinetics via Bioline (Bio-Logic SAS) software. The osmotic water permeability coefficients (P_f) were calculated as described by van Heeswijk and van Os (1986), using the rate constant of the exponential decay (k), the molar volume of water (V_W), the external osmolarity after the mixing event, and the initial mean protoplast volume and surface(S_0). The initial size of protoplasts was determined by light microscopy. For controls, calculation of P_f values was performed on at least four independent experiments of three independently transformed clones with an average of 20 measurements each (n 100). The corresponding curve (AoPIP2) on Figure 3.20(A) shows a much faster relaxation than the curve of the yeast protoplasts without plant AQPs (i.e., not induced). This indicates a significant increase in the water permeability of the yeast protoplasts by the PIP2 aquaporins. Expression of AoPIP2 (Pf = 180.3 +/- 20.2* 10-3 cm s-1) in yeast resulted in a 10- to 12-fold increase in water permeability of the yeast plasma membrane.

3.4.2 Alkaline / neutral invertase portion of gene (CINV2) coding for neutral / alkaline invertase protein

Using NCBI BLAST, sequence similarity to a protein called CINV2 was found in one of the positive samples sent for sequencing. Figure 3.21 shows an alignment of a putative alkaline/neutral invertase from *Arceuthobium oxycedri* to very similar proteins from different plants, ranging from 90% to 93% identity.

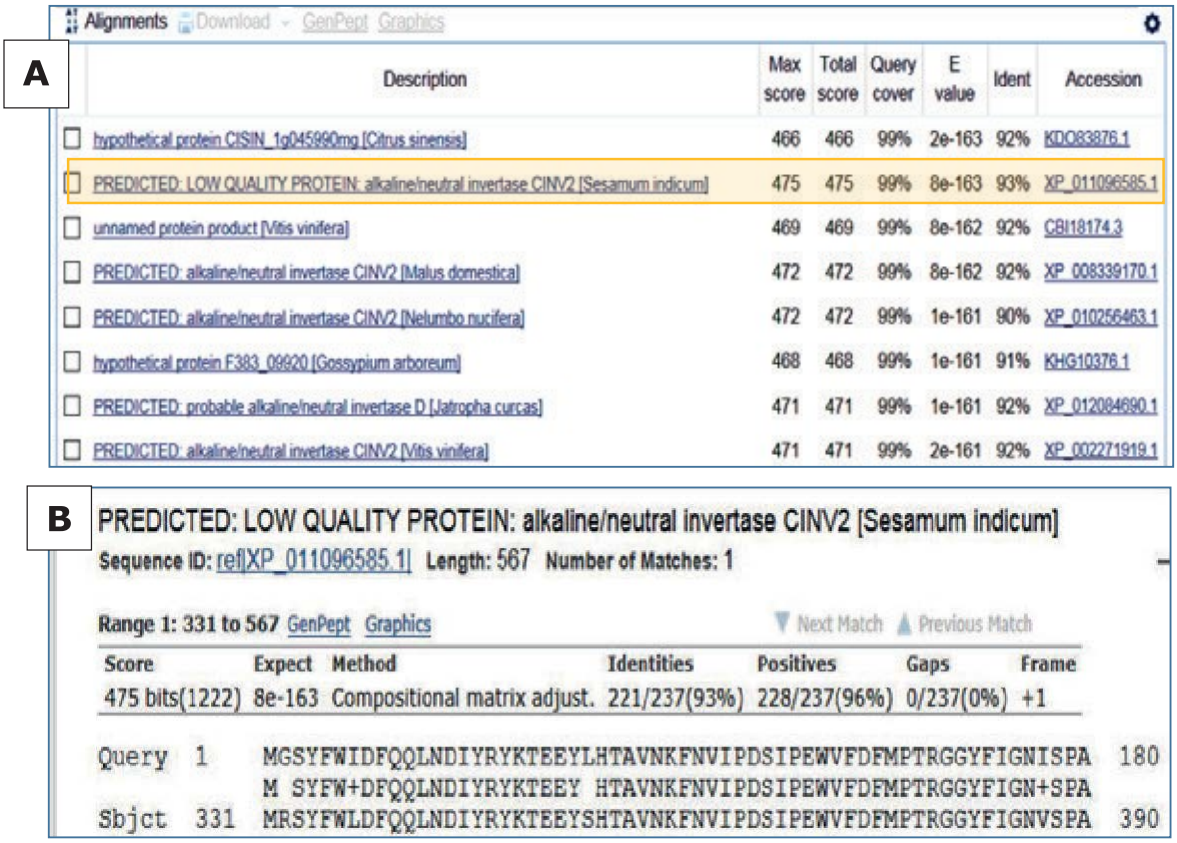

Figure 3.21 Blast (NCBI's BLAST) results of in silico translated nucleotide sequence. (A) Alignment of putative alkaline/neutral invertase from Arceuthobium oxycedri with similar proteins. (B) Specific sequence example from Sesamum indicum (orange box in part A).

3.4.2.1 Discussion

Neutral and alkaline invertases are an example of the cytoplasmic invertases necessary for heterotrophic plant survival. Invertases can be found in the mitochondria, chloroplast, and nuclei (Vargas & Salerno, 2010) of a plant. The most important function of neutral and alkaline invertases is hydrolysis of disaccharides, specifically sucrose, into hexoses, glucose, and fructose, which are fed into different metabolic pathways. Figure 3.22 shows plant invertases and their location in plant cells. Additionally, neutral and alkaline invertases are involved in plant growth and development, flowering, and seed germination (Barratt et al., 2009; Welham et al., 2009). They are also part of the antioxidant system involved in cellular reactive oxygen species homeostasis (Xiang et al., 2011).

Transcripts for neutral invertase are found with slightly higher levels in developing organs in comparison to other parts of the plant (Sturm et al., 1999; Fotopoulos, 2005).

The activity of cleavage enzymes in sink organs play a crucial role in the regulation of assimilate segregation through the creation of sugar gradients. These events are especially important when looking at fruit development (Nonis et al., 2007). For example, during grape berry ripening, sucrose is transported from the leaves and accumulated in the vacuoles of berries or hydrolysed into fructose and glucose (Davies & Robinson, 1996). Invertase activity in grape increases from flowering, peaking at 8 weeks, and then remaining constant until the fruit is ripe.

As dwarf mistletoes are responsible for only a small amount of the sucrose produced during the process of photosynthesis, most sucrose must be transported from a host to a pathogenic plant and then into each organ, including the fruit, where it can be cleaved into two hexoses to become an energy source. All mistletoe fruit consists of viscin cells that secrete mucilage ("viscin") (section 1), which is crucial for adhering a dispersed seed to a host. In the case of *Arceuthobium*, viscin also plays a critical role in creating the hygroscopic force needed for ballistic seed dispersal. Gedalovich-Shedletzky et al. (1989) and Kuijt & Bertel (2015) found that mistletoe fruit's viscin cell mucilage consists mostly of neutral polysaccharides such as xylose, arabinose, or glucose with significant amounts of uronic acids and proteins, as well as glycine and higher than average amounts of histidine. Perhaps invertase, by assisting in splitting sucrose into fructose and glucose, may be involved in establishing the osmotic gradient that helps the movement of water into a fruit. Also, during thermogenesis (deBruyn et al., 2015), the plant would need a large amount of chemical energy to fuel the heat production, so invertase is likely needed in a higher amount to help in obtaining glucose as a chemical energy source.

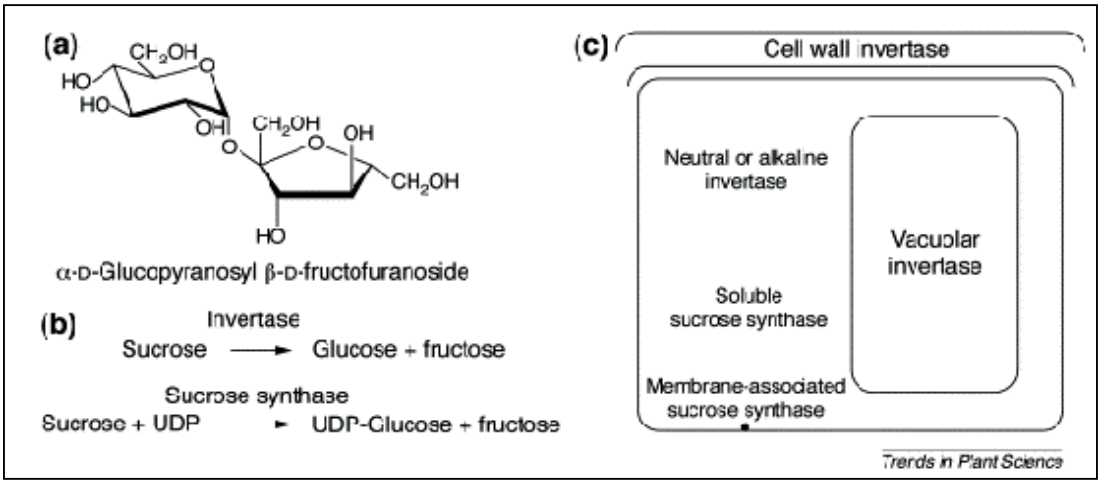

Figure 3.22 Plant invertases and synthases. a) Chemical composition of sucrose. b) Invertase as a hydrolase, cleaving sucrose into glucose and fructose. c) Isoforms of sucrose invertase and synthase and their different subcellular compartments (adapted from Sturm & Tang, 1999).

The Affymetrix results suggested that the expression of the neutral invertase gene was down-regulated in September, just before the time of seed dispersal, when compared to May.

3.4.3 ATP-binding cassette (ABC) transporter family protein, cholesterol/phospholipid flippase isoform

Using NCBI BLAST, sequence similarity to a gene called the ABC transporter family was found in one of the positive samples sent for sequencing. Figure 3.23 shows an alignment of a putative cholesterol/phospholipid flippase from *Arceuthobium oxycedri* to very similar proteins in different plants, ranging from 77% to 78% identity.

A

Description	Max score	Total score	Query cover	E value	Ident	Accession
ABC transporter family, cholesterol/phospholipid flippase isoform 2 [Theobroma cacao]	471	661	99%	2e-150	77%	XP_007028660.1
PREDICTED: ABC transporter A family member 1 isoform X2 [Vitis vinifera]	469	630	92%	2e-149	78%	XP_010653767.1
ABC transporter family, cholesterol/phospholipid flippase isoform 1 [Theobroma cacao]	472	662	99%	5e-149	77%	XP_007028659.1
unnamed protein product [Vitis vinifera]	471	632	92%	2e-148	78%	CBI29824.3
PREDICTED: ABC transporter A family member 1 isoform X1 [Vitis vinifera]	470	631	92%	2e-148	78%	XP_002284204.1
PREDICTED: ABC transporter A family member 1 isoform X4 [Populus euphratica]	464	625	94%	3e-148	77%	XP_011048076.1

B

ABC transporter family, cholesterol/phospholipid flippase isoform 2 [Theobroma cacao]

Sequence ID: ref|XP_007028660.1| **Length:** 1566 **Number of Matches:** 3

▸ See 1 more title(s)

Range 1: 1188 to 1479 GenPept Graphics ▼ Next Match ▲ Previous Match

Score	Expect	Method	Identities	Positives	Gaps	Frame
471 bits(1213)	2e-150	Compositional matrix adjust.	225/292(77%)	258/292(88%)	0/292(0%)	+1

```
Query  1     MLSGEEIPSSGSAFIFGRNIFSNPKTIRRHVGYCPQFDALLEYLTVQEHLELYARIKGVP
             ML+GEE P+ G+AFIFG++I SNPK  RRH+GYCPQFDALLEYLTVQEHLELYARIKGV
Sbjct  1188  MLTGEESPTEGTAFIFGKDIASNPKAARRHIGYCPQFDALLEYLTVQEHLELYARIKGVL
```

Figure 3.23 Blast (NCBI's BLAST) results of in silico translated nucleotides sequence. (A) Alignment of putative ABC transporter family protein from *A. oxycedri* with similar proteins. (B) Specific sequence example from Theobrama cacao (orange box in part A).

3.4.3.1 Discussion

This group of proteins comprises one of the largest universal protein families, composed of mostly transport proteins, and is present in all organisms on Earth (Lefèvre et al., 2015). Plant genomes consist of a large number of genes coding for

ABC transport proteins (120 in the case of *Arabidopsis thaliana).* These enzymes are nonspecific substrates; coupling the hydrolysis of ATP permits the active transport of substances such as sterols, lipids, sugars, ions, proteins, metal complexes, and antibiotics (Lefèvre et al., 2015). These proteins are involved in various physiological functions besides transport, such as signalling, growth and development, detoxification, lipid homeostasis, defence, and antigen presentation (Lewinson and Livnat-Levanon, 2017). Structurally, the ABC transporter enzyme consists of two cytosolic nucleotide-binding domains that supply energy by binding and hydrolysing ATP as well as two integral transmembrane domains that form the transmembrane permeation pathway. (Figure 3.24).

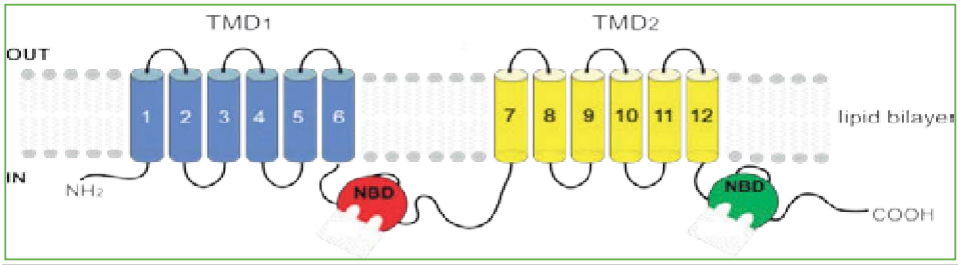

Figure 3.24 ABC full transporter. Representative structure of an ABC full transporter containing two transmembrane domains (TMDs), TMD_1 (blue) and TMD_2 (yellow), each containing six transmembrane segments and two nucleotide-binding domains (NBDs), NBD_1 (red) and NBD_2 (green; Deeley et al., 2006). Adapted from Dermauw & Van Leeuwen (2014).

According to the Affymetrix microarray results, many genes involved in transport were highly active within mistletoe fruit collected in May (see Section 3.3.2.2), a time when the plant begins actively growing and producing its new crop of flowers. As such, nutrient transport from the host to the mistletoe, as well as within the mistletoe plant itself, was increased. Among these genes are many ABC transporters. Additionally, results obtained from research done using the haustorium of other parasitic plants, namely *Cuscuta* (Ranjan et al., 2014) and a few species of *Orobanchaceae* (Young et al., 1999; Yang et al., 2015)) show increase in transport involved.

3.4.4 Sterol 14-demethylase-like protein

Figure 3.25 shows the results of BLAST (NCBI), which depicts alignment of putative Sterol 14-demethylase protein from *A. oxycedri* to similar proteins from different plants, ranging from 80% to 85% of identity.

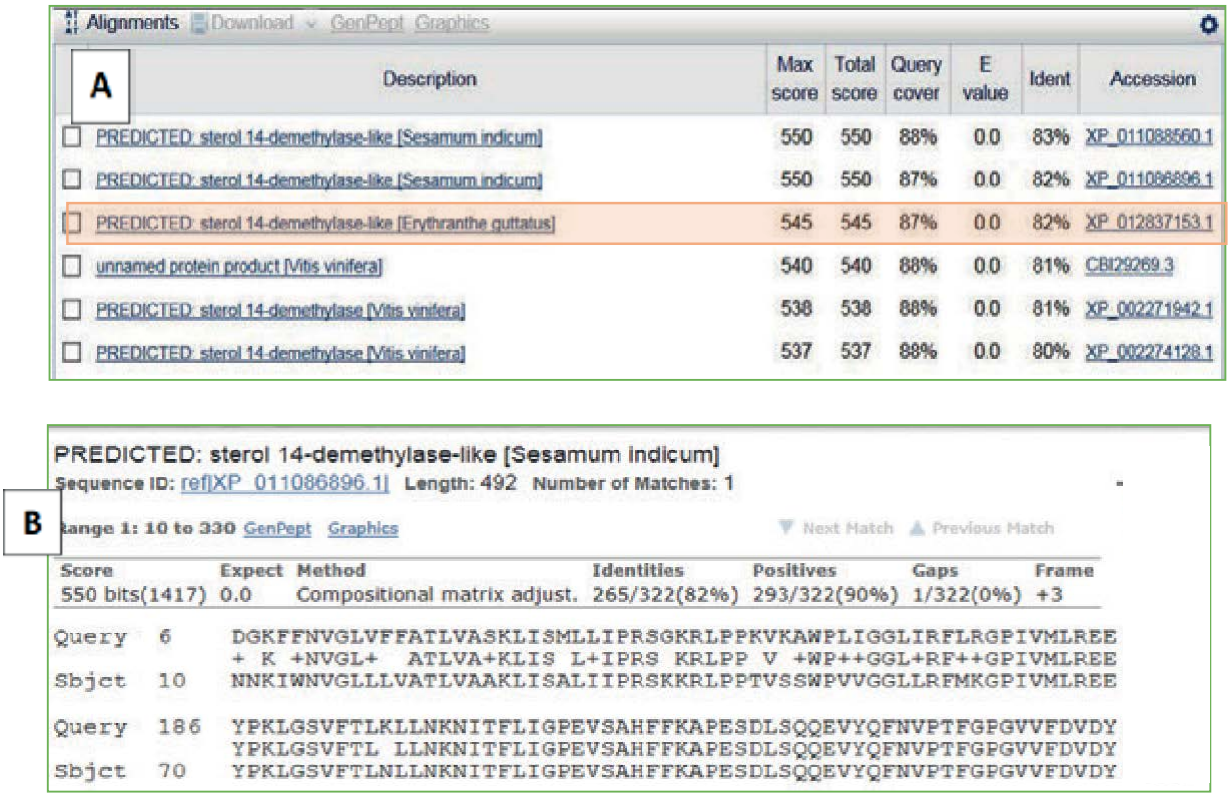

Figure 3.25 Blast (NCBI's BLAST) results of in silico translated nucleotide sequence. (A) Alignment of putative Sterol 14-demethylase-like protein from *A. oxycedri* with similar proteins. (B) Specific sequence example from *Sesamum indicum* (orange box in part A).

3.4.4.1 Discussion

Sterols are essential components of the cell membranes of all eukaryotes, including plants. They are involved in many biological functions, such as controlling the permeability and fluidity of plant membranes (Grunwald, 1971). Recent research has discovered new roles of sterols in the formation of lipids rafts (Ferrer et al., 2017), structures built between sterols (sitosterol and stigmasterol) and sphingolipids, which can be involved in many additional roles such as signalling, cellular sorting, and cytoskeleton rearrangement (Beck et al., 2007).

Plant sterols are steroid alcohols similar to cholesterol, the sterol in animals, in chemical structure and biological function. Both are biosynthetically derived from squalene and form a group of triterpenes (Piironen et al., 2000). Contrary to animals and fungi, plants produce a mixture of sterols that differ in side chains at position C17 as well as in the number of double bonds in the aromatic rings and longer chains (Figure 3.26). Sterol alpha demethylation is a part of sterol biosynthesis in eukaryotes, and 14-alpha demethylated products are intermediate products that lead

to the formation of cholesterol, ergosterol, and a variety of olefinated sterols in plants such as ergosterol and sitosterol (Lepesheva and Waterman, 2007).

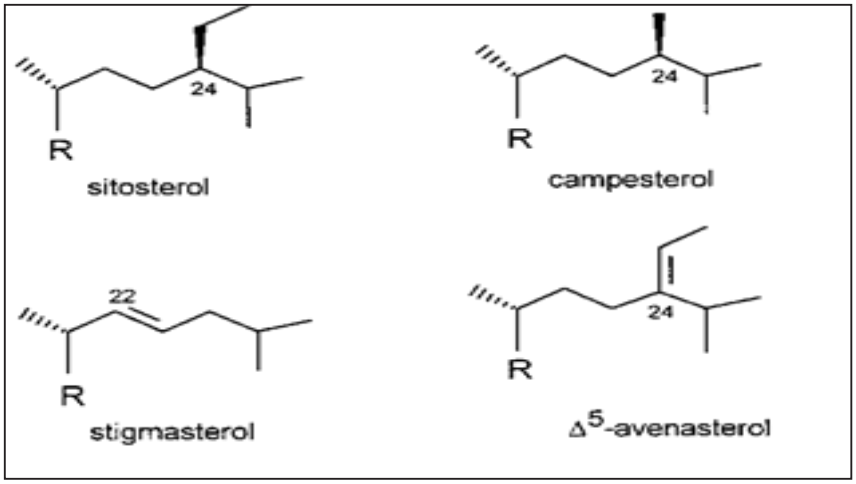

Figure 3.26 Structures of major plant sterols with a similar sterol nucleus (R): sitosterol (24a-ethylcholest-5-en-3b-ol), campesterol (24a-methylcholest-5-en-3b-ol), stigmasterol (24a-ethylcholest-5,22-en3b-ol), and D^5-avenasterol (Z-24-ethylidenecholest-5-en-3b-ol). Adopted from Piironen et al., 2000.

14-Alpha demethylase is an example of a cytochrome P450 (CYP) enzyme, which comprise a group of heme-containing monooxygenases that catalyze the metabolism of various endogenous and exogenous compounds. CYPs constitute a superfamily of enzymes present in various organisms, including plants. Though CYPs are diverse, and metabolize a wide selection of substrates, their structures are largely conserved. For example, enzyme 14-demethylase P450 (CYP51) is a highly conserved and essential enzyme seen in every kingdom of life; the first sterol (sterol 14-demethylase) in plants was found in 1996 in *Sorghum bicolor* (Kahn et al. 1996). Figure 3.27 shows the importance of the CYP51 enzyme in formation of sterols, and Figure 3.28 depicts the importance of the whole CYP family and other enzymes involved in the production of sterols in plants.

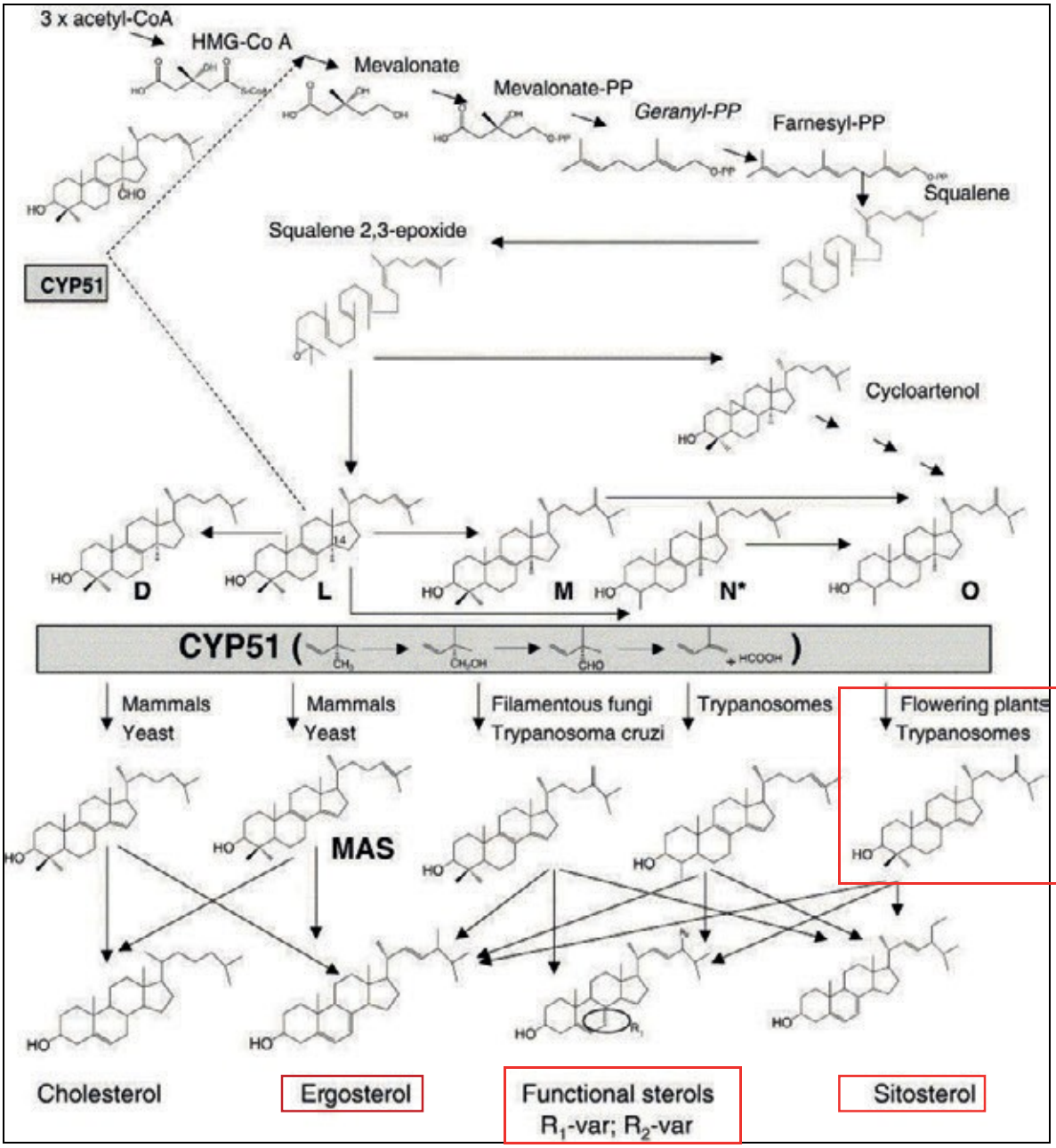

Figure 3.27 Cytochrome P450 (CYP) enzyme CYP51 main reactions and sterols biosynthesis. D) 24, 25-dihydrolanosterol; L) lanosterol; M) 24-methylenedihydrolanosterol; N) norlanosterol; O) obtusifoliol; R1) alkyl or alkylene group; R2) C6 or C7. Red boxes indicate products in plants (Adapted from Lepesheva and Waterman, 2007).

Sterol biosynthesis in plants has been very well investigated within the last decade. The sterol precursor cycloartenol is methylated either once or twice to produce a mixture of sterols, including sitosterol, stigmasterol, and campesterol. Campesterol is the precursor of brassinosteroids (BRs; Figure 3.28; Clouse, 2000).

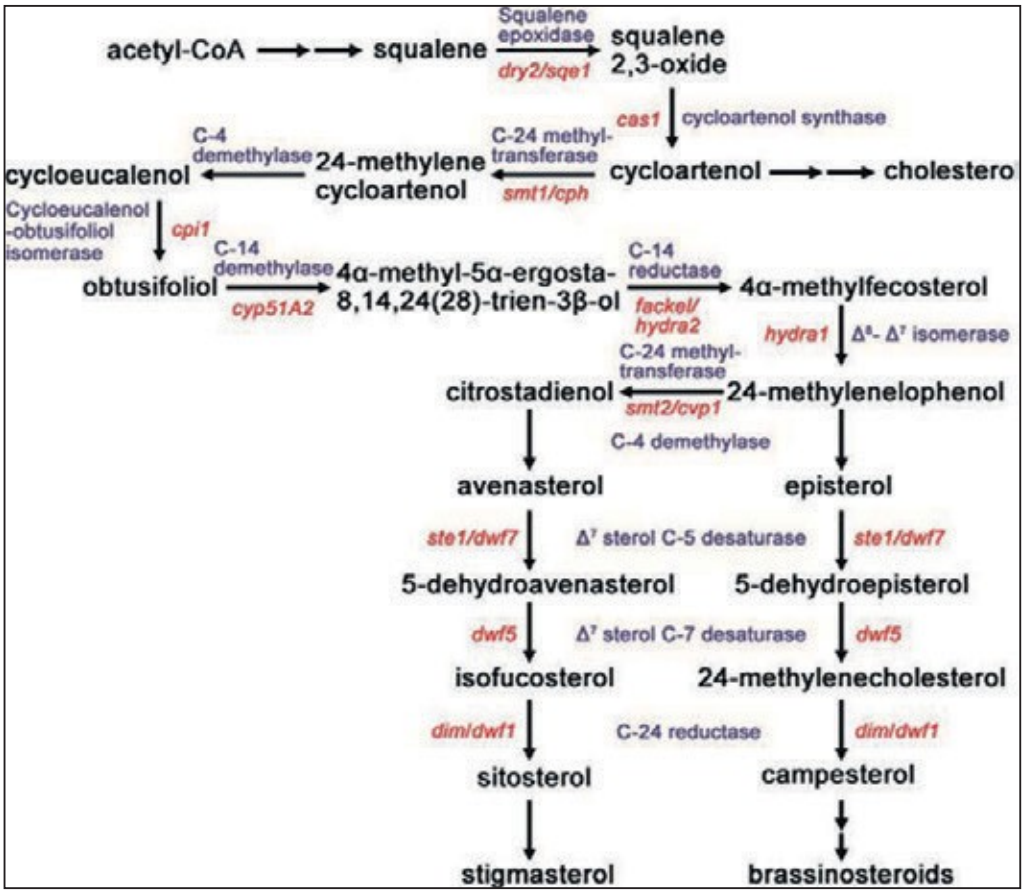

Figure 3.28 The detailed sterol biosynthetic pathway in *Arabidopsis thaliana*. A branch in the pathway results from either one or two methylation steps, producing two major end products, stigmasterol and campesterol. Campesterol is the precursor of brassinosteroids. Enzymes catalyzing these steps are shown in purple, and their corresponding mutants are shown in red (Jang et al., 2000; Schrick et al., 2000, 2002, 2004; Men et al., 2008).

Additionally, research done by Qian et al. (2013) suggests that sterols are required for *Arabidopsis* stomata pattering (Figure 3.29). More information about stomata and guard cells is given later.

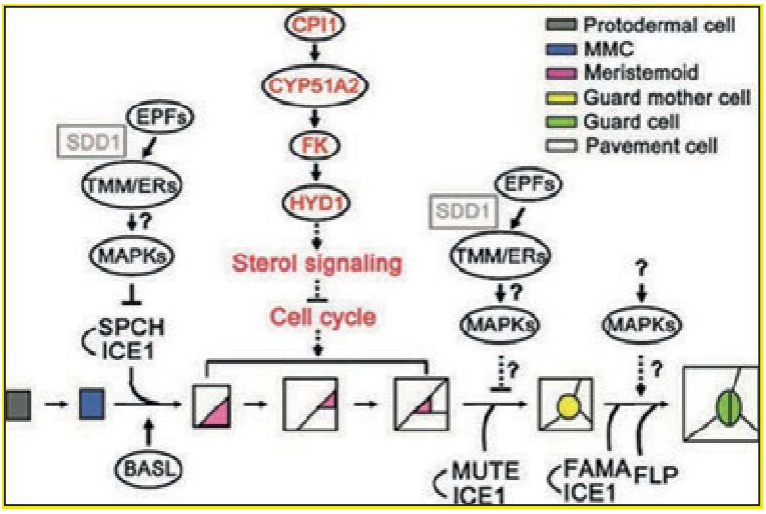

Figure 3.29 Simplified model of the initial steps of sterol biosynthesis (in red) involved in stomatal development. The EPF–TMM/ER–MAPK cascade, SDD1 and BASL, help bHLH and MYB transcription factors to determine three cell-type differentiations (Casson & Gray, 2008; Lampard et al., 2009; Pillitteri & Torii, 2012). In this proposed model sterol biosynthesis is involved in the cell-fate commitment of the stomatal lineage after asymmetric division (Adapted from Casson & Gray, 2008).

As thermogenesis occurs in dwarf mistletoe (deBruyn et al., 2015), the plasma membrane of viable cells in the fruit likely becomes more stressed, thus jeopardizing membrane integrity. With the production of more sterols (genes are up-regulated in May and down-regulated in September; Affymetrix results), the membranes probably become rigid and less likely to destabilize when thermogenesis initiates. In addition, sterols are highly hydrophobic. If sterols enforce the membranes of the vesicular cells, which form three to four outer mesocarp layers that envelop the viscin cells and their mucilage (“viscin”), sterol-enforced vesicular cells may function in sealing water within the viscin, thereby helping to establish the pressure needed for seed dispersal. Also, research conducted by Kai & Kaldenhoff (2014) demonstrates that sterols decrease water permeability of lipid bilayer membranes; as such, they can help in establishing the hydrostatic pressure inside the fruit. Furthermore, the lipid concentration in a fruit’s vesicular cells increases throughout their development (Kelly et al., 2009). Accompanying the enlargement of a fruit, intracellular triacylglycerides (TAGs), largely composed of 16-carbon and 18-carbon fatty acids, accumulate in vesicular cells and form large lipid bodies. These lipids probably also assist in sealing water within the viscin, allowing pressure to build. Immediately before discharge, vesicular cell boundaries become indistinct, and the cell contents become confluent, creating a lipid mass between the viscin cells and the exocarp (Kelly et al., 2009).

3.4.5 Ribulose-1,5-bisphophate carboxylase/oxygenase

Figure 3.30 shows BLAST (NCBI) results displaying alignment of a putative RuBisCo protein from *A. oxycedri* to similar proteins from different plants, with identity ranging from 85% to 88%.

A major enzyme, RuBisCo is involved in carbon fixation in plants, where carbon dioxide is converted to glucose in photosynthetic organisms (Andersson and Backlund, 2008). It is also involved in photorespiration as an oxygenase (Peterhansel et al., 2010).

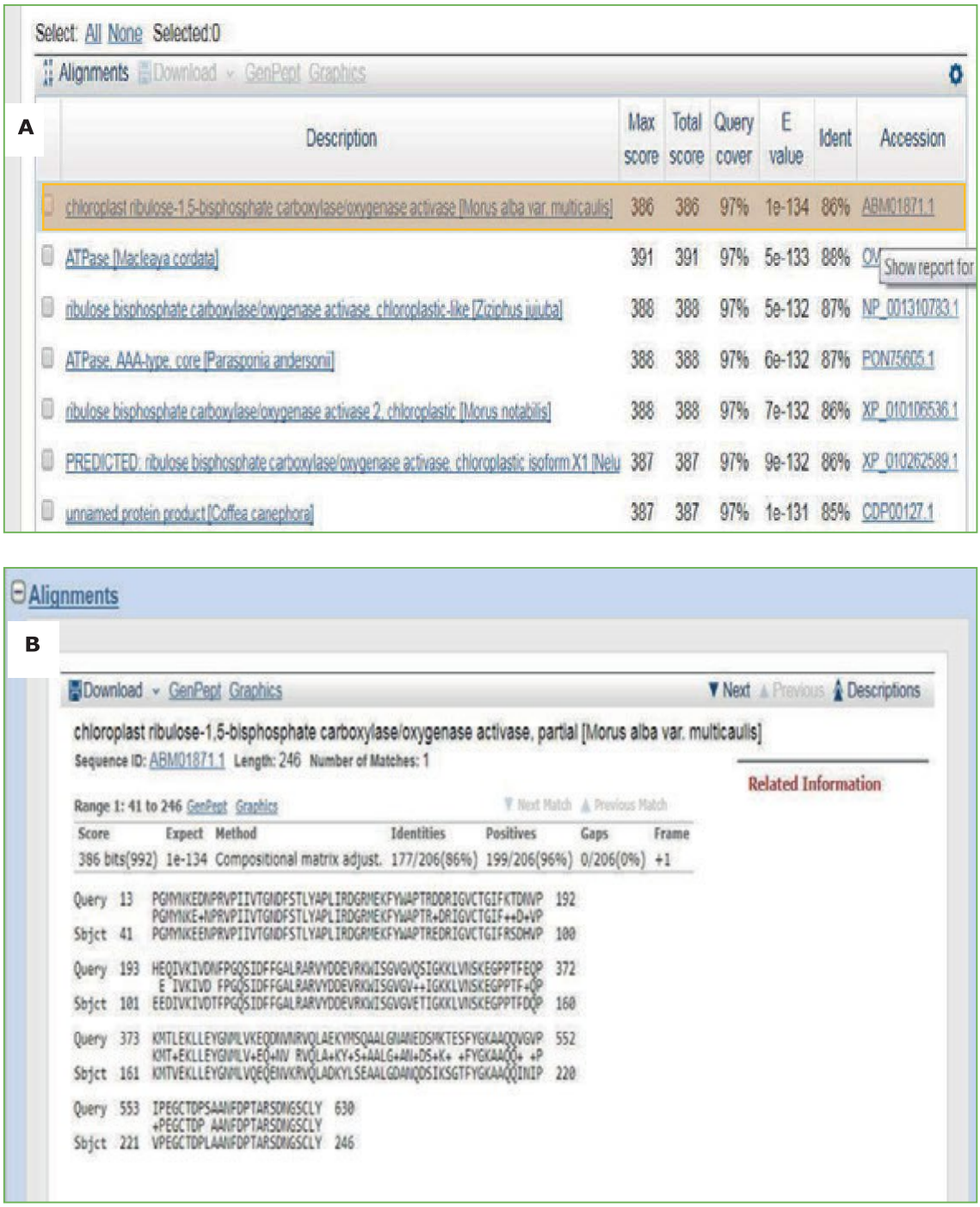

Figure 3.30 Blast (NCBI's BLAST) results of in silico translated nucleotide sequence. (A) Alignment of putative RuBisCo enzyme family protein from *A. oxycedri* with similar proteins from different plants. (B) Specific sequence example from *Morus alba* var. *multicaulis* (orange box in part A).

3.4.5.1 Discussion

Due to the RuBisCo protein's crucial role in photosynthetic carbon fixation, it is found in most autotrophic organisms, and it has been hypothesised that RuBisCo is probably the most abundant protein on Earth (Andersson & Backlund, 2008).

All RuBisCo molecules are multimeric (Figure 3.31) with two different types of subunits: large catalytic (L: 50–55 kDa) and small (S: 12–18 kDa) subunits. The most common form (form I) of RuBisCo is composed of large and small subunits in a hexadecameric structure: L8S8 (Figure 3.31B). This form exists in all higher plants.

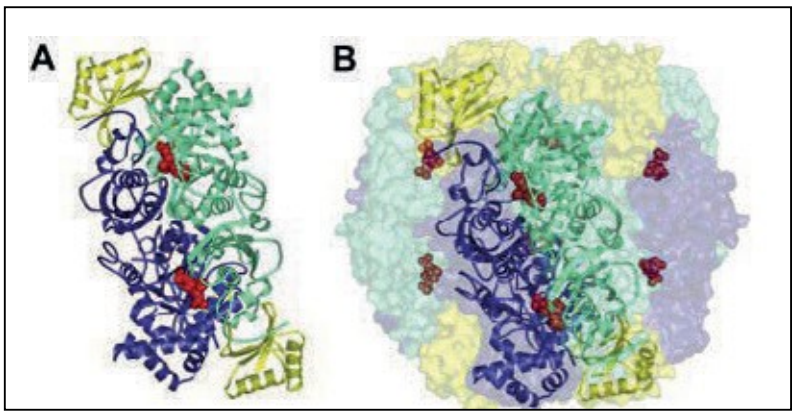

Figure 3.31 The quaternary structure of RuBisCo enzymes showing the molecular symmetry. A) The L2S2 unit of form I RuBisCo from spinach viewed along the 2-fold symmetry axis. Large subunits: blue and green colour, small subunits: yellow colour, and the substrate mimic (2CABP) is shown as red domains. B) The complete L8S8 hexadecamer (Adopted from Andersson & Backlund, 2008). The gene for the RuBisCO enzyme was used as reference gene for quantitative real time polymerase chain reaction.

The expression of the *RuBisCo* gene is steady during the second year of development for *Areuthobium* spp. (See qRt-PCR results); so, it could be used as a housekeeping gene for qRT-PCR purposes.

Mistletoes are hemiparasitic plants, and as such, they display a unique approach of obtaining resources by combining parasitism with their own photosynthetic activity, which is very limited in the dwarf mistletoes (Těšitel et al., 2010). Mistletoes have no root network, like holoparasites, but they can access water, minerals, and small amounts of carbon (to larger amounts, as in the dwarf mistletoes) from a host through haustorial sinkers. Additionally, they can balance the shortage or lack of organic carbon with their own photosynthetic activity (Watling & Press, 2001).

3.5 Other genes possibly involved in explosive seed dispersal

Results obtained from the Affymetrix array allowed the opportunity to identify approximately 1,000 genes highly differentially expressed in dwarf mistletoes during the second summer of fruit development. Consequently, this allowed a discussion of the molecular results to try and explain some of the physiological processes. However, as the main goal of this thesis was to elucidate potential molecular players engaged in explosive seed dispersal, the choice was made to focus on gene expression related to this event. Table 3.7 shows the genes potentially involved in the process of explosive seed dispersal. The AQPs were described in the Introduction.

Table 3.7 *Description of candidate genes potentially involved in explosive seed dispersal in Arceuthobium spp.*

Gene / Protein name	**TAIR**	**September expression in comparison to May**	**General protein function / putative physiological results in *Arceuthobium* spp.**
Plasma membrane intrinsic protein 2 PIP2 2 PIP1 4 PIP2 4	AT2G37170 AT4G00430 AT5G60660	-2.21 -1.1885 -1.207489	Water transport, Significant increase of fruit size over the growing season (Ziegler & Ross Friedman (2017a,b)
Stomatal cytokinesis defective2 (SCD2)	AT3G48860	-1.155	Mutated cell prevents the cell division of meristemoid/guard cells in the stomatal differentiation pathway. Stomata density decline during the growing season of fruit, scanning electron microscope (Ziegler and Ross Friedman 2017b)
Movement protein binding protein (MPB2)	AT5GO8120	-1.175	Influences stomatal patterning, overexpression leads to stomatal clustering and higher stomatal density Stomata density declines during the growing season of the fruit, scanning electron microscope (Ziegler and Ross Friedman 2017b)
ECERIFERUM 1 (CER1)	At1G02205	-1.95	Dvelopment of waxes within cuticle; alkane formation Cuticle thicker on mature fruit of *Areuthobium* spp.
Sterol-14 demethylase (CYP51) Member of P-450	AT1G11680 At1G50430	-1,13	Cell membrane sterol production Not reported/investigated in *Arceuthobium* spp.
SHINE2 (SHN2)	AT5G11190	2.05	The SHINE clade of AP2 involved in waxes formation Cuticle thicker on fruit of *Areuthobium* spp.
Alkaline/neutral invertase portion of gene (CINV2)	AT4G09510	Down-regulated	Splitting sucrose into fructose and glucose Not investigated in *Arceuthobium* spp.

As the fruit of all mistletoes within the former Viscaceae (now in Santalaceae) resembles berry/pseudoberry types of fruit (Polli et al., 2016), and as the *Vitis*

vinifera berry has been extensively studied (Zenoni et al., 2010), it was decided to look at genes that are similarly expressed in *Arceuthobium* as revealed in the Affymetrix microarray.

3.5.1 Stomata development

The anatomy and structure of *Arceuthobium* fruit have also been extensively studied, and as noted by Hawksworth and Wiens (1998) and Wilson and Calvin et al. (2006), fruits of *Arceuthobium* are divided into two distinct morphological zones. The distal upper one-third of the fruit (the remnant sepals) contains stomata, with stomatal density in nearly mature fruits having a concentration around 48 per mm^2. The lower two-thirds of the fruit (proximal zone) is completely devoid of stomata. This value corresponds with results obtained by Ziegler & Ross Friedman (2017b), who, using environmental scanning electron microscopy, observed fruit during a whole second summer (growing season) of development from late April until early September. These authors found that the density of stomata per mm^2 decreases and that the cuticle, which only covers the fruit body (not the sepals), gets thicker with development (Figure 3.32).

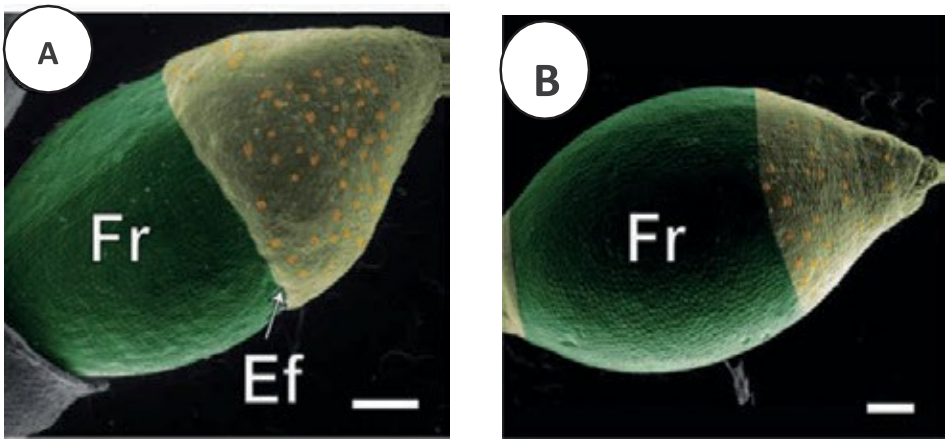

Figure 3.32 Images (environmental scanning electron microscopy) of second-year fruit from *Arceuthobium americanum* sampled in (A) late April (B) late August. The fruit body (Fr) is highlighted in green, the sepals are in beige, and the subsidiary cells of each stoma in orange; an epidermal fold (Ef) is evident where the sepals are united and inserted at the top of the ovary (modified from Ziegler & Ross Friedman, 2017b). Scale bar = 400 µm

The observed anatomical changes can be discussed on a molecular level to a certain degree based on the information-rich Affymetrix microarray results. A single stoma consists of a pair of guard cells (occasionally with subsidiary cells as well); its role is to facilitate gas and water-vapour exchange between plants and the environment. In

Arabidopsis, there are three key stomatal proteins: MUTE, and two paralogues, FAMA and SPEECHLESS. Together, they control stomatal development at three sequential steps: initiation, meristemoid differentiation, and guard cell morphogenesis (Pillitteri et al., 2007).

However, they were not detected in either May or September in *Arceuthobium americanum*, suggesting that the signal was very low and that they were filtered out from both 300 and 200 cut-off level intensity files. Therefore, probes representing these genes in *Arabidopsis* do not match a template from *Arceuthobium*. However, there are other genes that play an important role in fruit development and seed dispersal in *A. thaliana*, and they were significantly expressed in *A. americanum*.

There are two genes, among others, known to be related to stomata development: stomatal cytokinesis defective (SCD) 1 and SCD2. The respective proteins are important in clathrin-dependent trafficking during cytokinesis and cell expansion in *Arabidopsis thaliana.* If both genes are mutated, guard cells miss a part or a whole cell wall; also, cytokinesis of the epidermal pavement cells is then defective (McMichael et al., 2013). The homologues of SCD2 proteins are found in many divergent plant genera including *Ricinus* (castor bean), *Vitis* (grape), *Cucumis* (cucumber), *Solanum* (tomato), *Zea* (maize), *Glycine* (soybean), *Oryza* (rice), *Sorghum*, *Panicum* (switchgrass), *Picea* (spruce), and *Populus* (poplar; http://blast.ncbi.nlm.nih.gov/Blast.cgi). As this protein has never been found in protists, fungi, or animals, it must assist plants exclusively. To date, little is known about how SCD proteins can control cell division symmetry and stomatal patterning. According to the Affymetrix results, SCD2 is up-regulated in May with down-regulation (-1.12) in September. Generally, there are fewer stomata on mature mistletoe fruits, particularly in September, so this expression reduction makes sense in unmutated genes. It would be interesting to find out when exactly stomata develop.

Another protein, movement protein binding protein (MPB2), was down-regulated in September (-1.75). Research by Ruggenthaler et al. (2009) indicates that overexpression of MPB2 in *Arabidopsis* causes disturbed stomata pattering, stomatal clustering, and higher stomatal density. Therefore, the lower stomatal density observed in September *A. americanum* fruit makes sense. To date, not much research has been done regarding the effects of down-regulation of MPB2 on stomatas in plants.

3.5.2 Cuticle and wax production

The Affymetrix results indicate that a few genes were also likely involved in the synthesis of cuticle and waxes in *Arceuthobium*: ECERIFERUM 1 (CER 1) and SHINE 2 (SHN 2). These genes could be involved in seed dispersal as they are involved in wax and cutin production.

Plant aerial surfaces are separated from the outside environment by a cuticle that overlays the cell walls of epidermal cells (the outermost cells). The cuticle consists of cutin (composed mainly of esterified hydroxy and epoxy fatty acids, 16 and 18 carbons in length), waxes embedded as crystals in the cuticle, and epicuticular wax on the outermost surface of the cuticle (Figure 3.33; Commenil et al., 1997). Waxes in the cuticle consist mostly of saturated, very long fatty acids (more than 18 carbons in length), alcohols, ketones, esters, alkanes, and aldehydes.

The cuticle plays many important roles in a plant, such as protection against external environmental stressors and pathogens (Commenil et al., 1997) as well as controlling nonstomatal water loss and epidermal permeability (Aharoni et al. 2004; Petit et al., 2016). Considering the importance of water in the physiology of plant growth and development, the need for controlling and assisting in water retention in any environment, especially in summer, is paramount. Consequently, the capability to synthesize, transport, and accumulate a hydrophobic layer or cuticle over the surface of aerial organs appears to be critical (Budke et al., 2012). This is particularly true in the case of fruits, where there is a need to protect an embryo against desiccation and other environmental conditions, as well as maintain a high level of moisture in many fleshy fruits.

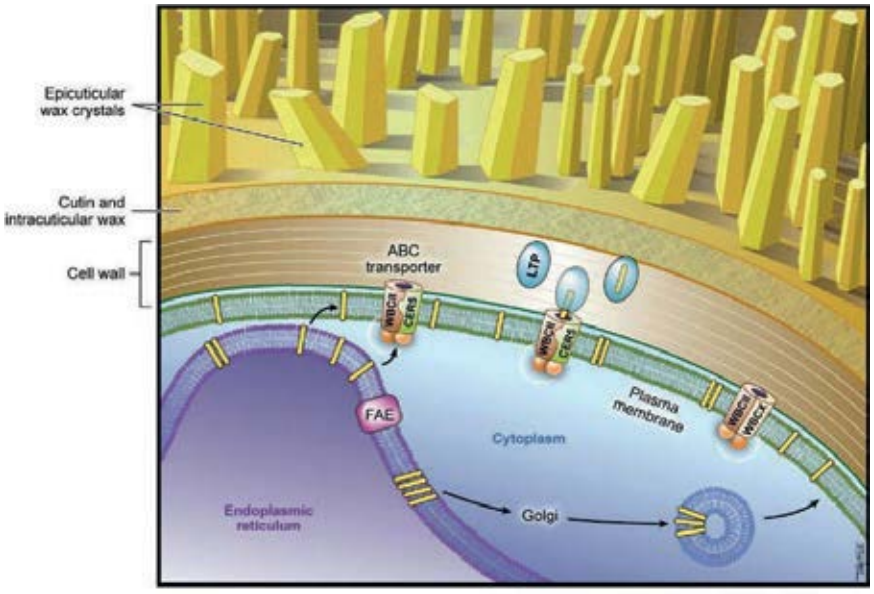

Figure 3.33 Generalized plant surface showing the major structural features of the cuticle, epidermal cell layer, and graphic model of cuticular wax secretion. Genes listed are ATP-binding cassette transporter (ABC); ECERIFERUM (CER)5; fatty acid elongase (FAE); lipid transfer protein (LTP); white-brown complex (WBC; Samuels et al., 2008). Only the ABC transporter gene was investigated in detail in this thesis.

To date, cuticle and wax biosynthesis has been extensively studied in *Arabidopsis*, a dry fruit-bearing plant that provides an excellent experimental model for the research (reviewed in Bernard & Joubès, 2013) and much information can be derived from this study in relation to cuticle development. Here, it was decided to concentrate on anatomical and molecular research done for fleshy type fruits, especially berry type such as *Vitis vinifera* and tomato (Pettit et al., 2016). For example, numerous researchers have tried to find a connection between the chemistry of a given cuticle's wax and the transpirational barrier properties of the cuticle. A study by Vogg et al. (2004) examined the developmental stage of dwarf tomato MicroTom; study of its *lecer6* mutant showed that water permeability of cuticle in the fruits was largely dependent on the aliphatic component of the intracuticular wax layer, which was modified by variable amounts of triterpenoids during the various maturation stages. Another study done by Leide et al. (2007) indicated that cuticular wax quality rather than quantity is more important in governing water barrier properties. Table 3.8 shows cuticular wax components and cutin monomers in different fleshy fruits from different plant species.

Table 3.8 Cuticular wax compositions and predominant cutin monomers in different fruit species. Adapted from Misra (2015).

Fruit	Fruit type	**Predominant wax components**	**Predominant cutin monomers**	**References**
Tomato (*Solanum lycopersicum*)	berry	n-hentriacontane (C_{31}) triterpenoid alcohols (α-, β-, and δ-amyrin)	C_{16} monomers (10,16-dihydroxy $C_{16:0}$)	Isaacson et al. (2009); Leide et al. (2007); Petit et al. (2014); Shi et al. (2013); Yeats et al. (2012a)
Grape (*Vitis vinifera*)	berry	Triterpernoid oleanoic acid n- alcohols (C24, C26, C28), n-aldehydes (mostly C28 and C30), esters, and free acids (largly C24, C26, and C28) n-hydrocarbons (mostly C25, C27, and C31)	Not reported	Casado & Heredia (1999); Comménil et al. (1997); Pensec et al. (2014); Radler (1965,1970); Radler & Horn (1965)
Plum (*Prunus domestica*)	drupe	(oleanolic acid)	not reported	Ismail et al. (1977)
Peach (*Prunus persica*)	berry	n-tricosane (C_{23}), n-pentacosane (C_{25}), n-heptacosane (C_{27}) triterpenoid acids (ursolic acid, oleanolic acid)	C_{18} monomers (ω-hydroxy $C_{18:1}$)	Belge et al. (2014a); Fernández et al. (2011)
Sweet cherry (*Prunus avium*)	drupe	n-nonacosane (C_{29}) triterpenoid acids (ursolic acid)	cultivar-dependent (dihydroxy $C_{16:0}$ or dihydroxy $C_{18:x}$ (mainly reported)	Belge et al. (2014b); Peschel et al. (2007)

Strawberry (*Fragaria* × *ananassa*)	etaerio	not reported	C16 monomers (9(10),16-dihydroxy C16:	Järvinen et al. (2010)
Cranberry (*Vaccinium oxycoccos*)	berry	not reported	C18 monomers (ω-hydroxy-9,10-epoxy C18:0)	Kallio et al. (2006)
Dwarf mistleto (*Arceuthobium* spp.)	berry/pseudoberry	not reported	not reported	Ziegler & Ross Friedman (2017a,b); Polli et al. (2016)

Similarly, based on these observations, there are many genes that could potentially be involved in cuticle/wax formation in dwarf mistletoe.

3.5.2.1 ECERIFERUM 1 gene

Many genes associated with cuticular wax metabolism in *Arabidopsis* have been isolated and characterized. The group of genes called ECERIFERUM (CER) genes affect wax biosynthesis at many levels of synthesis. As such, CER1 has been proposed to encode an aldehyde decarbonylase (Aarts et al., 1995; Bourdenx et al., 2011). It was noticed in the CER1 mutant that there is an increase in aldehydes and a reduction in levels of alkanes, secondary alcohols, and alkanest. Therefore, it was proposed that CER1 encodes a novel protein involved in the conversion of long-chain aldehydes to alkanes, a key step in wax biosynthesis.

3.5.2.2 SHINE2 - SHINE clade of AP2

Research done by Shi et al. (2011) using *Arabidopsis thaliana* suggests that SHINE (SHN) transcription factors have target genes within four cutin- and suberin-associated protein families comprising CYP86A cytochrome P450s, fatty acyl-CoA reductases, GSDL-motif lipases, and BODYGUARD1-like proteins. Besides controlling cuticular lipids metabolism, SHNs act to modify the epidermis cell wall through altering pectin metabolism and structural proteins. Specifically, SHINE2 promotes cuticle formation by inducing the expression of enzymes involved in wax biosynthesis. It binds to the GCC-box pathogenesis-related promoter element. It may also be involved in the regulation of gene expression by stress factors and components of stress signal transduction pathways (Aharoni et al., 2004).

3.6 General discussion

The main purpose of this thesis was to explore the potential molecular basis for explosive seed dispersal in dwarf mistletoes (*Arceuthobium* spp.), with focus on AQPs, which could be involved in the explosive seed dispersal by transporting water between cells. To achieve this goal, the research started with extraction of RNA from dwarf mistletoe; the process of extraction was very lengthy and difficult, but ultimately succesful.

To find AQPs and other possible genes, a heterologous microarray approach employing probes from unrelated plants was used. This technique was chosen because no genomic sequences currently exist in the NCBI database for any member of *Arceuthobium* or any other closely related plant. By using this approach, sequence similarity to PIP2, RuBisCo, Alk/N invertase, the ABC transporter group, and sterols was shown. For the PIP2 candidate, a physiological experiment on the presumed PIP2 gene was performed; and stopped-flow cytometry was used to prove that the sequenced molecule was indeed an AQP2.

Results initially obtained with the handheld MicroCASTer microarray system and heterologous approach encouraged continued experimentation with the Affymetrix microarray technique for *A. americanum* fruits to detect other genes and their expression over fruit development. The results obtained from the Affymetrix microarray were validated by performing qRT-PCR and comparing the expression results with the existing literature describing certain physiologically or anatomically relevant findings.

To explore and deliberate the results in light of both fruit development and explosive seed dispersal, the information obtained previously from research done on fruit development using the well-studied *A. thaliana* fruit (dry fruit) as well as fleshy fruit like *Vitis vinifera* and *Solanum lycopersicum* (fleshy berry type) was compared. During fleshy fruit development, as in *Vitis vinifera* (a plant that so far possesses one of the most extensively studied and characterized transcriptomes among fruit species: Terrier et al., 2005; Zenoni et al, 2010; di Genova et al., 2014; Balic et al. 2018) there are many developmental stages wherein many changes occur in terms of anatomy and physiology, and thus gene expression. Many genes are involved in the production of primary and secondary metabolites, water transport, and enzymes. As was shown by Terrier et al. (2005), genes important for ripening are mostly invertases that help in the accumulation of sugars (Terrier et al., 2005). Moreover, as fruit enlarges, water influx controlled by aquaporins is important (Fouquet et al., 2008).

Similarly, in dwarf mistletoe, it was concluded that in addition to genes regulating standard fruit maturation, which are similar in all berries, genes regulating explosive seed dispersal are also required. There are some plants that also rely on ejection of seeds from a fruit, but they depend on water evaporation from pods (*Papilionaceae* family). There are not many plants that eject their seeds similarly to dwarf mistletoes, although the squirting cucumber (*Ecballium elaterium*) belonging to the family *Cucurbitaceae* is an example, but there is no data for the molecular basis of “squirting” discharge, either.

All of the results from the Affymetrix array in terms of gene expression and potential roles in explosive seed dispersal are supported by physiological and anatomical changes observed by others and verified by the qRT-PCR results. As a result, an overarching general hypothesis was formed regarding explosive seed dispersal, which is supported by the molecular results.

These genes as well as their expression can be seen in Table 3.7 and include PIP2, alkaline/neutral invertase portion of gene (CINV2), stomatal cytokinesis defective2

(SCD2), movement protein binding (MPB2), CER1, sterol- 14 demetylase CYP51, and SHINE3.

Anatomically, in *Arceuthobium* spp fruit, vesicular cells are located outside viscin cells, which in turn surround its seed (endocarp, embryo, and endosperm). During fruit and seed development (late April to end of August of the second summer), water accumulates inside of the fruit, most notably in the viscin cell mucilage (viscin). Fruits grow by increasing in size, largelt due to water retention both inside and outside of viscin cells, mostly in the viscin. Water is drawn into the fruit from the rest of the mistletoe plant and host tree via transpiration in the apoplast (Ziegler & Ross Friedman, 2017b). Since the alkaline neutral invertase gene (CINV2) is up-regulated in Ma, in comparison to September, the resulting enzyme helps in movement of sucrose and in splitting it into glucose and fructose (Figure 3.34). This action would create an increasing solute concentration within the fruit (likely mucilage), which would continue to draw and hold water.

However, not all water movement would be apoplastic; movement of water from cell-to-cell (in the symplast) would also occur, and would be facilitated by AQPs. This result has been confirmed by the Affymerix results, which clearly show that the PIP2 gene in *Arceuthobium* spp. is up-regulated in May and down-regulated in September, just before seed dispersal. Similar results have been observed in the *Vitis vinifera* berry, where up-regulation of PIP2 genes was noticed just before ripening, with a decline over time (Fouquet et al. 2008). Also, immunogold-labelled tobacco PIP2 antibodies were used probe viscin tissue of *Arceuthobium americanum*, and the results show suggest that PIP2 proteins exist at higher concentrations in May and June in comparison to the time just before seed dispersal (Ross Friedman et al. 2010). Therefore, water transport between the living cells within the fruit must also be ongoing, with the most likely direction of transport being from the mesocarp cells at the base of the fruit (near the vascular tissue) toward the viscin cells, which are viable at maturity (Ross, 2006).

Concomitantly, vesicular cells become impregnated with fatty acids and sterols (CYP1 gene up-regulated in May, down in September), and the resulting cells become stiffer, forming a “lipid casing” around the viscin cells. Additionally, genes involved in stomatal expression, like SCD2 and MPB2C, show lower expression in September, evidenced by a deceased stomatal density on the distal part of the fruit, perhaps allowing the plant to retain water inside the fruit and help build the pressure until the time of dispersal arrives. Furthermore, *A. americanum* was recently observed to develop a particularly thick cuticle as dispersal approaches (Ziegler & Ross Friedman,

2017a,b), which may also facilitate pressurization. Genes like CER1 and SHINE 3 are certainly showing changes in gene expression at this time.

As both fruit length and diameter increased over most of the second year, and the stomatal density decreased on the distal part of the fruit, the reorientation of the fruit and stomata via the growth of a recurved pedicel may further play a role in optimizing dispersal. Naturally, the curvature enables the seed to be released at a 45-degree angle away from the plant axis, maximizing spread. However, orienting the stomata downward, away from the sun and natural transpiration pull, might help reduce the apoplastic flow of water into the fruit as dispersal approaches.

Results obtained by deBruyn et al. (2015) show that the process of thermogenesis (accumulation of heat energy before seed dispersal) is somehow intimately involved in discharge, perhaps by building pressure and/or perhaps by labilizing cellular components, potentially even destabilizing the cuticle around the abscission layer. In any case, thermogenesis would create a large demand for glucose and sucrose, so up-regulation of alkaline invertase makes sense. Figure 3.34 shows all genes investigated during the research and that may potentially be involved in explosive seed dispersal in *Arceuthobium* species.

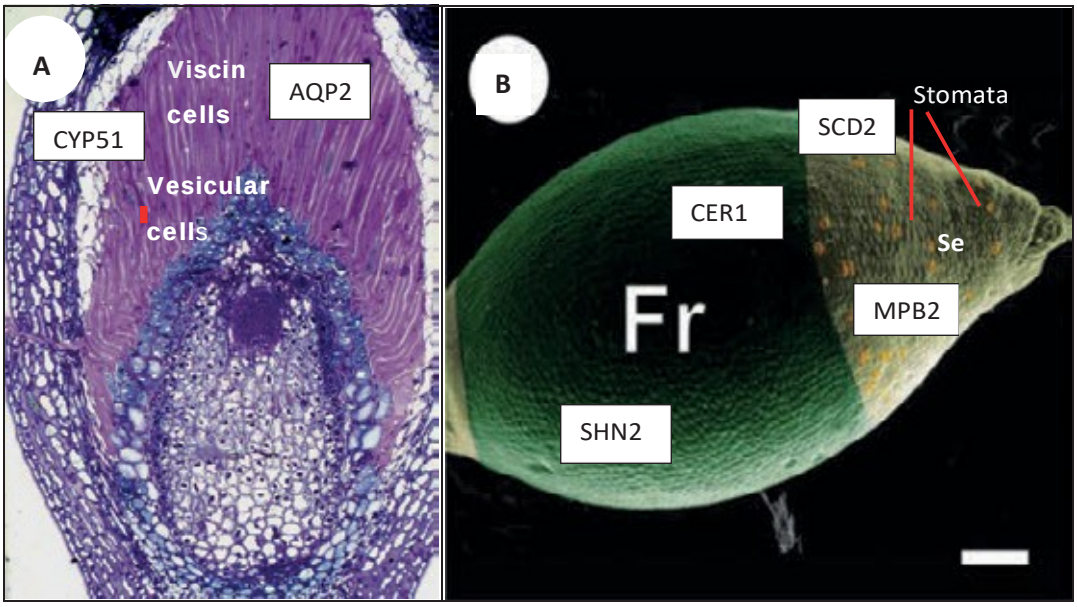

Figure 3.34 Distribution of genes potentially involved in explosive seed dispersal in second-year fruit from *Arceuthobium* spp. (A) Fruit as seen in longitudinal sectional view using brightfield microscopy and stained with toluidine blue O (Ross, 2006). (B) Environmental scanning electron micrograph of fruit (Ziegler & Ross Friedman, 2017b). Fruit (Fr); sepals (Se); aquaporins 2 (AQP2); cytochrome P450 (CYP5), sterol-14 demethylase; ECERIFERUM 1 (CER1); SHN2, SHINE2; stomatal cytokinesis defective2 (SCD2); Movement protein binding protein (MPB2,); alkaline/neutral invertase portion of gene (CINV2). Scale bar = 400 µm.

3.7 Future prospects

The present study dealing with the process of explosive seed dispersal could be a very useful platform for further investigations of similar processes in other plants. This study could provide novel, molecular insights into not only the explosive seed dispersal in dwarf mistletoe, but also into other processes within dwarf mistletoe. The preliminary studies described herein shed light on the seed dispersal process. The present work still leaves many questions unanswered, which need to be addressed, to better understand the physiology of this parasitic plant. At this point, it is crucial to emphasize that changes in mRNA accumulation may not always correlate with protein and enzyme activity; therefore, additional physiological studies, proteomics and transgenic approaches may be needed for better understanding and clarification of the process of seed dispersal.

To move forward using the results of this current research, I propose the following studies:

1. Western blots of the aquaporins should be performed to build the seasonal profile over the entire fruit development season.
2. Concentration and identification of fatty acids using gas chromatography (GC) (Mir et al., 2006) and the same for sterols using HPLC/mass spectrometry over an entire year (or at least the growing season) should be determined.
3. To further our knowledge about the influence of the stomata on the process of seed dispersal, transpiration rates, which are strongly related to stomatal regulation leading to explosive discharge, should be investigated.
4. And, in conjunction with the previous point, the composition of the cuticle throughout development should be determined to assess how the cuticle may be regulating transpiration.
5. More of the molecular drivers that control development of various tissues in the fruit (i.e., when the viscin cells begin to elongate, when they begin to secrete their mucilage, if the composition of the mucilage changes over time, how the vescicular cells develop, etc.) should be investigated.
6. The process of thermogenesis should be further investigated in terms of expression of AOX and PTOX genes, which are typically involved in this process. Q-RTPCR may help establish the profile of expression.

7. Affymetrix heterologous array results should be used for further investigation of other processes in dwarf mistletoe identified in the GO categories, such as development and reproduction, photosynthesis and response to light stimulus, as well as parasitism related gene expression.

8. The heterologous microarray data should be used as a basis for next gen sequencing, which should be run to obtain detailed transcriptomic resources.

Undertaking further studies in this vein will not only shed light on the intricate and unusual processes of fruit development and seed dispersal in *Arceuthobium*, but should also reveal sensitive points in fruit development, which in turn could potentially be targeted in dwarf mistletoe management.

4. SUMMARY

Worldwide, mistletoe plants are important forest pests, found in all continents aside from Antarctica. In North America, control of conifer parasitism by dwarf mistletoes, specifically *Arceuthobium americanum,* is challenging. Dwarf mistletoes are dioecious parasitic flowering plants with a unique and effective explosive seed dispersal mechanism. Due to the large accumulation of water within the fruit, which increases both the fruit size and its internal hydrostatic pressure, the transport of water into the fruit and the possible involvement of plasma membrane intrinsic proteins (PIPs), particularly aquaporins (AQPs), were the focus of the investigation. Notably, previous research also demonstrated that cuticle thickening, declining stomata number, and thermogenesis are potential “players” in forcible discharge. As such, molecular work was performed here to reveal genes involved in physiological processes potentially associated with explosive seed dispersal and to examine the expression of these genes. Therefore, the overarching goal of this project was to obtain gene sequencing and expression data for *Arceuthobium* spp. to gain insights into the involvement of AQPs and other proteins likely responsible for generating high hydrostatic pressure and discharge. Many methods were employed to extract the RNA from the fruit, including both traditional and commercially available methods, and following successful extraction, a cDNA library was constructed. A non-standard heterologous microarray hybridization, unconventionally used for transcription analysis of non-model species, employing both the MicroCASTer handheld system and an Affymetrix *Arabidopsis* Gene 1.0 ST microarray was used to determine gene sequence and expression. Five genes sequences were obtained from the handheld system: *AQP2, ABC transporter, Ribulose Bisphosphate Carboxylase-Oxygenase, Alkaline/neutral invertase,* and *Sterol-14 demethylase.* To confirm that *AQP2* codes for plasma membrane intrinsic protein 2 (PIP2), gateway cloning followed by a physiological study with stopped-flow spectroscopy was undertaken. Despite sequence divergence between the two species, 24.2% of *Arabidopsis* Gene 1.0 ST array was hybridized to dwarf mistletoe RNA; this hybridization identified approximately 1,000 genes that are highly differentially expressed in dwarf mistletoe during fruit development. Further investigation of the Affymetrix results revealed several additional mistletoe genes, *Stomatal cytokinesis defective2*, *Movement protein binding protein, Eceriferum1, and SHINE2*, that are seasonally up and down regulated (May vs. September) and are likely involved in the explosive seed dispersal process. With these results in hand, research can advance towards molecular insights into not only explosive seed dispersal in dwarf mistletoe, but also into other processes such as development, reproduction, photosynthesis light response, and parasitism-associated gene expression within dwarf mistletoe and

related plants. Ideally, this work will provide new opportunities for investigating novel avenues of plant-plant pest control.

Poster presentations / publications emerging from the thesis

Poster presentations

July 2015 Botany 2015: Science and Plants for People. International Conference, Edmonton, Alberta. Poster presentation: Urban, J., Kaldenhoff, R., Ross Friedman, C., Otto, B., and Bouditchevskaia, A. Gene expression in Dwarf Mistletoe during the Explosive Seed Dispersal with Special Attention to Aquaporins.

June 2013 49th Canadian Botanical Association Annual Meeting and Conference. Thompson Rivers University, Kamloops, BC. Poster presentation: Urban, J., Kaldenhoff R., Ross Friedman, C., Otto, B. Dwarf Mistletoe and Aquaporins.

Manuscripts in progress:

1. *Use of heterologous microarrays approach for investigation of gene expression in non-model plants.*
2. *Gene expression in dwarf mistletoe during explosive seed dispersal with special attention to aquaporins.*

REFERENCES

Aarts, M. G., Keijzer, C. J., Stiekema, W. J., & Pereira, A. (1995). Molecular characterization of the CER1 gene of arabidopsis involved in epicuticular wax biosynthesis and pollen fertility. *The Plant Cell*, *7*(12), 2115–2127. Retrieved from https://www.ncbi.nlm.nih.gov/pubmed/8718622

Abascal, F., Irisarri, I., & Zardoya, R. (2014). Diversity and evolution of membrane intrinsic proteins. *Biochimica et Biophysica Acta*, *1840*(5), 1468–1481. https://doi.org/10.1016/j.bbagen.2013.12.001

Agre, P., Preston, G. M., Smith, B. L., Jung, J. S., Raina, S., Moon, C., … Nielsen, S. (1993). Aquaporin CHIP: the archetypal molecular water channel. *The American Journal of Physiology, 265*(4 Pt 2), F463–F476. https://doi.org/10.1152/ajprenal.1993.265.4.F463

Aharoni, A., Dixit, S., Jetter, R., Thoenes, E., van Arkel, G., & Pereira, A. (2004). The NE clade of AP2 domain transcription factors activates wax biosynthesis, alters cuticle properties, and confers drought tolerance when overexpressed in Arabidopsis. *The Plant Cell*, *16*(9), 2463–2480. https://doi.org/10.1105/tpc.104.022897

Andersson, I., & Backlund, A. (2008). Structure and function of Rubisco. *Plant Physiology and Biochemistry: PPB / Societe Francaise de Physiologie Vegetale*, *46*(3), 275–291. https://doi.org/10.1016/j.plaphy.2008.01.001

Aranda, P. S., LaJoie, D. M., & Jorcyk, C. L. (2012). Bleach gel: a simple agarose gel for analyzing RNA quality. *Electrophoresis, 33*(2), 366–369. https://doi.org/10.1002/elps.201100335

Ashburner, M., Ball, C. A., Blake, J. A., Botstein, D., Butler, H., Cherry, J. M., … Sherlock, G. (2000). Gene ontology: tool for the unification of biology. The Gene Ontology Consortium. *Nature Genetics*, *25*(1), 25–9. https://doi.org/10.1038/75556

Auer, H., Newsom, D. L., & Kornacker, K. (2009). Expression Profiling Using Affymetrix GeneChip Microarrays. In U. Bilitewski (Ed.), *Microchip Methods in Diagnostics* (pp. 35–46). Totowa, NJ: Humana Press. https://doi.org/10.1007/978-1-59745-372-1_3

Balic, I., Vizoso, P., Nilo-Poyanco, R., Sanhueza, D., Olmedo, P., Sepúlveda, P., … Campos-Vargas, R. (2018). Transcriptome analysis during ripening of table grape berry cv. Thompson Seedless. *PloS One, 13*(1), e0190087. https://doi.org/10.1371/journal.pone.0190087

Barlow, J. J., Mathias, A. P., Williamson, R., & Gammack, D. B. (1963). A simple method for the quantitative isolation of undegraded high molecular weight ribonucleic acid. *Biochemical and Biophysical Research Communications*, *13*, 61–6. Retrieved from http://www.ncbi.nlm.nih.gov/pubmed/14069514

Barratt, D. H. P., Derbyshire, P., Findlay, K., Pike, M., Wellner, N., Lunn, J., … Smith, A. M. (2009). Normal growth of *Arabidopsis* requires cytosolic invertase but not sucrose synthase. *Proceedings of the National Academy of Sciences of the United States of America*, *106*(31), 13124–13129. https://doi.org/10.1073/pnas.0900689106

Beck, J. G., Mathieu, D., Loudet, C., Buchoux, S., & Dufourc, E. J. (2007). Plant sterols in “rafts”: a better way to regulate membrane thermal shocks. *The FASEB Journal*. https://doi.org/10.1096/fj.06-7809com

Belge, B., Llovera, M., Comabella, E., Graell, J., & Lara, I. (2014a). Fruit cuticle composition of a melting and a nonmelting peach cultivar. *Journal of Agricultural and Food Chemistry, 62*(15), 3488–3495. https://doi.org/10.1021/jf5003528

Belge, B., Llovera, M., Comabella, E., Gatius, F., Guillén, P., Graell, J., & Lara, I. (2014b). Characterization of cuticle composition after cold storage of “Celeste” and “Somerset” sweet cherry fruit. *Journal of Agricultural and Food Chemistry, 6*2(34), 8722–8729.https://doi.org/10.1021/jf502650t

Benjamini, Y., & Hochberg, Y. (1995). Controlling the false discovery rate: A practical and powerful approach to multiple testing. *Journal of the Royal Statistical Society. Series B, Statistical Methodology, 57*(1), 289–300. Retrieved from http://www.jstor.org/stable/2346101

Bernard, A., & Joubès, J. (2013). *Arabidopsis* cuticular waxes: advances in synthesis, export and regulation. *Progress in Lipid Research*, *52*(1), 110–129. https://doi.org/10.1016/j.plipres.2012.10.002

Bertl, A., Slayman, C. L., & Gradmann, D. (1993). Gating and conductance in an outward-rectifying K+ channel from the plasma membrane of Saccharomyces cerevisiae. *The Journal of Membrane Biology, 132*(3), 183–199. Retrieved from https://www.ncbi.nlm.nih.gov/pubmed/8492306

Biela, A., Grote, K., Otto, B., Hoth, S., Hedrich, R., & Kaldenhoff, R. (1999). The *Nicotiana tabacum* plasma membrane aquaporin NtAQP1 is mercury-insensitive and permeable for glycerol. *The Plant Journal: For Cell and Molecular Biology, 18*(5), 565–570. Retrieved from https://www.ncbi.nlm.nih.gov/pubmed/10417707

Birtić, S., & Kranner, I. (2006). Isolation of high-quality RNA from polyphenol-, polysaccharide- and lipid-rich seeds. *Phytochemical Analysis : PCA*, *17*(3), 144–148. Retrieved from http://www.ncbi.nlm.nih.gov/pubmed/16749420

Bots, M., Vergeldt, F., Wolters-Arts, M., Weterings, K., van As, H., & Mariani, C. (2005). Aquaporins of the PIP2 class are required for efficient anther dehiscence in tobacco. *Plant Physiology, 137*(3), 1049–1056. https://doi.org/10.1104/pp.104.056408

Boudichevskaia, A., Heckwolf, M., Althaus, L., & Kaldenhoff, R. (2015). Transcriptome analysis of the aquaporin AtPIP1;2 deficient line in Arabidopsis thaliana. *Genomics Data*, *4*, 162–4. https://doi.org/10.1016/j.gdata.2015.04.018

Bourdenx, B., Bernard, A., Domergue, F., Pascal, S., Léger, A., Roby, D., … Joubès, J. (2011). Overexpression of Arabidopsis ECERIFERUM1 promotes wax very-long-chain alkane biosynthesis and influences plant response to biotic and abiotic stresses. *Plant Physiology, 156*(1), 29–45. https://doi.org/10.1104/pp.111.172320

Boyle, E. I., Weng, S., Gollub, J., Jin, H., Botstein, D., Cherry, J. M., & Sherlock, G. (2004). GO::TermFinder--open source software for accessing Gene Ontology information and finding significantly enriched Gene Ontology terms associated with a list of genes. *Bioinformatics*, *20*(18), 3710–3715. https://doi.org/10.1093/bioinformatics/bth456

Budke, J. M., Goffinet, B., & Jones, C. S. (2012). The cuticle on the gametophyte calyptra matures before the sporophyte cuticle in the moss *Funaria hygrometrica* (Funariaceae). *American Journal of Botany*, *99*(1), 14–22. https://doi.org/10.3732/ajb.1100311

Bumgarner, R. (2013). Overview of DNA microarrays: types, applications, and their future. *Current Protocols in Molecular Biology / Edited by Frederick M. Ausubel ... [et Al.]*, *Chapter 22*, Unit 22.1. https://doi.org/10.1002/0471142727.mb2201s101

Calvin, C. L., and Wilson, C. A. 1996. Endophytic system. In F. G. Hawksworth and D. Wiens (Eds.), *Dwarf Mistletoes: Biology, Pathology, and Systematics*. Washington, D.C.: United States Department of Agriculture, Forestry Service: Agricultural Handbook 709.

Casado, C. G., & Heredia, A. (1999). Structure and dynamics of reconstituted cuticular waxes of grape berry cuticle (*Vitis vinifera* L.). *Journal of Experimental Botany, 50*(331), 175–182. https://doi.org/10.1093/jxb/50.331.175

Casson, S., & Gray, J. E. (2008). Influence of environmental factors on stomatal development. *The New Phytologist*, *178*(1), 9–23. https://doi.org/10.1111/j.1469-8137.2007.02351.x

Ciesla, W. M., Geils, B. W., & Adams, R. P. (2002). Hosts and geographic distribution of *Arceuthobium oxycedri*. *(Revised 2004). RMRS-RN-11. Fort Collins, CO: US Department of Agriculture, Forest Service, Rocky Mountain Research Station, 11*. Retrieved fromhttps://www.fs.usda.gov/treesearch/pubs/4616

Chang, S., Puryear, J., & Cairney, J. (1993). A simple and efficient method for isolating RNA from pine trees. *Plant Molecular Biology Reporter / ISPMB*, *11*(2), 113–116. https://doi.org/10.1007/BF02670468

Chaumont, F., & Tyerman, S. D. (2014). Aquaporins: highly regulated channels controlling plant water relations. *Plant Physiology, 164*(4), 1600–1618. https://doi.org/10.1104/pp.113.233791

Clouse, S. D. (2000). Plant development: A role for sterols in embryogenesis. *Current Biology: CB, 10*(16), R601–R604. Retrieved from https://www.ncbi.nlm.nih.gov/pubmed/10985378

Commenil, P., Brunet, L., & Audran, J.-C. (1997). The development of the grape berry cuticle in relation to susceptibility to bunch rot disease. *Journal of Experimental Botany, 48*(8), 1599–1607. https://doi.org/10.1093/jxb/48.8.1599

Conzone, S. D., & Pantano, C. G. (2004). Glass slides to DNA microarrays. *Materials Today*, *7*(3), 20–26. https://doi.org/10.1016/S1369-7021(04)00122-1

Coram, T. E., & Pang, E. C. K. (2006). Expression profiling of chickpea genes differentially regulated during a resistance response to *Ascochyta rabiei*. *Plant Biotechnology Journal*, *4*(6), 647–666. https://doi.org/10.1111/j.1467-7652.2006.00208.x

Crandall, E. D., Klocke, R. A., & Forster, R. E. (1971). Hydroxyl ion movements across the human erythrocyte membrane. Measurement of rapid pH changes in red cell suspensions. *The Journal of General Physiology, 57*(6), 664–683. Retrieved from https://www.ncbi.nlm.nih.gov/pubmed/5576765

Dalma-Weiszhausz, D. D., Warrington, J., Tanimoto, E. Y., & Miyada, C. G. (2006). [1] The affymetrix geneChip® platform: an overview. *Methods in Enzymology*, *410*, 3–28. https://doi.org/10.1016/S0076-6879 (06)10001-4

Dalziel, K. (1957). Initial steady state velocities in the evaluation of enzyme-coenzyme-substrate reaction mechanisms. *Acta Chemica Scandinavica, 11*(1), 706–723. Retrieved from http://actachemscand.dk/pdf/acta_vol_11_p1706-1723.pdf

Davey, M. W., Graham, N. S., Vanholme, B., Swennen, R., May, S. T., & Keulemans, J. (2009). Heterologous oligonucleotide microarrays for transcriptomics in a non-model species; a proof-of-concept study of drought stress in *Musa*. *BMC Genomics*, *10*, 436. https://doi.org/10.1186/1471-2164-10-436

Davies, C., & Robinson, S. P. (1996). Sugar accumulation in grape berries. Cloning of two putative vacuolar invertase cDNAs and their expression in grapevine tissues. *Plant Physiology*, *111*(1), 275–283. Retrieved from https://www.ncbi.nlm.nih.gov/pubmed/8685267

deBruyn, R. A. J., Paetkau, M., Ross, K. A., Godfrey, D. V., & Friedman, C. R. (2015). Thermogenesis-triggered seed dispersal in dwarf mistletoe. *Nature Communications, 6*, 6262. https://doi.org/10.1038/ncomms7262

Deeley, R. G., Westlake, C., & Cole, S. P. C. (2006). Transmembrane transport of endo- and xenobiotics by mammalian ATP-binding cassette multidrug resistance proteins. *Physiological Reviews*, *86*(3), 849–899. https://doi.org/10.1152/physrev.00035.2005

DeRisi, J., Penland, L., Bittner, M. L., Meltzer, P. S., Ray, M., Chen, Y., … Trent, J. M. (1996). Use of a cDNA microarray to analyse gene expression. *Nature Genetics, 14*, 457–460. Retrieved from https://www.nature.com/articles/ng1296-457

Dermauw, W., & Van Leeuwen, T. (2014). The ABC gene family in arthropods: comparative genomics and role in insecticide transport and resistance. *Insect Biochemistry and Molecular Biology*, *45*, 89–110. https://doi.org/10.1016/j.ibmb.2013.11.001

Die, J. V., & Román, B. (2012). RNA quality assessment: a view from plant qPCR studies. *Journal of Experimental Botany*, *63*(17), 6069–6077. https://doi.org/10.1093/jxb/ers276

Di Genova, A., Almeida, A. M., Muñoz-Espinoza, C., Vizoso, P., Travisany, D., Moraga, C., … Maass, A. (2014). Whole genome comparison between table and wine grapes reveals a comprehensive catalog of structural variants. *BMC Plant Biology, 14*, 7. https://doi.org/10.1186/1471-2229-14-7

Dowd, C., Wilson, I. W., & McFadden, H. (2004). Gene expression profile changes in cotton root and hypocotyl tissues in response to infection with *Fusarium oxysporum* f. sp. vasinfectum. *Molecular Plant-Microbe Interactions: MPMI*, *17*(6), 654–667. https://doi.org/10.1094/MPMI.2004.17.6.654

Elashry, A., Okumoto, S., Siddique, S., Koch, W., Kreil, D. P., & Bohlmann, H. (2013). The AAP gene family for amino acid permeases contributes to development of the cyst nematode Heterodera schachtii in roots of Arabidopsis. *Plant Physiology and Biochemistry*, *70*, 379–386. https://doi.org/10.1016/J.PLAPHY.2013.05.016

Fernández, V., Khayet, M., Montero-Prado, P., Alejandro Heredia-Guerrero, J., Liakopoulos, G., Karabourniotis, G., … Heredia, A. (2011). New insights into the properties of pubescent surfaces: peach fruit as a model 1[OA]. https://doi.org/10.1104/pp.111.176305

Ferrer, A., Altabella, T., Arró, M., & Boronat, A. (2017). Emerging roles for conjugated sterols in plants. *Progress in Lipid Research*, *67*, 27–37. https://doi.org/10.1016/j.plipres.2017.06.002

Festa, F., Steel, J., Bian, X., & Labaer, J. (2013). High-throughput cloning and expression library creation for functional proteomics. *Proteomics*, *13*(9), 1381–1399. https://doi.org/10.1002/pmic.201200456

Finn, R. N., & Cerdà, J. (2015). Evolution and functional diversity of aquaporins. *The Biological Bulletin*, *229*(1), 6–23. https://doi.org/10.1086/BBLv229n1p6

Fotopoulos, V. (2005). Plant invertases: structure, function and regulation of a diverse enzyme family. *Journal of Biological Research, 4*, 127-137. http://www.jbr.gr/main/index.htm

Fouquet, R., Léon, C., Ollat, N., & Barrieu, F. (2008). Identification of grapevine aquaporins and expression analysis in developing berries. *Plant Cell Reports, 27*(9), 1541–1550. https://doi.org/10.1007/s00299-008-0566-1

Gadkar, V. J., & Filion, M. (2015). Validation of endogenous reference genes in Buglossoides arvensis for normalizing RT-qPCR-based gene expression data. *SpringerPlus*, *4*, 178. https://doi.org/10.1186/s40064-015-0952-4

Gao, M., Liu, Y., Ma, X., Shuai, Q., Gai, J., & Li, Y. (2017). Evaluation of reference genes for normalization of gene expression using quantitative RT-PCR under aluminum, cadmium, and heat stresses in soybean. *PloS One*, *12*(1), e0168965. https://doi.org/10.1371/journal.pone.0168965

Gedalovich-Shedletzky, E., Delmer, D. P., & Kuijt, J. (1989). Chemical composition of viscin mucilage from three mistletoe species—A comparison. *Annals of Botany*, *64*(3), 249–252. https://doi.org/10.1093/oxfordjournals.aob.a087838

Gehrig, H. H., Winter, K., Cushman, J., Borland, A., & Taybi, T. (2000). An improved RNA isolation method for succulent plant species rich in polyphenols and polysaccharides. *Plant Molecular Biology Reporter / ISPMB*, *18*(4), 369–376. https://doi.org/10.1007/BF02825065

Grunstein, M., & Hogness, D. S. (1975). Colony hybridization: a method for the isolation of cloned DNAs that contain a specific gene. *Proceedings of the National Academy of Sciences of the United States of America, 72*(10), 3961–3965. Retrieved from https://www.ncbi.nlm.nih.gov/pubmed/1105573

Grunwald, C. (1971). Effects of free sterols, steryl ester, and steryl glycoside on membrane permeability. *Plant Physiology*, *48*(5), 653–655. Retrieved from https://www.ncbi.nlm.nih.gov/pubmed/16657855

Gupta, A. B., & Sankararamakrishnan, R. (2009). Genome-wide analysis of major intrinsic proteins in the tree plant *Populus trichocarpa*: characterization of XIP subfamily of aquaporins from evolutionary perspective. *BMC Plant Biology, 9*, 134. https://doi.org/10.1186/1471-2229-9-134

Hammond, J. P., Broadley, M. R., Craigon, D. J., Higgins, J., Emmerson, Z. F., Townsend, H. J., … May, S. T. (2005). Using genomic DNA-based probe-selection to improve the sensitivity of high-density oligonucleotide arrays when applied to heterologous species. *Plant Methods*, *1*(1), 10. https://doi.org/10.1186/1746-4811-1-10

Harr, B., & Schlötterer, C. (2006). Comparison of algorithms for the analysis of Affymetrix microarray data as evaluated by co-expression of genes in known operons. *Nucleic Acids Research*, *34*(2), e8–e8. https://doi.org/10.1093/nar/gnj010

Hawksworth, F. G. (1959). Ballistics of dwarf mistletoe seeds. *Science, 130*(3374), 504–504. https://doi.org/10.1126/science.130.3374.504

Hawksworth, F. G., & Dooling, O. J. (1984). *Lodgepole Pine Dwarf Mistletoe.* US Department of Agriculture, Forest Service. Retrieved from http://dnrc.mt.gov/divisions/forestry/docs/assistance/pests/fidls/018.pdf

Hawksworth, F. G., & Wiens, D. (1972). *Biology and Classification of Dwarf Mistletoe (*Arceuthobium*).* Forest Service. United States Department of Agriculture.

Hawksworth, F. G., & Wiens, D. (1998). *Dwarf Mistletoes: Biology, Pathology, and Systematics*. DIANE Publishing. Retrieved from https://market.android.com/details?id=book-bdfXQ4c5h4IC

Heid, C. A., Stevens, J., Livak, K. J., & Williams, P. M. (1996). Real time quantitative PCR. *Genome Research*, *6*(10), 986–994. https://doi.org/10.1101/gr.6.10.986

Heide-Jørgensen, H. (2008). *Parasitic flowering plants.* BRILL. Retrieved from https://market.android.com/details?id=book-wUOwCQAAQBAJ

Hinds, T. E., & Hawksworth, F. G. (1965). Seed dispersal velocity in four dwarfmistletoes. *Science, 148*(3669), 517–519. https://doi.org/10.1126/science.148.3669.517

Hinds, T. E., Hawksworth, F. G., & McGinnies, W. J. (1963). Seed discharge in Arceuthobium: a photographic study. *Science*, *140*(3572), 1236 LP-1238. https://doi.org/10.1126/science.140.3572.1236

Honaas, L. A., Wafula, E. K., Yang, Z., Der, J. P., Wickett, N. J., Altman, N. S., … dePamphilis, C. W. (2013). Functional genomics of a generalist parasitic plant: laser microdissection of host-parasite interface reveals host-specific patterns of parasite gene expression. *BMC Plant Biology*, *13*, 9. https://doi.org/10.1186/1471-2229-13-9

Hu, C. G., Honda, C., Kita, M., Zhang, Z., Tsuda, T., & Moriguchi, T. (2002). A simple protocol for RNA isolation from fruit trees containing high levels of polysaccharides and polyphenol compounds. *Plant Molecular Biology Reporter / ISPMB*, *20*(1), 69a – 69g. Retrieved from https://link.springer.com/article/10.1007%2FBF02801935

Iandolino, A. B., Goes da Silva, F., Lim, H., Choi, H., Williams, L. E., & Cook, D. R. (2004). High-quality RNA, cDNA, and derived EST libraries from grapevine (*Vitis vinifera* L.). *Plant Molecular Biology Reporter / ISPMB*, *22*(3), 269–278. https://doi.org/10.1007/BF02773137

Ikeda, S., Nasrallah, J. B., Dixit, R., Preiss, S., & Nasrallah, M. E. (1997). An aquaporin-like gene required for the *Brassica* self-incompatibility response. *Science, 276*(5318), 1564–1566. Retrieved from https://www.ncbi.nlm.nih.gov/pubmed/9171060

Imbeaud, S., Graudens, E., Boulanger, V., Barlet, X., Zaborski, P., Eveno, E., … Auffray, C. (2005). Towards standardization of RNA quality assessment using user-independent classifiers of microcapillary electrophoresis traces. *Nucleic Acids Research*, *33*(6), e56. https://doi.org/10.1093/nar/gni054

Inoue, H., Nojima, H., & Okayama, H. (1990). High efficiency transformation of *Escherichia coli* with plasmids. *Gene, 96*(1), 23–28. Retrieved from https://www.ncbi.nlm.nih.gov/pubmed/2265755

Irizarry, R. A., Hobbs, B., Collin, F., Beazer-Barclay, Y. D., Antonellis, K. J., Scherf, U., & Speed, T. P. (2003). Exploration, normalization, and summaries of high density oligonucleotide array probe level data. *Biostatistics, 4*(2), 249–264. https://doi.org/10.1093/biostatistics/4.2.249

Isaacson, T., Kosma, D. K., Matas, A. J., Buda, G. J., He, Y., Yu, B., … Rose, J. K. C. (2009). Cutin deficiency in the tomato fruit cuticle consistently affects resistance to microbial infection and biomechanical properties, but not transpirational water loss. *The Plant Journal: For Cell and Molecular Biology, 60*(2), 363–377. https://doi.org/10.1111/j.1365-313X.2009.03969.x

Ismail, H. M., Brown, G. A., Tucknott, O. G., Holloway, P. J., & Williams, A. A. (1977). Nonanal in epicuticular wax of golden egg plums (*Prunus domestica*). *Phytochemistry, 16*(6), 769–770. https://doi.org/10.1016/S0031-9422(00)89254-7

Iyer, V. R., Eisen, M. B., Ross, D. T., Schuler, G., Moore, T., Lee, J. C., … Brown, P. O. (1999). The transcriptional program in the response of human fibroblasts to serum. *Science*, *283*(5398), 83–87. Retrieved from https://www.ncbi.nlm.nih.gov/pubmed/9872747

Jacobi, W. R., & Swift, C. E. (2005). Dwarf Mistletoe Management. *Diseases Fact Sheet No. 2.925*. Fort Collins, CO: Colorado State University Cooperative Extension. https://static.colostate.edu/client-files/csfs/pdfs/DMT.pdf

Jang, J. C., Fujioka, S., Tasaka, M., Seto, H., Takatsuto, S., Ishii, A., … Sheen, J. (2000). A critical role of sterols in embryonic patterning and meristem programming revealed by the fackel mutants of *Arabidopsis thaliana*. *Genes & Development, 14*(12), 1485–1497. Retrieved from https://www.ncbi.nlm.nih.gov/pubmed/10859167

Järvinen, R., Kaimainen, M., & Kallio, H. (2010). Cutin composition of selected northern berries and seeds. *Food Chemistry, 122*(1), 137–144. https://doi.org/10.1016/j.foodchem.2010.02.030

Johanson, U., Karlsson, M., Johansson, I., Gustavsson, S., Sjövall, S., Fraysse, L., … Kjellbom, P. (2001). The complete set of genes encoding major intrinsic proteins in *Arabidopsis* provides a framework for a new nomenclature for major intrinsic proteins in plants. *Plant Physiology, 126*(4), 1358–1369. Retrieved from https://www.ncbi.nlm.nih.gov/pubmed/11500536

Kahn, R. A., Bak, S., Olsen, C. E., Svendsen, I., & Møller, B. L. (1996). Isolation and reconstitution of the heme-thiolate protein obtusifoliol 14α-demethylase from *Sorghum bicolor* (L.) Moench. *Journal of Biological Chemistry*, *271*(51), 32944–32950. https://doi.org/10.1074/jbc.271.51.32944

Kai, L., & Kaldenhoff, R. (2014). A refined model of water and CO2 membrane diffusion: Effects and contribution of sterols and proteins. *Scientific Reports*, *4*, 6665. Retrieved from http://dx.doi.org/10.1038/srep06665

Kaiser, C. Michaelis, S. & Mitchell A., & Cold Spring Harbor Laboratory (1994). *Methods in yeast genetics: A Cold Spring Harbor Laboratory course manual*. Plainview, N.Y: Cold Spring Harbor Laboratory Press. Retrieved from https://trove.nla.gov.au/work/8137194

Kaldenhoff, R. (2006). Besides water: Functions of plant membrane intrinsic proteins and aquaporins. In K. Esser, U. Lüttge, W. Beyschlag, & J. Murata (Eds.), *Progress in Botany* (pp. 206–218). Berlin, Heidelberg: Springer Berlin Heidelberg. https://doi.org/10.1007/3-540-27998-9_10

Kaldenhoff, R., Bertl, A., Otto, B., Moshelion, M., & Uehlein, N. (2007). Chapter Twenty-Eight - Characterization of Plant Aquaporins. In D. Häussinger & H. Sies (Eds.), *Methods in Enzymology (428)*, 505–531. Academic Press. https://doi.org/10.1016/S0076-6879(07)28028-0

Kaldenhoff, R., & Eckert, M. (1999). Features and function of plant aquaporins. *Journal of Photochemistry and Photobiology. B, Biology, 52*(1), 1–6. https://doi.org/10.1016/S1011-1344(99)00140-2

Kaldenhoff, R., & Fischer, M. (2006). Aquaporins in plants. *Acta Physiologica, 187*(1-2), 169–176. https://doi.org/10.1111/j.1748-1716.2006.01563.x

Kallio, H., Nieminen, R., Tuomasjukka, S., & Hakala, M. (2006). Cutin composition of five Finnish berries. *Journal of Agricultural and Food Chemistry, 54*(2), 457–462. https://doi.org/10.1021/jf0522659

Kassahn, K. S. (2008). Microarrays for comparative and ecological genomics: beyond single-species applications of array technologies. *Journal of Fish Biology*, *72*(9), 2407–2434. https://doi.org/10.1111/j.1095-8649.2008.01890.x

Kelly, S. K., Ross Friedman, C. M., & Smith, R. G. (2009). Vesicular cells of the lodgepole pine dwarf mistletoe *(Arceuthobium americanum*) fruit: development, cytochemistry, and lipid analysis. *Botany, 87*(12), 1177–1185. https://doi.org/10.1139/B09-079

Krajinski, F., Biela, A., Schubert, D., Gianinazzi-Pearson, V., Kaldenhoff, R., & Franken, P. (2000). Arbuscular mycorrhiza development regulates the mRNA abundance of Mtaqp1 encoding a mercury-insensitive aquaporin of *Medicago truncatula*. *Planta, 211*(1), 85–90. https://doi.org/10.1007/s004250000263

Kruse, E., Uehlein, N., & Kaldenhoff, R. (2006). The aquaporins. *Genome Biology, 7*(2), 206.https://doi.org/10.1186/gb-2006-7-2-206

Kuijt, J., & Bertel, H. (2015). *Flowering Plants. Eudicots: Santalales, Balanophorales*. Springer. Retrieved from https://market.android.com/details?id=book-iUEBBQAAQBAJ

Kukulski, W., Schenk, A. D., Johanson, U., Braun, T., de Groot, B. L., Fotiadis, D., … Engel, A. (2005). The 5 Å structure of heterologously expressed plant aquaporin SoPIP2;1. *Journal of Molecular Biology*, *350*(4), 611–616. https://doi.org/10.1016/J.JMB.2005.05.001

Lampard, G. R., Lukowitz, W., Ellis, B. E., & Bergmann, D. C. (2009). Novel and expanded roles for MAPK signaling in *Arabidopsis* stomatal cell fate revealed by cell type--specific manipulations. *The Plant Cell*, *21*(11), 3506–3517. Retrieved from http://www.plantcell.org/content/21/11/3506.short

Lee, D., Polisensky, D. H., & Braam, J. (2005). Genome-wide identification of touch- and darkness-regulated *Arabidopsis* genes: A focus on calmodulin-like and XTH genes. *The New Phytologist, 165*(2), 429–444. https://doi.org/10.1111/j.1469-8137.2004.01238.x

Lefèvre, F., Baijot, A., & Boutry, M. (2015). Plant ABC transporters: time for biochemistry? *Biochemical Society Transactions*, *43*(5), 931–936. https://doi.org/10.1042/BST20150108

Leide, J., Hildebrandt, U., Reussing, K., Riederer, M., & Vogg, G. (2007). The developmental pattern of tomato fruit wax accumulation and its impact on cuticular transpiration barrier properties: effects of a deficiency in a beta- ketoacyl-coenzyme A synthase (LeCER6). *Plant Physiology*, *144*(3), 1667–1679. https://doi.org/10.1104/pp.107.099481

Lepesheva, G. I., & Waterman, M. R. (2007). Sterol 14alpha-demethylase cytochrome P450 (CYP51), a P450 in all biological kingdoms. *Biochimica et Biophysica Acta*, *1770*(3), 467–477. https://doi.org/10.1016/j.bbagen.2006.07.018

Lewinson, O., & Livnat-Levanon, N. (2017). Mechanism of action of ABC importers: Conservation, divergence, and physiological adaptations. *Journal of Molecular Biology*, *429*(5), 606–619. https://doi.org/10.1016/j.jmb.2017.01.010

López, M.M., Bertolini, E., Caruso, P., Penyalver, R, Marco-Noales, E., Gorris, M.T., Morente, C., Salcedo, C., Cambra, M., & Llop, P. (2005). Advantages of an integrated approach for diagnosis of quarantined pathogenic bacteria in plant material. *Phyopathol. Polonica 35*, 49-56. http://www.up.poznan.pl/~ptfit1/pdf/PP35/PP_35_05.pdf

Loulakakis, K. A., Roubelakis-Angelakis, K. A., & Kanellis, A. K. (1996). Isolation of functional RNA from grapevine tissues poor in nucleic acid content. *American Journal of Enology and Viticulture*, *47*(2), 181–185. Retrieved from http://www.ajevonline.org/content/47/2/181.short

Marella, H. H., Nielsen, E., Schachtman, D. P., & Taylor, C. G. (2013). The amino acid permeases AAP3 and AAP6 are involved in root-knot nematode parasitism of *Arabidopsis*. *Molecular Plant-Microbe Interactions: MPMI*, *26*(1), 44–54. https://doi.org/10.1094/MPMI-05-12-0123-FI

McMichael, C. M., Reynolds, G. D., Koch, L. M., Wang, C., Jiang, N., Nadeau, J., … Bednarek, S. Y. (2013). Mediation of clathrin-dependent trafficking during cytokinesis and cell expansion by Arabidopsis STOMATAL CYTOKINESIS DEFECTIVE proteins W. https://doi.org/10.1105/tpc.113.115162

Men, S., Boutté, Y., Ikeda, Y., Li, X., Palme, K., Stierhof, Y.-D., … Grebe, M. (2008). Sterol-dependent endocytosis mediates post-cytokinetic acquisition of PIN2 auxin efflux carrier polarity. *Nature Cell Biology*, *10*(2), 237–244. https://doi.org/10.1038/ncb1686

Mir, P. S., Bittman, S., Hunt, D., Entz, T. and Yip, B. (2006). Lipid content and fatty acid composition of grasses sampled on different dates through the early part of the growing season. *Canadian Journal of Animal Science* 86: 279–290

Misra, C. S. (2015). *Characterization of grapevine (*Vitis vinifera *L.) berry cuticle for its role in water stress response* (Master's thesis). Retrieved from https://fenix.tecnico.ulisboa.pt/downloadFile/563345090414184/Thesis_CS Misra.pdf

Montojo, J., Zuberi, K., Rodriguez, H., Kazi, F., Wright, G., Donaldson, S. L., … Bader, G. D. (2010). GeneMANIA Cytoscape plugin: fast gene function predictions on the desktop. *Bioinformatics , 26*(22), 2927–2928. https://doi.org/10.1093/bioinformatics/btq562

Moshelion, M., Becker, D., Biela, A., Uehlein, N., Hedrich, R., Otto, B., … Kaldenhoff, R. (2002). Plasma membrane aquaporins in the motor cells of *Samanea saman*: diurnal and circadian regulation. *The Plant Cell, 14*(3), 727–739. Retrieved from https://www.ncbi.nlm.nih.gov/pubmed/11910017

Munro, K. C., Jackson, J. R. M., Hartling, I., Sumner, M. J., & Ross Friedman, C. M. (2014). Anther and pollen development in the lodgepole pine dwarf mistletoe (*Arceuthobium americanum*) staminate flower. *Botany*, *92*(3), 203–214. https://doi.org/10.1139/cjb-2013-0276

Murata, K., Mitsuoka, K., Hirai, T., Walz, T., Agre, P., Heymann, J. B., … Fujiyoshi, Y. (2000). Structural determinants of water permeation through aquaporin-1. *Nature, 407*(6804), 599–605. https://doi.org/10.1038/35036519

Nakamura, K., Tanaka, T., & Takeo, K. (1989). Characterization of protein binding to a nitrocellulose membrane. *Seibutsu Butsuri Kagaku, 33*(6), 293–303. https://doi.org/10.2198/sbk.33.293

Nickrent, D. L., Garcia, M. A., Martin, M. P., & Mathiasen, R. L. (2004). A phylogeny of all species of *Arceuthobium* (Viscaceae) using nuclear and chloroplast DNA sequences. *American Journal of Botany, 91* (1), 125-138. http://doi.wiley.com/10.3732/ajb.91.1.125

Nonis, A., Ruperti, B., Falchi, R., Casatta, E., Thamasebi Enferadi, S., & Vizzotto, G. (2007). Differential expression and regulation of a neutral invertase encoding gene from peach (*Prunus persica*): evidence for a role in fruit development. *Physiologia Plantarum*, *129*(2), 436–446. https://doi.org/10.1111/j.1399-3054.2006.00832.x

Okumoto, S., Koch, W., Tegeder, M., Fischer, W. N., Biehl, A., Leister, D., Frommer, W. B. (2004). Root phloem-specific expression of the plasma membrane amino acid proton co-transporter AAP3. *Journal of Experimental Botany*, *55*(406), 2155–2168. https://doi.org/10.1093/jxb/erh233

Opperman, C. H., Taylor, C. G., & Conkling, M. A. (1994). Root-knot nematode--directed expression of a plant root--specific gene. *Science, 263(5144)*, 221–223. https://doi.org/10.1126/science.263.5144.221

Otto, B., & Kaldenhoff, R. (2000). Cell-specific expression of the mercury-insensitive plasma-membrane aquaporin NtAQP1 from *Nicotiana tabacum*. *Planta, 211*(2), 167–172. https://doi.org/10.1007/s004250000275

Pensec, F., Pączkowski, C., Grabarczyk, M., Woźniak, A., Bénard-Gellon, M., Bertsch, C., … Szakiel, A. (2014). Changes in the triterpenoid content of cuticular waxes during fruit ripening of eight grape (*Vitis vinifera*) cultivars grown in the Upper Rhine Valley. *Journal of Agricultural and Food Chemistry, 62*(32), 7998–8007. https://doi.org/10.1021/jf502033s

Peschel, S., Franke, R., Schreiber, L., & Knoche, M. (2007). Composition of the cuticle of developing sweet cherry fruit. *Phytochemistry, 68*(7), 1017–1025. https://doi.org/10.1016/j.phytochem.2007.01.008

Peterhansel, C., Horst, I., Niessen, M., Blume, C., Kebeish, R., Kürkcüoglu, S., & Kreuzaler, F. (2010). Photorespiration. *The Arabidopsis Book*, *8*, e0130. https://doi.org/10.1199/tab.0130

Petit, J., Bres, C., Just, D., Garcia, V., Mauxion, J.-P., Marion, D., … Rothan, C. (2014). Analyses of tomato fruit brightness mutants uncover both cutin-deficient and cutin-abundant mutants and a new hypomorphic allele of GDSL lipase. *Plant Physiology, 164*(2), 888–906. https://doi.org/10.1104/pp.113.232645

Petit, J., Bres, C., Mauxion, J.-P., Tai, F. W. J., Martin, L. B. B., Fich, E. A., … Rothan, C. (2016). The glycerol-3-phosphate acyltransferase GPAT6 from tomato plays a central role in fruit cutin biosynthesis. *Plant Physiology*, *171*(2), 894–913. https://doi.org/10.1104/pp.16.00409

Pfaffl, M. W. (2001). A new mathematical model for relative quantification in real-time RT–PCR. *Nucleic Acids Research*, *29*(9), e45–e45. https://doi.org/10.1093/nar/29.9.e45

Piironen, V., Lindsay, D. G., Miettinen, T. A., Toivo, J., & Lampi, A. M. (2000). Plant sterols: Biosynthesis, biological function and their importance to human nutrition. *Journal of the Science of Food and Agriculture*. https://doi.org/10.1002/(SICI)1097-0010(20000515)80:7<939::AID-JSFA644>3.0.CO;2-C

Pillitteri, L. J., Sloan, D. B., Bogenschutz, N. L., & Torii, K. U. (2007). Termination of asymmetric cell division and differentiation of stomata. *Nature*, *445*(7127), 501–505. https://doi.org/10.1038/nature05467

Pillitteri, L. J., & Torii, K. U. (2012). Mechanisms of stomatal development. *Annual Review of Plant Biology*, *63*, 591–614. https://doi.org/10.1146/annurev-arplant-042811-105451

Polli, A., de Souza, L. A. & de Almeida, O. J. G. (2016). Structural development of the fruits and seeds in three mistletoe species of Phoradendron (Visceae: Santalaceae). *Rodriguésia*, *67*(3), 649–659. https://doi.org/10.1590/2175-7860201667309

Qian, P., Han, B., Forestier, E., Hu, Z., Gao, N., Lu, W., … Hou, S. (2013). Sterols are required for cell-fate commitment and maintenance of the stomatal lineage in Arabidopsis. *The Plant Journal*, *74*(6), 1029–1044. https://doi.org/10.1111/tpj.12190

Radler, F. (1965). The surface waxes of the Sultana vine (*Vitis vinifera* Cv. Thompson Seedless). *Australian Journal of Biological Sciences, 18*(5), 1045–1056. https://doi.org/10.1071/bi9651045

Radler, F. (1970). Investigations on the cuticular wax of *Vitis vinifera* ssp. *tylvestrit* and *Vitis vinifera* ssp. *vinifera*. *Angewandte Botanik 44*, 187-195. Retrieved from https://www.cabdirect.org/cabdirect/abstract/19710303691

Radler, F., & Horn, D. (1965). The composition of grape cuticle wax. *Australian Journal of Chemistry, 18*(7), 1059–1069. https://doi.org/10.1071/ch9651059

Ranjan, A., Ichihashi, Y., Farhi, M., Zumstein, K., Townsley, B., David-Schwartz, R., & Sinha, N. R. (2014). De novo assembly and characterization of the transcriptome of the parasitic weed dodder identifies genes associated with plant parasitism. *Plant Physiology*, *166*(3), 1186–1199. https://doi.org/10.1104/pp.113.234864

Reid, N., & Shamoun, S. F. (2008). Contrasting research approaches to managing mistletoes in commercial forests and wooded pastures. This minireview is one of a collection of papers based on a presentation from the Stem and Shoot Fungal Pathogens and Parasitic Plants: the Values of Biological Diversity session of the XXII International Union of Forestry Research Organization World Congress meeting held in Brisbane, Queensland, Australia, in 2005. *Botany*, *87*(1), 1–9. https://doi.org/10.1139/B08-109

Ringler, P., Borgnia, M. J., Stahlberg, H., Maloney, P. C., Agre, P., & Engel, A. (1999). Structure of the water channel AqpZ from *Escherichia coli* revealed by electron crystallography. *Journal of Molecular Biology, 291*(5), 1181–1190. https://doi.org/10.1006/jmbi.1999.3031

Ross, C. M. (2006). Viscin cells in the dwarf mistletoe *Arceuthobium americanum*– “green springs” with potential roles in explosive seed discharge and seed adhesion. *Davidsonia, 17.*

Ross Friedman, C. M., Ross, B. N., & Martens, G. D. (2010). Antibodies raised against tobacco aquaporins of the PIP2 class label viscin tissue of the explosive dwarf mistletoe fruit. *Plant Biology, 12*(1), 229–233. https://doi.org/10.1111/j.1438-8677.2009.00223.x

Ross Friedman, C., Ross, B. N., & Martens, G. D. (2013). An antibody against a conserved C-terminal consensus motif from plant alternative oxidase (AOX) isoforms 1 and 2 label plastids in the explosive dwarf mistletoe (*Arceuthobium americanum*, Santalaceae) fruit exocarp. *Protoplasma, 250*(1), 317–323. https://doi.org/10.1007/s00709-012-0414-6

Ruggenthaler, P., Fichtenbauer, D., Krasensky, J., Jonak, C., & Waigmann, E. (2009). Microtubule-associated protein AtMPB2C plays a role in organization of cortical microtubules, stomata patterning, and tobamovirus infectivity. *Plant Physiology*, *149*(3), 1354–1365. https://doi.org/10.1104/pp.108.130450

Sambrook, J., Fritsch, E. F., Maniatis, T. & Cold Spring Harbor Laboratory (1989). *Molecular cloning: a laboratory manual* (2nd ed.). Cold Spring Harbor, N.Y: Cold Spring Harbor Laboratory Press. https://trove.nla.gov.au/version/180145381

Samuels, L., Kunst, L., & Jetter, R. (2008). Sealing plant surfaces: cuticular wax formation by epidermal cells. *Annual Review of Plant Biology*, *59*, 683–707. https://doi.org/10.1146/annurev.arplant.59.103006.093219

Schmittgen, T. D., & Livak, K. J. (2008). Analyzing real-time PCR data by the comparative C(T) method. *Nature Protocols*, *3*(6), 1101–1108. Retrieved from https://www.ncbi.nlm.nih.gov/pubmed/18546601

SCHOTT Technical Glass Solutions GmbH. 2010. *NEXTERION™ product catalogue*. Otto-Schott-Straße 13 Jena, Germany. www.schott.com/nexterion

Schrick, K., Fujioka, S., Takatsuto, S., Stierhof, Y.-D., Stransky, H., Yoshida, S., & Jürgens, G. (2004). A link between sterol biosynthesis, the cell wall, and cellulose in *Arabidopsis*. *The Plant Journal For Cell and Molecular Biology*, *38*(2), 227–243. https://doi.org/10.1111/j.1365-313X.2004.02039.x

Schrick, K., Mayer, U., Horrichs, A., Kuhnt, C., Bellini, C., Dangl, J., … Jürgens, G. (2000). FACKEL is a sterol C-14 reductase required for organized cell division and expansion in *Arabidopsis* embryogenesis. *Genes & Development*, *14*(12), 1471–1484. Retrieved from https://www.ncbi.nlm.nih.gov/pubmed/10859166

Schrick, K., Mayer, U., Martin, G., Bellini, C., Kuhnt, C., Schmidt, J., & Jürgens, G. (2002). Interactions between sterol biosynthesis genes in embryonic development of *Arabidopsis*. *The Plant Journal for Cell and Molecular Biology*, *31*(1), 61–73. Retrieved from https://www.ncbi.nlm.nih.gov/pubmed/12100483

Shamoun, S. F., & Dewald, L. E. (2002). Chapter 7 Management Strategies for Dwarf Mistletoes: Biological, Chemical, and Genetic Approaches. In *Mistletoes of North American Conifers*. USDA Forest Service. https://www.fs.fed.us/rm/pubs/rmrs_gtr098/rmrs_gtr098_075_082.pdf

Shamoun, S. F., Ramsfield, T. D., Van Der Kamp, B. J., & Others. (2003). Biological control approach for management of dwarf mistletoes. *New Zealand Journal of Forestry Science, 33*(3), 373–384. Retrieved from http://www.cfs.nrcan.gc.ca/pubwarehouse/pdfs/24754.pdf

Shaw, D. C., Watson, D. M., & Mathiasen, R. L. (2004). Comparison of dwarf mistletoes (*Arceuthobium* spp., Viscaceae) in the western United States with mistletoes (*Amyema* spp., Loranthaceae) in Australia—ecological analogs and reciprocal models for ecosystem management. *Australian Journal of Botany, 52*(4), 481. https://doi.org/10.1071/bt03074

Shi, J. X., Malitsky, S., De Oliveira, S., Branigan, C., Franke, R. B., Schreiber, L., & Aharoni, A. (2011). SHINE transcription factors act redundantly to pattern the archetypal surface of *Arabidopsis* flower organs. *PLoS Genetics*, *7*(5), e1001388. https://doi.org/10.1371/journal.pgen.1001388

Shi, J. X., Adato, A., Alkan, N., He, Y., Lashbrooke, J., Matas, A. J., … Aharoni, A. (2013). The tomato SlSHINE3 transcription factor regulates fruit cuticle formation and epidermal patterning. *The New Phytologist, 197*(2), 468–480. https://doi.org/10.1111/nph.12032

Siefritz, F., Tyree, M. T., Lovisolo, C., Schubert, A., & Kaldenhoff, R. (2002). PIP1 plasma membrane aquaporins in tobacco: from cellular effects to function in plants. *The Plant Cell, 14*(4), 869–876. Retrieved from https://www.ncbi.nlm.nih.gov/pubmed/11971141

Siefritz, F., Otto, B., Bienert, G. P., van der Krol, A., & Kaldenhoff, R. (2004). The plasma membrane aquaporin NtAQP1 is a key component of the leaf unfolding mechanism in tobacco. *The Plant Journal: For Cell and Molecular Biology, 37*(2), 147–155. Retrieved from https://www.ncbi.nlm.nih.gov/pubmed/14690500

Sturm, A., Hess, D., Lee, H.-S., & Lienhard, S. (1999). Neutral invertase is a novel type of sucrose-cleaving enzyme. *Physiologia Plantarum*, *107*(2), 159–165. https://doi.org/10.1034/j.1399-3054.1999.100202.x

Sturm, A., & Tang, G. Q. (1999). The sucrose-cleaving enzymes of plants are crucial for development, growth and carbon partitioning. *Trends in Plant Science*, *4*(10), 401–407. Retrieved from https://www.ncbi.nlm.nih.gov/pubmed/10498964

Suzuki, T., Miwa, K., Ishikawa, K., Yamada, H., Aiba, H., & Mizuno, T. (2001). The *Arabidopsi*s sensor His-kinase, AHk4, can respond to cytokinins. *Plant & Cell Physiology*, *42*(2), 107–113. Retrieved from https://www.ncbi.nlm.nih.gov/pubmed/11230563

Tani, K., & Fujiyoshi, Y. (2014). Water channel structures analysed by electron crystallography. *Biochimica et Biophysica Acta, 1840*(5), 1605–1613. https://doi.org/10.1016/j.bbagen.2013.10.007

Terrier, N., Glissant, D., Grimplet, J., Barrieu, F., Abbal, P., Couture, C., … Hamdi, S. (2005). Isogene specific oligo arrays reveal multifaceted changes in gene expression during grape berry (*Vitis vinifera* L.) development. *Planta*, *222*(5), 832–847. https://doi.org/10.1007/s00425-005-0017-y

Těšitel, J., Plavcová, L., & Cameron, D. D. (2010). Heterotrophic carbon gain by the root hemiparasites, *Rhinanthus minor* and *Euphrasia rostkoviana* (Orobanchaceae). *Planta*, *231*(5), 1137–1144. https://doi.org/10.1007/s00425-010-1114-0

Thellin, O., ElMoualij, B., Heinen, E., & Zorzi, W. (2009). A decade of improvements in quantification of gene expression and internal standard selection. *Biotechnology Advances*, *27*(4), 323–333. Retrieved from https://www.ncbi.nlm.nih.gov/pubmed/19472509

Thellin, O., Zorzi, W., Lakaye, B., De Borman, B., Coumans, B., Hennen, G., … Heinen, E. (1999). Housekeeping genes as internal standards: use and limits. *Journal of Biotechnology*, *75*(2-3), 291–295. Retrieved from https://www.ncbi.nlm.nih.gov/pubmed/10617337

Thimm, O., Bläsing, O., Gibon, Y., Nagel, A., Meyer, S., Krüger, P., … Stitt, M. (2004). Mapman: a user-driven tool to display genomics data sets onto diagrams of metabolic pathways and other biological processes. *The Plant Journal: For Cell and Molecular Biology, 37*(6), 914–939. Retrieved from http://onlinelibrary.wiley.com/doi/10.1111/j.1365-313X.2004.02016.x/full

Tyerman, S. D., Niemietz, C. M., & Bramley, H. (2002). Plant aquaporins: multifunctional water and solute channels with expanding roles. *Plant, Cell & Environment, 25*(2), 173–194. Retrieved from https://www.ncbi.nlm.nih.gov/pubmed/11841662

Uehlein, N., & Kaldenhoff, R. (2008). Aquaporins and plant leaf movements. *Annals of Botany, 101*(1), 1–4. https://doi.org/10.1093/aob/mcm278

Umekawa, Y., Seymour, R. S., & Ito, K. (2016). The biochemical basis for thermoregulation in heat-producing flowers. *Scientific Reports*, *6*(1), 24830. https://doi.org/10.1038/srep24830

van Dongen, J. T., Schuurmans, J. A. M. J., Deen, P. M. T., & Borstlap, A. C. (2000). Analysis of four MIP-like proteins from the developing pea seed coat. In S. Hohmann & S. Nielsen (Eds.), *Molecular Biology and Physiology of Water and Solute Transport* (pp. 331–338). Boston, MA: Springer US. https://doi.org/10.1007/978-1-4615-1203-5_45

van Heeswijk, M. P., & van Os, C. H. (1986). Osmotic water permeabilities of brush border and basolateral membrane vesicles from rat renal cortex and small intestine. *The Journal of Membrane Biology, 92*(2), 183–193. Retrieved from https://www.ncbi.nlm.nih.gov/pubmed/3761362

Vargas, W. A., & Salerno, G. L. (2010). The Cinderella story of sucrose hydrolysis: Alkaline/neutral invertases, from cyanobacteria to unforeseen roles in plant cytosol and organelles. *Plant Science: An International Journal of Experimental Plant Biology*, *178*(1), 1–8. https://doi.org/10.1016/j.plantsci.2009.09.015

Vogg, G., Fischer, S., Leide, J., Emmanuel, E., Jetter, R., Levy, A. A., & Riederer, M. (2004). Tomato fruit cuticular waxes and their effects on transpiration barrier properties: functional characterization of a mutant deficient in a very-long-chain fatty acid beta-ketoacyl-CoA synthase. *Journal of Experimental Botany*, *55*(401), 1401–1410. https://doi.org/10.1093/jxb/erh149

Vomelová, I., Vanícková, Z., & Sedo, A. (2009). Methods of RNA purification. All ways (should) lead to Rome. *Folia Biologica*, *55*(6), 243–251. Retrieved from https://www.ncbi.nlm.nih.gov/pubmed/20163774

Watling, J. R., & Press, M. C. (2001). Impacts of infection by parasitic angiosperms on host photosynthesis. *Plant Biology*, *3*(3), 244–250. https://doi.org/10.1055/s-2001-15195

Welham, T., Pike, J., Horst, I., Flemetakis, E., Katinakis, P., Kaneko, T., … Wang, T. L. (2009). A cytosolic invertase is required for normal growth and cell development in the model legume, *Lotus japonicus*. *Journal of Experimental Botany*, *60*(12), 3353–3365. https://doi.org/10.1093/jxb/erp169

Werner, T., Motyka, V., Strnad, M., & Schmülling, T. (2001). Regulation of plant growth by cytokinin. *Proceedings of the National Academy of Sciences of the United States of America, 98*(18), 10487–10492. https://doi.org/10.1073/pnas.171304098

Westwood, J. H., dePamphilis, C. W., Das, M., Fernández-Aparicio, M., Honaas, L. A., Timko, M. P., … Yoder, J. I. (2012). The parasitic plant genome project: New tools for understanding the biology of *Orobanche* and *Striga*. *Weed Science*, *60*(2), 295–306. https://doi.org/10.1614/WS-D-11-00113.1

Wilson, C. A., & Calvin, C. L. (2006). An origin of aerial branch parasitism in the mistletoe family, Loranthaceae. *American Journal of Botany*, *93*(5), 787–796. https://doi.org/10.3732/ajb.93.5.787

Winfrey, M. R., Rott, M. A., & Wortman, A. T. (1997). *Unraveling DNA: Molecular biology for the laboratory*. Upper Saddle River, NJ: Prentice-Hall.

Worrall, J., & Geils, B. (2006). Dwarf mistletoe. *The Plant Health Instructor*. https://doi.org/10.1094/phi-i-2006-1117-01

Xiang, L., Li, Y., Rolland, F., & Van den Ende, W. (2011). Neutral invertase, hexokinase and mitochondrial ROS homeostasis: emerging links between sugar metabolism, sugar signaling and ascorbate synthesis. *Plant Signaling & Behavior*, *6*(10), 1567–1573. https://doi.org/10.4161/psb.6.10.17036

Yang, Z., Wafula, E. K., Honaas, L. A., Zhang, H., Das, M., Fernandez-Aparicio, M., … dePamphilis, C. W. (2015). Comparative transcriptome analyses reveal core parasitism genes and suggest gene duplication and repurposing as sources of structural novelty. *Molecular Biology and Evolution*, *32*(3), 767–790. https://doi.org/10.1093/molbev/msu343

Yeats, T. H., Buda, G. J., Wang, Z., Chehanovsky, N., Moyle, L. C., Jetter, R., … Rose, J. K. C. (2012a). The fruit cuticles of wild tomato species exhibit architectural and chemical diversity, providing a new model for studying the evolution of cuticle function. *The Plant Journal: For Cell and Molecular Biology, 69*(4), 655–666. https://doi.org/10.1111/j.1365-313X.2011.04820.x

Yool, A. J., & Weinstein, A. M. (2002). New roles for old holes: ion channel function in aquaporin-1. *News in Physiological Sciences: An International Journal of Physiology Produced Jointly by the International Union of Physiological Sciences and the American Physiological Society, 17*, 68–72. Retrieved from https://www.ncbi.nlm.nih.gov/pubmed/11909995

Young, N. D., Steiner, K. E., & dePamphilis, C. W. (1999). The evolution of parasitism in Scrophulariaceae/Orobanchaceae: Plastid gene sequences refute an evolutionary transition series. *Annals of the Missouri Botanical Garden. Missouri Botanical Garden, 86*(4), 876–893. https://doi.org/10.2307/2666173

Zhao, S., Fung-Leung, W.-P., Bittner, A., Ngo, K., & Liu, X. (2014). Comparison of RNA-Seq and microarray in transcriptome profiling of activated T cells. *PLoS ONE*, *9*(1), e78644. https://doi.org/10.1371/journal.pone.0078644

Ziegler, D. J., & Ross Friedman, C. (2017a). Vegetative and floral development in the pistillate plant of *Arceuthobium americanum* (lodgepole pine dwarf mistletoe): an environmental scanning electron microscopy study of its phenology and shoot organization. *Botany, 95*(3), 337–346. https://doi.org/10.1139/cjb-2016-0253

Ziegler, D. J., & Ross Friedman, C. (2017b). Morphology and stomatal density of developing Arceuthobium americanum (lodgepole pine dwarf mistletoe) fruit: a qualitative and quantitative analysis using environmental scanning electron microscopy. *Botany*, *95*(3), 347–356. https://doi.org/10.1139/cjb-2016-0187

Zenoni, S., Ferrarini, A., Giacomelli, E., Xumerle, L., Fasoli, M., Malerba, G., … Delledonne, M. (2010). Characterization of transcriptional complexity during berry development in *Vitis vinifera* using RNA-Seq. *Plant Physiology, 152*(4), 1787–1795. https://doi.org/10.1104/pp.109.149716

APPENDIX I

Sequenced genes

1(A). AQP

```
   1 atggccaagg acgttgaggc tggtgctacc ggcgtcactg tgaacaccgt caaggactac
  61 gaagaccctc cgccggctcc tctgttcgag ccacatgagc ttttgagttg gtctttttac
 121 agagctgcca tcgcggagtt catagccacg cttctgttcc tctacatcac tgtactcacc
 181 gtcatcggct acaaaagcca gaccgactct aaactcacgc cttccgaccc gtgcggtggc
 241 gtgggagtcc tcggcatcgc ctggtccttc ggcggcatga ttttcgtcct cgtctactgc
 301 accgccggca tctccggggg gcatattaac ccggcggtga cgttcggatt gtttctagct
 361 cggaagctga cgctggtgcg agccgtggtg tatatatcgg ctcagtgcct gggagcgatc
 421 tgtggagtgg gtcttgttcg tgctttccaa tcttcccatt actttcgtta cggcggcgga
 481 gccaacatgc tcatggacgg ctacagtacc ggcacggggc tcgccgccga gataattgga
 541 actttcgtgc tagtctacac cgtcttctcc gctaccgatc ccaaacgcag cgccagggat
 601 tcccatgttc ccgtacttgc accgcttcct attgggttcg cagtgttcgt ggttcatctt
 661 gccacgatcc ccatcaccgg cacgagcatc aaccctgctc ggagtctggg agccgctgtc
 721 atatataata gagaccaaga atgggatgac cagtggattt tctgggtagg gccattgttg
 781 ggagcggcca ttgcagcaat atatcatcaa ttcattctga gagcaggggc tgtgaaggca
 841 ctggggtcat tcatggagtc accacccaca tctgatttc ggttcagtaa tttgatttac
 901 tcanttatgg attaa
```

1(B). Alignment of predicted amino acid sequence of *Arceuthobium oxycedri* PIP2 (AoPIP2) with other PIP2 (300 aa) aquaporins (Clustal W) from different plant groups. Asterisks (*) indicate conserved regions (identical amino acids). NPA (Asn-Pro- Ala) = highly conserved regions. Rc–*Ricinus communis*; Pc-*Pyrus communis*; Vv-*Vitis vinifera*; Hb-*Hevea brasiliensis*; Zm-*Zea mays;* Fa-*Fragaria ananasa*; At-*Arabidopsis thaliana.*

```
                                    10        20        30        40        50
PUTATIVE AoPIP              -MAKDVEAGATGVTVNTVKDYEDPPPAPLFEPHELLSWSFYRAAIAEFIA
RcPIP2.                     -MVKDMEVGERG--PFSAKDYHDPPPAPLIDAVELTKWSFYRALIAEFIA
PcPIP2-                     -MAKDMEVAERG--SFSAKDYHDPPPAPLIDAAELTKWSFYRALIAEFVA
VvPIP2-                     -MTKDVEVAEHG--SFSAKDYHDPPPAPLFDSVELTKWSFYRALIAEFIA
VvPIP2-                     -MTKDVEVAEHG--SFSAKDYHDPPPAPLFDSVELTKWSFYRALIAEFIA
HbPIP2-                     -MAKDVEVGGQGG-EFQAKDYNDPPPAPLIDAEEFTQWSFYRAIIAEFIA
FaPIP2-                     -MAKDVEVAERG--SFSAKDYHDPPPAPLFDSVELTKWSFYRAVIAEFIA
ZmPIP2-                     -MAKDIEASGPEAGEFSAKDYTDPPPAPLVDAEELTQWSLYRAVIAEFIA
AtPIP2-                     -MAKDVEGP--EG--FQTRDYEDPPPTPFFDADELTKWSLYRAVIAEFVA
AtPIP2-                     -MAKDVEAVPGEG--FQTRDYQDPPPAPFIDGAELKKWSFYRAVIAEFVA
AtPIP2-                     -MAKDVEGP--DG--FQTRDYEDPPPTPFFDAEELTKWSLYRAVIAEFVA
                               .*:           .:** ****:*:.:  *: .**:*** ****:*
                                    60        70        80 90             100
PUTATIVE AoPIP              TLLFLYITVLTVIGYKSQTDSKLTP-SDPCGGVGVLGIAWSFGGMIFVLV
RcPIP2.                     TLLFLYITVLTVIGYKSQSESDS------CGGVGILGIAWAFGGMIFILV
PcPIP2-                     TLLFLYVTVLTVIGYKSQTDPAVN--ADACGGVGILGIAWAFGGMIFVLV
VvPIP2-                     TLLFLYITVLTVIGYKSQTAGG-----DPCGGVGILGIAWSFGGMIFILV
VvPIP2-                     TLLFLYITVLTVIGYKSQTAGG-----DPCGGVGILGIAWSFGGMIFILV
HbPIP2-                     TLLFLYITVLTVIGYKSQTDPAKN--ADPCGGVGILGIAWAFGGMIFILV
FaPIP2-                     TLLFLYITVLTVIGYKSQIDADLG--GDACGGVGILGIAWAFGGMIFILV
ZmPIP2-                     TLLFLYITVATVIGYKHQTDASASGPDAACGGVGILGIAWAFGGMIFILV
AtPIP2-                     TLLFLYITVLTVIGYKIQSDTKAGG--VDCGGVGILGIAWAFGGMIFILV
AtPIP2-                     TLLFLYITVLTVIGYKIQSDTDAGG--VDCGGVGILGIAWAFGGMIFILV
AtPIP2-                     TLLFLYVTVLTVIGYKIQSDTKAGG--VDCGGVGILGIAWAFGGMIFILV
                            ******:** ****** *           *****:*****:******:**
                                   110       120     130       140     150
PUTATIVE AoPIP              YCTAGISGGHINPAVTFGLFLARKLTLVRAVVYISAQCLGAICGVGLVRA
RcPIP2.                     YCTAGISGGHINPAVTFGLFLARKVSLVRAIMYMVAQCLGAICGVGLVKA
PcPIP2-                     YCTAGISGGHINPAVTFGLFLARKVSLVRAVLYMVAQSLGAIAGVALVKA
VvPIP2-                     YCTAGISGGHINPAVTFGLFLARKVSLIRAILYMVAQCLGAICGVGLVKA
VvPIP2-                     YCTAGISGGHINPAVTFGLFLARKVSLIRAILYMVAQCLGAICGVGLVKA
HbPIP2-                     YCTAGISGGHINPAVTLGLFLARKVSLVRAILYMAAQCLGAICGCGLVKA
```

```
FaPIP2-                 YCTAGISGGHINPAVTFGLFLARKVSLVRAVMYIVAQSLGAIAGVGLVKA
ZmPIP2-                 YCTAGISGGHINPAVTFGLFLARKVSLVRALLYIVAQCLGAICGVGLVKG
AtPIP2-                 YCTAGISGGHINPAVTFGLFLARKVSLIRAVLYMVAQCLGAICGVGFVKA
AtPIP2-                 YCTAGISGGHINPAVTFGLFLARKVSLPRALLYIIAQCLGAICGVGFVKA
AtPIP2-                 YCTAGISGGHINPAVTFGLFLARKVSLIRAVLYMVAQCLGAICGVGFVKA
                        ****************:*******::* **::*: **.****.* .:*:.
                                 160       170       180       190    200
PUTATIVE AoPIP          FQSSHYFRYGGGANMLMDGYSTGTGLAAEIIGTFVLVYTVFSATDPKRSA
RcPIP2.                 FQSSHYKRYGGGANTLDDNYSTGVGLGAEIIGTFVLVYTVFSATDPKRSA
PcPIP2-                 FQKSYYIKYGGGANSLSDGYSTGVGLAAEIIGTFVLVYTVFSATDPKRSA
VvPIP2-                 FQSAYYDRYGGGANELSTGYSKGTGLGAEIIGTFVLVYTVFSATDPKRSA
VvPIP2-                 FQSAYYDRYGGGANELSTGYSKGTGLGAEIIGTFVLVYTVFSATDPKKSA
HbPIP2-                 FQKAYYNRYGGGANELADGYSKGTGLGAEIIGTFVLVYTVFSATDPKRNA
FaPIP2-                 FQKSYYTKYGGGANELADGYSTGVGLAAEIIGTFVLVYTVFSATDPKRSA
ZmPIP2-                 FQSAYYVRYGGGANELSDGYSKGTGLAAEIIGTFVLVYTVFSATDPKRSA
AtPIP2-                 FQSSYYDRYGGGANSLADGYNTGTGLAAEIIGTFVLVYTVFSATDPKRNA
AtPIP2-                 FQSSYYTRYGGGANSLADGYSTGTGLAAEIIGTFVLVYTVFSATDPKRSA
AtPIP2-                 FQSSHYVNYGGGANFLADGYNTGTGLAAEIIGTFVLVYTVFSATDPKRNA
                        **.::: .****** *  .*. *.**.*********************:.*
                                 210       220       230       240   250
PUTATIVE AoPIP          RDSHVPVLAPLPIGFAVFVVHLATIPITGTSINPARSLGAAVIYNRDQEW
RcPIP2.                 RDSHVPVLAPLPIGFAVFMVHLATIPITGTGINPARSLGAAVIYNQDKAW
PcPIP2-                 RDSHVPVLAPLPIGFAVFIVHLATIPITGTGINPARSLGAAVIYNKDKAW
VvPIP2-                 RDSHVPVLAPLPIGFAVFMVHLATIPITGTGINPARSLGAAVIYNNEKAW
VvPIP2-                 RDSHVPVLAPLPIGFAVFMVHLATIPITGTGINPARSLGAAVIYNNEKAW
HbPIP2-                 RDSHVPVLAPLPIGFAVFMVHLATIPVTGTGINPARSFGAAVIYNQDKAW
FaPIP2-                 RDSHVPVLAPLPIGFAVFMVHLATIPITGTGINPARSLGAAVIYDKKKAW
ZmPIP2-                 RDSHVPVLAPLPIGFAVFMVHLATIPITGTGINPARSLGAAVIYNKDKAW
AtPIP2-                 RDSHVPVLAPLPIGFAVFMVHLATIPITGTGINPARSFGAAVIYNKSKPW
AtPIP2-                 RDSHVPVLAPLPIGFAVFMVHLATIPITGTGINPARSFGAAVIYNKSKPW
AtPIP2-                 RDSHVPVLAPLPIGFAVFMVHLATIPITGTGINPARSFGAAVIFNKSKPW
                        ******************:*******:***.******:*****:::.: *

                                  260       270       280       290  300
PUTATIVE AoPIP          DDQWIFWVGPLLGAAIAAIYHQFILRAGAVKALGSFMESPPTSDFRFSNL
RcPIP2.                 DDQWIFWVGPFIGAAIAAFYHQFILRAGAVKALGSFRSNPTV-------
PcPIP2-                 DDQWIFWVGPFIGAAIAAFYHQFILRAGAVKALGSFRSNPHV--------
VvPIP2-                 DDQWIFWVGPFIGAAIAAFYHQFILRAGAVKALGSFRSTTHV--------
VvPIP2-                 DDQWIFWVGPFIGAAIAAFYHQFILRAGAVKALGSFRSTAHV--------
HbPIP2-                 DDQWIFWVGPFIGAAIAAFYHQYILRAAAVKALGSFRSTSNI--------
FaPIP2-                 DDQWIFWVGPFIGAAIAAFYHQFILRAGAVKALGSFRSNA----------
ZmPIP2-                 DDQWIFWVGPLIGAAIAAAYHQYVLRASATKLG-SYRSNA----------
AtPIP2-                 DDHWIFWVGPFIGAAIAAFYHQFVLRASGSKSLGSFRSAANV--------
AtPIP2-                 DDHWIFWVGPFIGAAIAAFYHQFVLRASGSKSLGSFRSAANV--------
AtPIP2-                 DDHWIFWVGPFIGATIAAFYHQFVLRASGSKSLGSFRSAANV--------
                        **:*******::**:*** ***::***.. *   *: .  .

                              310
PUTATIVE AoPIP          IYSXMD
RcPIP2.                 ------
PcPIP2-                 ------
VvPIP2-                 ------
VvPIP2-                 ------
HbPIP2-                 ------
FaPIP2-                 ------
ZmPIP2-                 ------
AtPIP2-                 ------
AtPIP2-                 ------
AtPIP2-                 ------
```

2. Alkaline/Neutral invertase (CINV2)

atggggagttacttttggattgatttccagcagctcaacgacatctaccgatataagacc
Gaggagtacttgcacacggcggtcaataagtttaacgtgattcccgattcgattcccgag
Tgggtttttgatttcatgcccacacgcggaggctacttcatcgggaatattagccccgcg
Agaatggatttccggtggtttgctttgggtaattgtgttgctatcctatcctctcttgcg
Actcctgagcagtctttggctatcatggatctgatcgaagcgcggtgggaagagctggtt
Ggggaaatgcccttaaagatttgctatcccgccattgaaactcatgaatggaggattact
Acgggctgtgatcctaagaatacgagatggagttatcataatgggggatcttggccagtt
Cttttgtggatcttgacggctgcgtgcataaagacggggcggcctcagatcgctcggcgc
Gcgattgatcttgcggaatcgcggctgttgaaggactcgtggccggaatattacgatgga
Aagcaaggtaggtatattgggaaacaagctaggaaattccagacatggtcgattgctgga
Tacttggtggcaaagatgctgcttgaggatccgtcgcacttgggaatgatatctcttgaa
gaagacaagcagatgaaacctttatcaagagatccctctcctggaactgctga

3. ABC transporter family

atgctttct
ggggaagagattccatctagtggatctgcatttatttttggaagaaatatattttcaaac
ccgaagactattcgtcgccatgttggttattgtccccaattcgatgccctgctggagtat
ttaactgttcaagagcatcttgagctttatgcaagaataaaaggtgtcccaggttaccag
ttggaagatgttgttatgcagaagttattggagtttgatttgttaaagcatgctagtaaa
ccatcattttctcttagtggtggaaacaagcgtaaattatctgtagcaattgctatgatt
ggggatcccccaatagttattcttgatgagccatccacaggtatggatcctattgccaaa
agattcatgtgggaagtcatatctcgcatatcaacaagaagagaaaagactgcagttatt
cttactacacacagcatggatgaggctcaagcactttgtacccgaatcggaataatggtt
ggaggtcggctaagatgcattggaagtccccaacatcttaaaacacgatttggaaatcat
atagagctagaggtgaaaccagctgatgttagtcccgaggagttgggaaacctatgtaaa
acaatacaagacaggcttattgacattccttgccctcaaaggagcatcctcagtgacctt
gaaacctgcattggtggaatagactccaatatctcagaaaatgcatcagtttcagaaatt
tccttgtcccttgaaatgatgattataattggccggtggcttgggaatgaagatctggta
 aggatgcttgcttcagaaatcaaatcttctaatggggcttttggtgaacaattatcaaaa
cagcttctccctggatgggggtacccctttacgggtgttttcaaaatggtggctaaccaa
aaaaaaattttccggaattga

4. Sterol 14-demethylase

atggatgtggatggcaagttcttcaatgtcggtcttgttttttcgcgacactggtcgcgtctaagcttata
tctatgcttctgattcccagatctggaaagcgcttgcctcccaaagtaaaggcatggccattgattggtggt
cttataagatttttgagaggcccgatcgtcatgcttcgcgaagagtatcccaagcttgggagcgtcttcaca
ctcaagttattaaacaagaacattacattcttaataggtccagaggtctcggcgcatttcttcaaggctcca
gaatcggatcttagccagcaggaggtgtaccagttcaatgtccctacctttggacctggcgtggtctttgat
gtggattactctatacggcaagagcagttccggttcttcactgagtcgttgagagttgtgaaattgaagggt
tatgttgatcagatggttatggaagcagaggattacttctcaaagtgggggaaagcggtgaggtggatctc
aagtatgaactggagcatctaatcatcttaacagccagccgatgtcttttgggtgaagaagttcgcaacaaa
cttttcgatgacgtgtcatctctcttccatgatctcgacaatggcatgctccccataagtgtcatcttcccc
tacttacccatcccagcccaccgccgccgtgaccaggcccgcaaaaagatcgccgacattttctcaaccata
atcgcttcgcgcaagaacaccggccaatcacaaaatgacatgttgcaatcgttcatagactcaaaatacaaa
gatgggcggtccaccacagattctgaagtcaccgggcttctcattgcagctttgttcgcaggacagcacaaa
agctccatcacggccacctggaccggggcctacttgctgaatcccccaagctttttaagtgccccccttgg
aacaaacaaaaaaagcttaataaaaaacattgggaaaaaaggtggatcccaaatgtttttccggaaatgga
actgtttgtttccggggcctccaaaaaggccctaaaggtctccccccctcccttataatgtctcctaa

5. Ribulose biphosphate carboxylase/oxylase (RuBisCo):

atgtccaactccccggggatgtacaataaagaggacaatccgcgagtcccgatcatt
gtcacgggtaacgacttttcgacgctttatgcgccgctaatccgtgacgggcgaatggag
aaattctattgggcccctactcgggacgaccgcatcggcgtttgtaccgggattttcaaa
acggataatgtcccgcacgagcaaattgtgaagatcgtggataatttcccgggacaatct

```
atcgatttttcggtgcgctgcgggcgcgagtgtacgatgacgaagtgaggaaatggata
tcgggagtgggagttcagagcatcggtaagaagctggttaactcaaaggagggtccgccc
actttcgagcaaccgaaaatgactctcgagaagcttctcgagtacgggaacatgctcgtc
aaagaacaagacaatgttaacagggttcaattagccgagaagtacatgagccaagcggct
cttggaaatgctaatgaagattccatgaaaacggagagcttctacgggaaggcagcccaa
caagtcggtgttcctatcccggaagggtgcacggacccttctgcggccaatttcgaccct
acggcaaggagtgataatgggagttgcctgtattga
```

APPENDIX II

PCR and qRT-PCR data

1. Primers for the fusion of a cDNA with recognition sequences for the Gateway® gene-specific sequence for PIP2 gene

AoAQPgate Sense	5‘-GGGGACAAGTTTGTAC AAAAAAGCAG GCTTAACCATGGCCAAGGACGTTGAG-3’	100	75	GatewayprimerAoPIP2
AoAQPgate Antisense	5‘-GGGGAC CACTTTGTAC AAGAAAGCTG GGTATTAATCCATAATTGAGTAAATCAA-3‘	100	72.9	GatewayprimerAoPIP2

2. List of primers that produced amplicons in qRTPCR when using *A. americanum*.

Sequence 5’ – 3’	*source*	gene
GTGGAGTGGGTCTTGTTCGT	*Arceuthobium oxycedri*	Aquaporin PIP2.1 (JN857944.1)
AGCGGAGAAGACGGTGTAGA	*Arceuthobium oxycedri*	Aquaporin PIP2.1 (JN857944.1)
ATATTAACCCGGCGGTGACG	*Arceuthobium oxycedri*	PIP2.1
ACGAACAAGACCCACTCCAC	*Arceuthobium oxycedri*	PIP2.1
AATGGTTGGAGGTCGGCTAAG	*Arceuthobium oxycedri*	ATPase
ATAGGTTTCCCAACTCCTCGG	*Arceuthobium oxycedri*	ATPase
AAACGGATAATGTCCCGCAC	*Arceuthobium oxycedri*	RUBISCO
ACTTCGTCATCGTACACTCGC	*Arceuthobium oxycedri*	RUBISCO

APPENDIX III

Affimetrix microarray data: Please access data using attached flash drive.

APPENDIX IV

Stopped-flow data and calculations

	1a										65.2		1.98E-01								9.96		0.03031037
diameter, radius, volume, surface											60.94		1.85E-01								0.49		0.00149117
	d	r	V	S							69.59		2.12E-01								5.63		0.01713327
	4.93	0.0002465	0.00000	7.6356E-07							61.28		1.86E-01								6.48		0.01972
		cm	cm^3	cm^2							61.59		1.87E-01								5.1		0.01552037
											60.29		1.83E-01								5.63		0.01713327
Molar volume of water, osmotic gradient											54.08		1.65E-01								0.25		0.0007608
Vw	18	cm^3/mol									63.35		1.93E-01								5.11		0.0155508
Cout	1.5 M Sorbitol	1.50E-03									63.87		1.94E-01								4.5		0.01369444
											64.99		1.98E-01								5.1		0.01552037
V/(S*Vw*cOUT)		3.04E-03									61.62		1.88E-01								6.6		0.02008519
											57.92		1.76E-01								4.9		0.01491173
	K-Werte		Pf-Werte								66.02		2.01E-01								4.29		0.01305537
											57.72		1.76E-01								4.46		1.36E-02
	4.6		0.01400								63.35		1.93E-01								7.2		2.19E-02
	0.49		0.00149				4.6		0.01399877		65.44		1.99E-01								6.65		2.02E-02
	5.63		0.01713				0.49		0.00149117		66.83		2.03E-01								3.2		9.74E-03
	6.48		0.01972				5.63		0.01713327		66.94		2.04E-01								3.98		1.21E-02
	5.1		0.01552				6.48		0.01972		56.82		1.73E-01								6.9		0.02099815
	3		0.00974				5.1		0.01552037		68.2		2.08E-01								9.2		0.02799753
	5.11		0.01555				3.2		0.00973827		59.98		1.83E-01								7.72		0.02349358
	4.5		0.01369				5.11		0.0155508		50.02		1.52E-01								6.9		0.02099815
	5.1		0.01552				4.5		0.01369444		55.96		1.70E-01									Avergae	0.01663391
	6.6		0.02009				5.1		0.01552037		53.59		1.63E-01									STDEV	0.00707371
	4.9		0.01491				6.6		0.02008519		58.12		1.77E-01										
	5.76		0.01753				4.9		0.01491173		56.16		1.71E-01										
	4		0.01306				5.76		0.01752889		59.12		1.80E-01										
	4.46		0.01357				4.29		0.01305537		74.75		2.27E-01										
	7.2		0.02191				4.46		0.01357272		64.84		1.97E-01										
	6.65		0.02024				7.2		0.02191111		69.47		2.11E-01										
	3.2		0.00974				6.65		0.02023735		64.38		1.96E-01										
	3.98		0.01211				3.2		0.00973827		58.83		1.79E-01										
	6.9		0.02100				3.98		0.01211198		71.45		2.17E-01										
	8.2		0.02495				6.9		0.02099815		59.89		1.82E-01										
	5		0.01522				8.2		0.02495432		6.57E+01		2.00E-01										
	7.72		0.02349				5		0.01521605		66.398		2.02E-01										
	6.9		0.02100				7.72		0.02349358		71.64		2.18E-01										
			0.00000				6.9		0.02099815		57.95		1.76E-01										
			0.00000						0.01613827														
			0.00000						0.00523662		54.34		1.65E-01										
			0.00000																				
			0.00000								53.18		1.62E-01										
			0.00000								52.59		1.60E-01										
			0.00000								62.88		1.91E-01										
			0.00000																				
			0.00000								49.72		1.51E-01										
			0.00000								55.34		1.68E-01										
			0.00000								58.26		1.77E-01										
			0.00000								60.53		1.84E-01										
			0.00000								57.61		1.75E-01										